

School of Computer Science, Engineering and Mathematics

Design and Optimisation of a Solar Array for the Flinders Solar Car

Master Thesis (18-units)

5th December, 2016

Name: Syed Wahb Mehdi Rizvi (2142342)

Academic Supervisor: Dr. Stuart Wildy

This thesis was submitted to the School of Computer Science, Engineering, and Mathematics in the Faculty of Science and Engineering in partial fulfilment of the requirements for the degree of Engineering (Electronic) at Flinders University – Adelaide, Australia.

Declaration

I certify that this work does not incorporate without acknowledgment any material previously submitted for a degree or diploma in any university, and that to the best of my knowledge and belief it does not contain any material previously published or written by another person except where due reference is made in the text.



Syed Wahb Mehdi Rizvi

5th December, 2016

Acknowledgments

First and foremost I would like to thank my university supervisor, Dr. Stuart Wildy for his extreme support in this real world engineering project and giving me the opportunity to undertake a study, which will further enhance my learning and understanding of solar array design. I must thank him for his time, guidance, enduring advice and the academic knowledge that he has forwarded to me all the way through the duration of this project.

Secondly, I would like to thank, Professor David Lewis, for sharing his vital research knowledge and his experience with me in the field of solar cells technology. I must show appreciation to the academic and technical staff at Flinders University, in particular, Dr. Andrew Lammas, Damian Kleiss and Craig Peacock for their technical feedback and guidance throughout the project.

Finally, I must thank my family for moral support at the whole time of the project. Through all the struggles in life, we have remained a team and always been there for each other. Particularly, to my mother, who support, encourage and the unconditional love and effort she has spent on me. My parents have provided me the opportunities and luxuries in life and have continuously promoted the importance of education in my life and encouraged me to believe in myself. Their love and guidance are the true reason for my success. I dedicate this thesis to my parents.

Abstract

This thesis is written on the design of a solar array for the Flinders University Solar Car. Flinders Automotive Solar Team (FAST) was formed in late 2015 and aims to take part in the World Solar Challenge in 2017. The World Solar Challenge (WSC) is a solar car competition held in Australia, where cars travel 3000km from Darwin to Adelaide. During the race, the illumination of the sunlight will change continuously. Therefore, to make sure of the success of the team, an efficient design of a solar array is required.

Before designing the Photovoltaic (PV) system, a few steps need to be taken. These steps include the best solar cells selection, calculation of available area for the solar cells on the body of the car and optimal arrangement of the solar cells, as well as determining the sun position during the race.

Since Flinders University is developing a solar racing car for the first time, the work completed in this project is developed from the ground up. A selection is made to use mono-crystalline silicon cells for the design of the solar array. After that the optimum arrangement of the selected solar cells to complete the solar array design is determined. Moreover, the importance and the selection of an appropriate Maximum Power Point Tracker (MPPT) and encapsulation techniques are also covered in this project.

After the design of a prototype of the solar array, the thesis will include the analysis of the performance of the solar array under environmental changes. During the analytical examinations, various post-design responses including change in sunlight, change in angle of incidence and change in temperature are calculated. These responses show the impacts on the overall solar output power and efficiency of the solar array.

The platform has been established with expandability in mind. So, additional future works can be easily undertaken by another student in the following years. Future enhancement includes the addition of more solar cells in order to boost solar output, the study for more suitable encapsulation techniques and the data acquisition system of solar radiation during the competition.

Table of Contents

DECLARATION	2
ACKNOWLEDGMENTS	3
ABSTRACT	4
LIST OF FIGURES	8
LIST OF TABLES	10
CHAPTER 1 - PROJECT INTRODUCTION AND SIGNIFICANCE.....	11
1.1 SOLAR CAR.....	12
1.2 CRUISER CLASS CAR	13
1.3 GOALS OF PROJECT	14
1.4 THESIS OUTLINE	15
CHAPTER 2 - LITERATURE REVIEW.....	16
2.1 BACKGROUND.....	16
2.2 SOLAR TECHNOLOGY	17
2.2.1 <i>Crystalline Silicon</i>	18
2.2.2 <i>Thin Film Cells</i>	19
2.2.3 <i>Organic/Polymer Cells</i>	19
2.2.4 <i>Hybrid Cells</i>	20
2.3 SHADING AND CONFIGURATION OF CELLS	20
2.4 ANGLES OF THE SOLAR CELLS	23
2.5 TEMPERATURE EFFECTS	26
2.5.1 <i>Analysis by SABER Modelling</i>	27
2.5.2 <i>Cooling Technique</i>	28
2.6 MAXIMUM POWER POINT TRACKER.....	30
2.6.1 <i>Perturb and Observe</i>	32
2.6.2 <i>Incremental Conductance</i>	34
2.6.3 <i>Comparison of MPPT Control Algorithm</i>	34
2.7 ENCAPSULATION	36
2.8 DESIGN TECHNIQUES OF PREVIOUS SOLAR CAR TEAMS	39
2.9 SUMMARY	42

CHAPTER 3 - SOLAR ARRAY MODELLING	43
3.1 SOLAR CELL MODEL	43
3.1.1 Short Circuit Current (I_{sc}).....	43
3.1.2 Open Circuit Voltage (VOC)	44
3.1.3 Fill Factor (F.F)	44
3.1.4 Maximum Output Power (P_{max}).....	45
3.1.5 Efficiency (η_{max}).....	45
3.2 SOFTWARE TESTING	46
3.3 RESISTANCE EFFECT	48
3.3.1 Series Resistance (R_s)	49
3.3.2 Series Resistance R_s on I-V Characteristics Curve.....	49
3.3.3 Shunt Resistance	50
3.3.4 Shunt Resistance R_{SH} on I-V Characteristics Curve.....	50
3.3.5 Results and Discussion.....	50
3.4 PROPOSED SOLAR ARRAY DESIGN	51
3.4.1 General Design	51
3.4.2 Partial Shading	52
3.5 FINAL SOLAR ARRAY DESIGN	54
3.5.1 Design Scheme of Solar Array.....	55
3.5.2 Prototype Design.....	56
3.5.3 Strength and Weaknesses of the Design.....	58
3.6 MAXIMUM POWER POINT TRACKER.....	60
CHAPTER 4 - PERFORMANCE ANALYSIS OF DESIGNED SOLAR ARRAY.....	63
4.1 TEMPERATURE EFFECTS	63
4.2 SHADING ANALYSIS	67
4.3 ANALYSIS OF OPTIMUM TILT ANGLE	70
4.3.1 Power and Efficiency Losses vs. Tilt Angles.....	70
CHAPTER 5 - DESIGN CHALLENGES AND CONSTRAINTS.....	77
5.1 AREA LIMITATIONS	77
5.2 AERODYNAMICS VS. SOLAR ARRAY.....	77
5.3 SOLDERING AND RECONFIGURATION.....	78

CHAPTER 6 - CONCLUSION	79
6.1 FUTURE WORK	81
6.1.1 Increment of Solar Cells.....	81
6.1.2 Data Logging	81
6.1.3 Additional Sensors.....	82
6.1.4 Efficient Enclosure and Encapsulation.....	82
REFERENCES	83
A. APPENDICES.....	87
A.1 APPENDIX A- SUNPOWER SOLAR CELL DATASHEET	87
A.2 APPENDIX B- MPPT DATASHEETS	89
A.3 APPENDIX C- MATLAB SIMULINK MODELS AND CODING	94
A.4 APPENDIX D- TEMPERATURE AND SHADING CALCULATIONS	98

LIST OF FIGURES

Figure 1: Development of Renewable Technologies [1].	11
Figure 2: Basic Structure of the Solar Car [4].	12
Figure 3: Basic Electrical Diagram of PV Array System	17
Figure 4: Photovoltaic Materials in Market [5].	17
Figure 5: Amorphous Silicon Cell [14].	19
Figure 6: Current and Voltage (I-V) curve [19].	21
Figure 7: Different Configurations and their Effect on P-V Curve [18].	22
Figure 8: Altitude and Declination Angles [20].	24
Figure 9: Hour Angle [20].	24
Figure 10 Effect of Temperature on Output Power [22].	26
Figure 11 Cooling Technique of a Solar Array [23].	28
Figure 12: Solar Array Temperature vs. irradiation [23].	29
Figure 13: I-V Curve with Different MPP [24].	30
Figure 14: P-V Curve with Different MPP [24].	31
Figure 15: Effect of MPPT [24].	31
Figure: 16 Perturb and Observe Algorithm [28].	33
Figure 17: Mathematical Model to Test MPPT Algorithm [28].	34
Figure 18: Different Encapsulation Techniques and overall output [31].	37
Figure 19: Comparison of EVA and Silicone Encapsulations by I-V Curve [33].	37
Figure 20 Front Side View of Solar Array of Gato Del Sol Car.	39
Figure 21: Eindhoven University Solar Car [37].	40
Figure 22: Kogakuin University Solar Car [38].	41
Figure 23: Single Diode Ideal model for a Solar cell [18].	43
Figure 24: I-V Curve with maximum power points [39].	44
Figure 25: MATLAB Simulation for P-V and I-V Curve	46
Figure 26: Power-Voltage (P-V) Curve.	47
Figure 27: Current-Voltage (I-V) Curve.	47
Figure 28: Single Diode Solar Cell Model with Parasitic Elements [39].	48
Figure 29: Power vs Load Resistance Curve [39].	48
Figure 30: I-V Characteristics with Varying Series Resistance at Fixed Illumination.	49

Figure 31: I-V Characteristics with Varying Shunt Resistance at Fixed Illumination.....	50
Figure 32: System diagram of a PV system on solar car [40].	52
Figure 33: Influence of Bypass diode [40].	53
Figure 34: Influence of Bypass diode [41].	53
Figure 35: Preliminary Solar Array Design	55
Figure 36: Prototype of Solar Array.	56
Figure 37: Final Model of the Solar Car.	58
Figure 38: Total Area for Solar Cells.	59
Figure 39: MPPT Hardware Module of Aurora/Symtech [45].	61
Figure 40: Power vs Efficiency Graph of Aurora/Symtech MPPT [45].	62
Figure 41: Temperature Variations of Solar Panel.	66
Figure 42: Effects of shading with and without bypass diode.	68
Figure 43: Change in Current, Voltage and Power vs. Tilt Angle.....	71
Figure 44: Change in Efficiency vs. Tilt Angle.	72
Figure 45: Optimum Tilt Angle for Darwin from 8 am to 5 pm.....	73
Figure 46: Optimum Tilt Angle from Darwin to Adelaide.....	75
Figure 47: Angle at Current FAST Car Model.	76

LIST OF TABLES

Table 1 Allowable Solar Cells Area for Cruiser Class	13
Table 2 Comparison of Crystalline Silicon Technology.....	18
Table 3: Value of 'n' for the first day of month	25
Table 4 : Perturb and Observe (P&O) Procedure [25].....	32
Table 5 Comparison of MPPT Algorithms [28]	35
Table 6 Electrical Specification of Gato Del Sol car.....	39
Table 7 Electrical Specification of Stella Lux Solar Car.....	40
Table 8 Electrical Specification of Aurora 101 Solar Car	41
Table 9 : Electrical characteristics of Sunpower C60 cell [42]	54
Table 10 : Physical characteristics of Sunpower C60 cell [42]	54
Table 11 Comparison of Different MPPT [45],[46],[47]	61
Table 12 Effect of Temperature on Output Power for Ideal Radiations (1kW/m2).....	65
Table 13 Effect of Bypass Diode on Output Power.....	68
Table 14 Electrical Specifications of Tindo karra-250 (tindosolar.com.au)....	70
Table 15 Optimum Tilt Angle for Complete Day at Darwin.....	73
Table 16 Optimum Tilt Angles for Complete Race at Solar Noon.....	74
Table 17 Reduction in Total Power	78

CHAPTER 1

PROJECT INTRODUCTION AND SIGNIFICANCE

Energy is the prime mover of financial growth and also one of the key factors in the growth of a country [1]. In 2011, Sarikprueck et al. [1] reveals that the future of carbon-constrained energy technologies such as solar power and wind power are very bright as they are reliable, affordable and have clean energy properties. The development of renewable technologies and their anticipated cost of full-scale application can be seen in Figure 1. Some of these technologies, including wind and the photovoltaic (PV) energy are in the deployment stage. Whereas, some renewable energy sources such as wave energy are still under development [2].

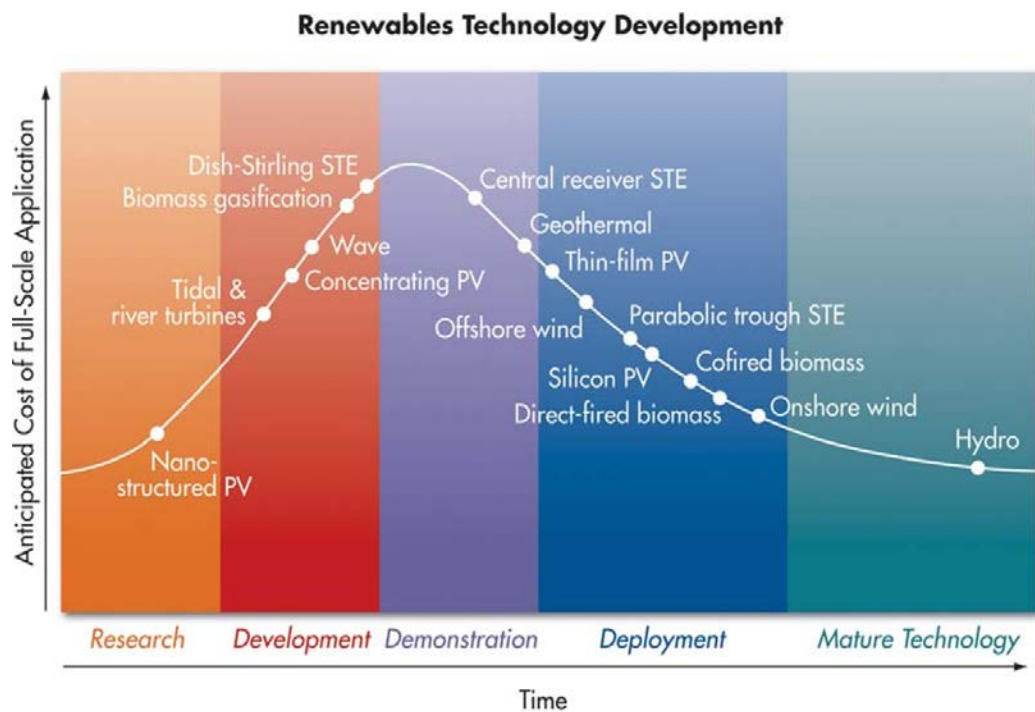


Figure 1: Development of Renewable Technologies [1].

The photovoltaic effect is the process of converting photons from sunlight into electricity. This process requires semiconductors to convert one form of energy (solar energy) into electrical energy. These semiconductors are commonly known as the solar cells. The solar cells produce Direct Current (DC) output, which may later convert into Alternating Current (AC) using DC to AC inverters.

Vehicles that run on electric energy are known as Electric Vehicles (EV's). In the last ten years, an increase in the development of EV's has been seen. This increase is because of the increase in pollution and high oil prices in the market [1]. EV's currently exists in the market in various forms such as hybrid, plug-in hybrid, and solar vehicles. The idea of a solar powered vehicle was first introduced in late 1970's [3]. Solar collectors are placed on the top part of the body of a car to capture photons from sunlight, and the produced energy is stored by using efficient battery systems.

1.1 Solar Car

Electric Vehicles that are powered by solar energy are called solar cars. The basic system structure of the solar car includes the solar array, power point tracker, battery pack, motor controller and a motor that runs the car as shown in Figure 2.

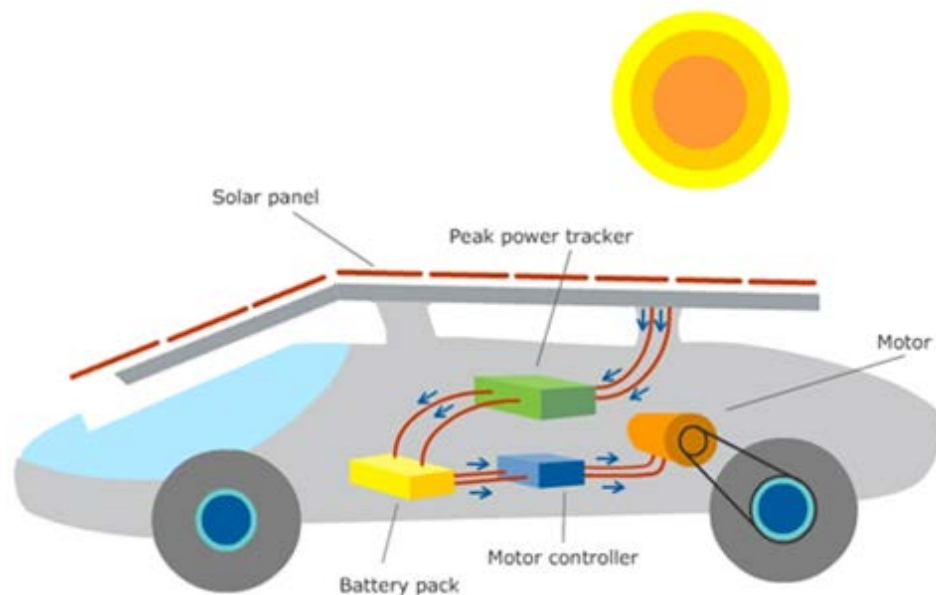


Figure 2: Basic Structure of the Solar Car [4].

Several efforts have been undertaken to push forward the idea of making a solar car more viable and common in the market, including solar car racing competition (world-nuclear.org). The first solar car race was held in 1985 in Switzerland, which led to numerous solar cars races, such as The World Solar Challenge, American Solar Challenge, and South African Solar Challenge (solarcarchallenge.org). From 1987, a racing event named The World Solar Challenge has been held after every two years in Australia (worldsolarchallenge.org).

The World Solar Challenge (WSC) is one of the most important events that promote the development of solar vehicles by organizing the 3000km race (Darwin to Adelaide). The WSC competition has different classes for racing including the Challenger Class, Cruiser Class, and Adventure Class. Flinders Automotive Solar Team (FAST) is competing for the first time within the Cruiser Class of the WSC in 2017. According to the WSC regulation [2.1.1], the Cruiser Class will be judged by its practicality and efficiency.

1.2 Cruiser Class Car

In WSC, 2017, the total allowable silicon cells area for the cruiser class vehicle is 5 square meters [2.4.2] as shown in Table 1. However, the core function of the PV array system is just to enhance the energy storage system of the car. At the time of energy deficiency, the car can be charged from external source as there is no restriction on the size of the batteries and the number of times the batteries being charged [3.18.2]. Therefore, for Flinders Solar Car, the solar array system is designed to work as a supplement for the energy storage system and not the only source of energy the runs the car.

Table 1 Allowable Solar Cells Area for Cruiser Class

PV Cell Chemistry	Allowable Total Cell Area (m²)
Silicon	5.000
Thin film GaAs	4.440
Multi-junctio	3.300

1.3 Goals of Project

The aim of the research in this project is to design, develop and analyse the performance of the Solar Array for the Flinders Solar Car to compete in WSC 2017. As mentioned in introduction, Flinders University has no prior experience in this field. Thus all the components including the solar array and the body of the car will be designed from the ground up.

The Design of a solar car consists of various steps. Initially, a model of the car needs to be finalized then the design of the solar car body, including a design of the solar array needs to be completed. To design an optimal solar collector several things need to be considered such as the PV cells arrangement, the angle of cells, connections and protection of the complete solar array.

The objectives for this project include:

- Research on previous solar array designs and analyse their advantages and possible gaps.
- Develop the optimized solar array for Flinders Solar Car that satisfies the regulations of the World Solar Challenge.
- Design the prototype of the solar array, computation of best angle to receive most of the sun radiations throughout the race.
- Comparatively analyse and test the design under different irradiation levels and different latitudes.
- Select and connect strategy of Maximum Power Point Tracker (MPPT) in order avoid mismatch between the solar arrays.
- Undertake a risk and precautionary analysis of the connection between solar array and batteries of the solar car, as well as develop safety circuitry to prevent high reverse current flow from the battery to the solar system.
- Propose a suitable encapsulation technique for the solar array design.

The above objectives led to the proficient design of the solar array for the Flinders Solar Car. Since the solar radiations are the only source of energy to run the solar car in WSC 2017. Therefore, the most important part is the optimal design of the solar array. Thus,

this project presents a detailed analytical study for the efficient design of the solar array to achieve the best performance of the solar car. As a result of this project an optimal design of the solar array and the most appropriate configurations of the solar arrays will be developed. The developed design will be further tested and compared with other possible configurations to produce maximum power on a limited area of the car.

1.4 Thesis Outline

This thesis presents the comprehensive research on the design of the solar array specifically for the solar car. The thesis comprises of 6 Chapters in total, following this introduction, Chapter 2 will outline the background information of Photovoltaic (PV) cells and working principles of a solar cell. In addition, the literature review in Chapter 2 covers the research conducted on the design of the solar array, the configuration of the solar array and methods to maximise efficiency under continuous environmental changes.

The design of the solar array for the Flinders Solar Car is presented in Chapter 3. This Chapter also explicitly describes the configuration techniques of the solar arrays. Moreover, the proposed design for the Flinders Solar Car is presented in this Chapter. Furthermore, Chapter 3 outlines the selection of optimum Maximum Power Point Tracker (MPPT) and encapsulation techniques. Chapter 4 compares and analyses the algorithms for the design of the PV system. This Chapter also presents the calculations for the produced power during different conditions such as, shaded conditions, change of locations (latitude) with the passage of time.

Chapter 5 concentrates on the limitations in the design of the solar array, including the area restriction of the solar cells by the World Solar Challenge regulation [2.4.2]. Moreover, the compromise on the optimum angle of the solar array because of the aerodynamics of the car. The limitation of reconfiguration of the solar array is also discussed in Chapter 5. Future research to increase the solar power is highlighted in Chapter 6, as well as a conclusion of the overall work, in the form of discussion and analysis, of the project work.

CHAPTER 2

LITERATURE REVIEW

This Chapter discusses the previous research in the area of designing a solar array followed by the background information of solar technology. At the end of this Chapter, a brief summary outlines the results and gaps of the research in the field of solar technology.

2.1 Background

The design of a solar array is the key feature of any solar powered car. During configuration of the solar cells several things need to be considered, such as mismatching of the cells, optimum tilt angle, shading of the cells and temperature effect [5]. This review will discuss the various past literatures on semiconductors that are used in solar cells, environmental and operational issues and achievements in designing the best possible solar array.

A literature review is divided into multiple sections including the background section discusses the past researchers on various substances that can be used as a solar cell. After that, Chapter 2 will talk about matching and mismatching of the solar cells and shading effect also analyse the optimum arrangement of the photovoltaic silicon cells. Weather conditions such as, total irradiation, cloudy weather plays an important role in the efficiency of solar cells [6]. Hence one of the sections will discuss the issues and also provides the solutions for the change in temperature. Finally to maximize the overall output of the solar array; this review will shed some light on the Maximum Power Point Trackers (MPPT), which are pivotal in increasing the efficiency of a photovoltaic cells [7].

The fundamental components of a PV system are shown in Figure 3. It can be seen that MPPT is connected with each solar module which will help to enhance the system efficiency by tracking the maximum power points of the solar cells. After that MPPT's are connected to the batteries to charge and batteries to the load (motor).

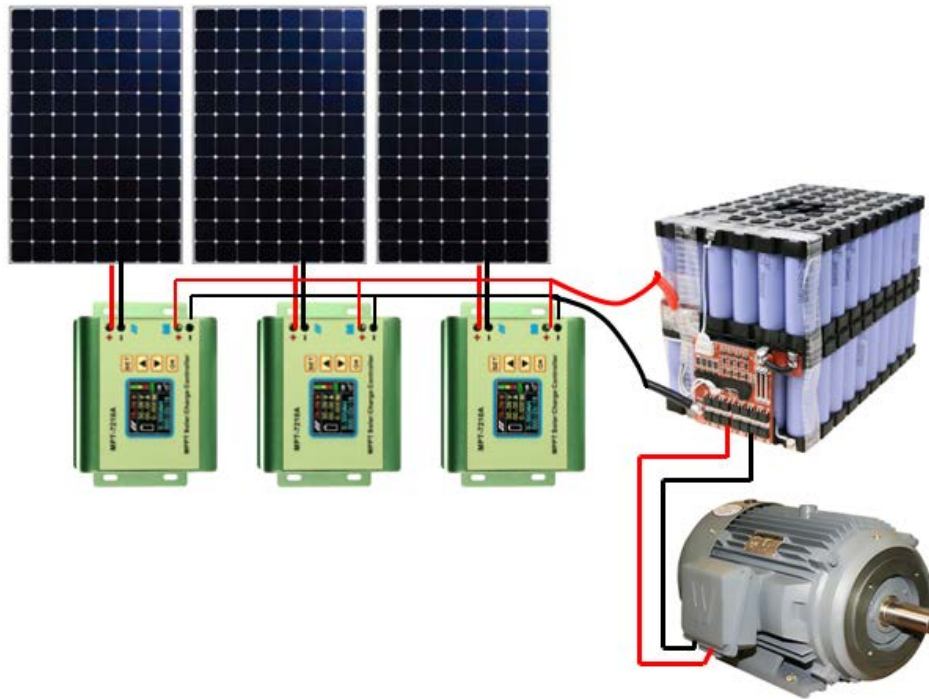


Figure 3: Basic Electrical Diagram of PV Array System

2.2 Solar Technology

Among all the advanced technologies, silicon is the best material to use as a solar cell because of its effectiveness, easy manufacturing, reliability and cost [5].

Following chart in Figure 4 shows the several types of cells which are currently available in the market and few of them are discussed below.

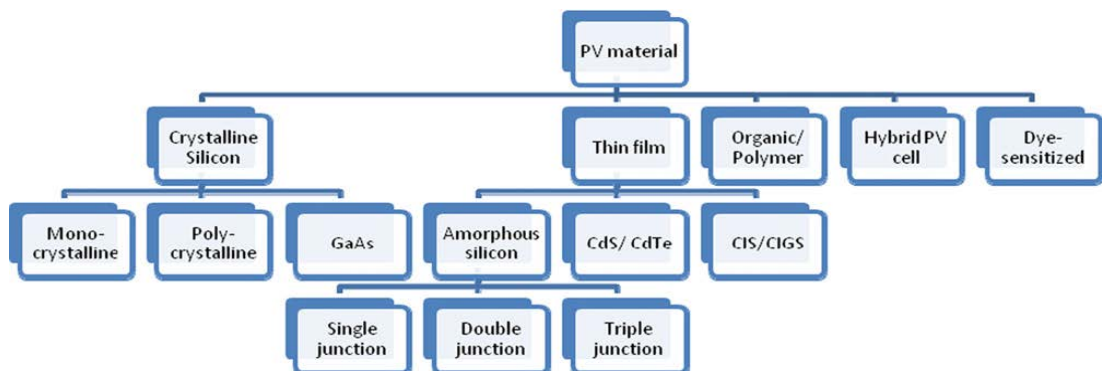


Figure 4: Photovoltaic Materials in Market [5].

Figure 4 shows that photovoltaic cells can be made by several substances. However, the Crystalline silicon and Thin film are two most common types, as well as organic, hybrid and Dye-sensitized may also use to make solar cells [5].

2.2.1 Crystalline Silicon

Among all the semiconductors, crystalline silicon is the best material to make solar cells because of its greater efficiency and easy availability [5]. Crystalline materials are further divided into subcategories including Mono-crystalline, Poly-crystalline, and Gallium Arsenide. Table 2 illustrates the physical structure and compares the crystalline silicon cells in terms of efficiency, cost and reliability.

Table 2 Comparison of Crystalline Silicon Technology

Mono-crystalline	Poly-crystalline	Gallium Arsenide (GaAs)
<p>Manufacturing Mono-crystalline silicon is developed by melting high-purity silicon material in a crucible, most of the time quartz. This process is known as the Czochralski process [5].</p>	<p>Manufacturing Polycrystalline silicon is manufactured by melting and then solidifies melted silicon into orient crystals and sliced into wafers [8].</p>	<p>Manufacturing Gallium and arsenide are compounded to make a semiconductor that has a similar structure to silicon [9].</p>
<p>Efficiency 15% - 21% [10].</p>	<p>Efficiency 13% - 16% [11].</p>	<p>Efficiency 20% - 35% [12].</p>
<p>Cost Mono-crystalline technology is costly but cheaper than GaAs.</p>	<p>Cost Cheapest available crystalline solar cell technology.</p>	<p>Cost Most expensive crystalline solar cell technology.</p>
<p>Typical life 25 years [11].</p>	<p>Typical life 25 years [11].</p>	<p>Typical life 25 – 30 years [13].</p>

2.2.2 Thin Film Cells

In 2013, Tyagi et al. [5] investigated that the amorphous silicon can be used to make thin film solar cells. Also, thin film cells require less materials and small manufacturing process. Among all solar cells, thin film cells are the cheapest solar cells available in the market [5].

a. Amorphous silicon

Amorphous silicon is the least efficient solar cell in the photovoltaic materials. It has non-uniform structure and non-crystalline form of silicon as shown in Figure 5. Due to its disordered structure, its band gap energy is very high i.e. 1.7eV. However, amorphous silicon is less expensive and more flexible than crystalline silicon [5].



Figure 5: Amorphous Silicon Cell [14].

2.2.3 Organic/Polymer Cells

Polymer cell is the new technology and currently in its developing phase. The efficiency of polymer cells has risen from 4% to 6.77% [15]. Polymer solar cells have some advantages regarding its cost-effectiveness, light-weight structure, ultraviolet stability and flexibility. Therefore, it is considered a most promising future technology for the production of clean energy at low cost [16].

2.2.4 Hybrid Cells

Hybrid cells are one of the most efficient technologies on the solar cell market [17]. It is a combination of crystalline and non-crystalline silicon. The two main advantages of hybrid cells are that; it has a relatively simple structure and is easy to implement or non-ideal impact are reduced [17]. A solar cell manufacturing company from Japan, Sanyo claims that they have been developing 21% efficient hybrid solar cell by a combining Hetero-junction and intrinsic thin film layer cells (HIT). Its base is composed of n-type silicon and works as a light absorber [17].

2.3 Shading and Configuration of Cells

This section discusses the term conducted by V.Di Dio et al. in 2009 [18] and C Vimalarani et al. in 2015 [19]. Mismatching represents the inadequate electrical configuration of photovoltaic (PV) cells or asymmetrical arrangement of solar cells in a solar module/array. This mismatching leads to reduce the performance of whole solar array (combination of solar modules); even if only a few of the modules are mismatched. There are two most important factors that cause mismatching; one of them is manufacturing defects, while the second is due to poor encapsulation and non-uniform radiation on the cells [18].

The asymmetrical arrangement of cells under partial shading (shaded by clouds or other means) can cause less output power as required. Hence, the shaded cells heat other cells in order to produce more power and meet the desired output power requirement. This heating of cells reduces performance or may damage (possibly break) cells. Those heated cells are known as Hot-Spot. Studies revealed that minor shading causes a major drop in the power output of the photovoltaic array.

To avoid this drawback, in 2009 V. Di Dio [18] conducted research to find out the effect of shading on the module and overall photovoltaic module performance. As a result, it concluded that “Bypass Diode” is the best remedy to avoid decrease of efficiency due to non-uniform light. It maintains the array voltage and minimizes hot-spots (heating), as wells as damage of other cells due to the connected shaded cell.

Bypass diode should be connected in parallel with a photovoltaic module. When any of the cells is heated due to increasing in its resistance or excessive voltage applied, that particular solar cell resist the flow of current and cause a thermal effect (heating). In that condition, bypass diode starts conduction and reduce overall module resistance. In results, the performance of photovoltaic module increases [18].

By the shading of only one cell, there is a significant decrease in whole array output. Figure 6 represents the output characteristics (I-V curve) of shaded and unshaded modules. It depicts that, with only one shaded cell, the maximum power point decrease from 21.48Watt to 15.44Watt [19].

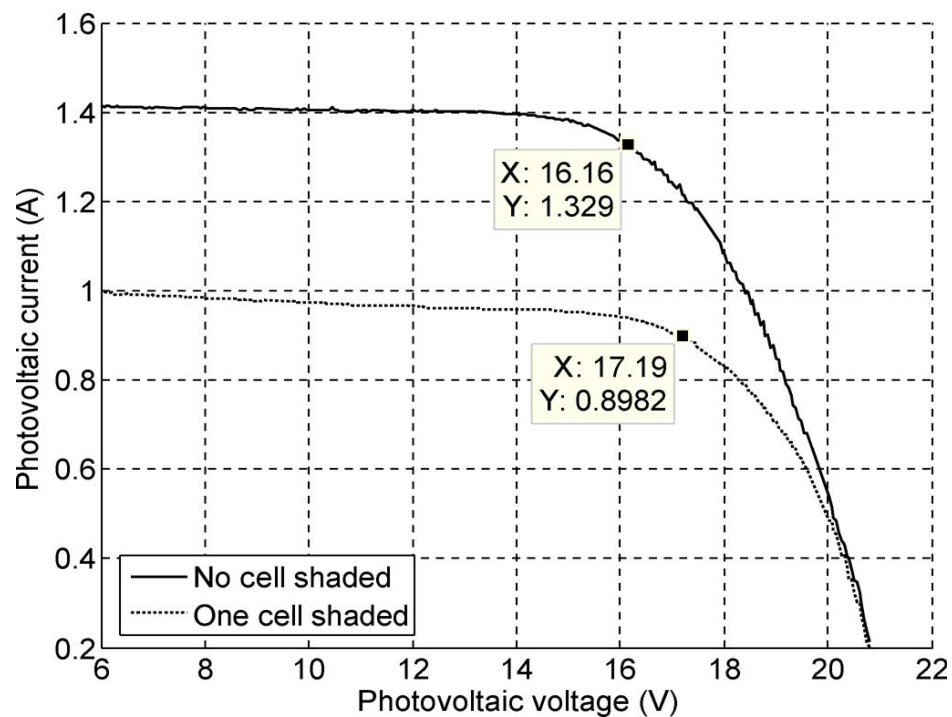


Figure 6: Current and Voltage (I-V) curve [19].

In 2009, V. Di Dio et al. [18] did the experiment with the PV array formed by four modules in a different configuration as well as under different irradiation levels. Considering irradiation of 800W/m^2 with un-shaded module while, the shaded module is equivalent to 500W/m^2 irradiation.

A different arrangement of modules leads to different output under shading condition as seen in Figure 7. The preferred configuration is the configuration that has output curve in black colour. In this configuration, series of two parallel modules are connected

in which one module is shaded as shown in Figure 7. In this case, power losses are minimised and comparable to an unshaded, just 14.3% loss of power. While the curve showed in brown colour has the worst connection of modules where three parallel connected modules are in series with one shaded module. It has power losses as compared to the case of equal radiations is 65.2% [18].

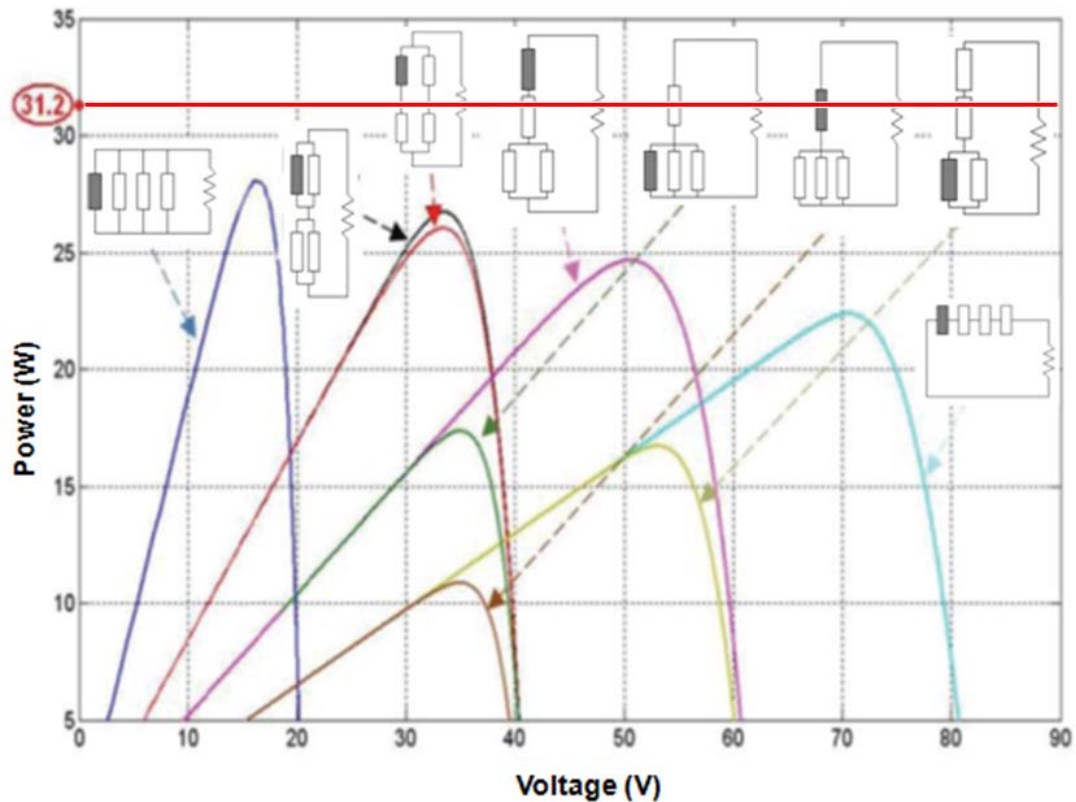


Figure 7: Different Configurations and their Effect on P-V Curve [18].

V. Di Dio et al. [18] also found that the best possible configuration of PV modules is the scheme of all parallel modules, but when one cell shaded, parallel connected cell acts as resistance. Hence, the overall configuration generates a high output current.

To overcome the high output current issue, a series connection of two parallel modules or parallel connection of two series modules can be implemented. This configuration provides a bypass path for current to flow when one cell is shaded as shown in black colour in Figure 7. In result, high current reduces as well as solar modules will give better performance.

2.4 Angles of the Solar Cells

During the daytime, the solar cells should face the sun directly to extract the maximum energy from the sunlight. Therefore, before the designing of the solar array, angle calculations should be necessarily done.

According to regulations [3.26.1] of the World Solar Challenge 2017, all vehicles must stop at designated control stops. Control stops are provided to all team managers by the event organizers. In this section, the brief description of different angles is presented in order to perform calculation of optimum tilt angle at all control stops in Chapter 4 (analysis).

Solar Declination Angle (δ)

The angle between centre of the sun and the plane of equator is known as solar declination angle as shown in Figure 8 and represented by δ . It varies between $\pm 23.5^\circ$ over the year [20]. The solar declination angle can be calculated as:

$$\delta = 23.45 \sin \left[\frac{360}{365} (n - 81) \right] \quad \text{Equation 2- 1}$$

'n' is the number of days of the year.

Altitude Angle (β_N)

The angle between the sun and the local horizon is known as Altitude angle as shown in Figure 8 and expressed by β_N [20]. For solar noon, the formula for altitude angle is shown in Equation 2-2. However, later the relationship was derived to calculate altitude angle for different timings as shown in Equation 2-3[20].

$$\beta_N = 90^\circ - L + \delta \quad \text{Equation 2- 2}$$

$$\sin \beta = \cos L \cos \delta \cos H + \sin L \sin \delta \quad \text{Equation 2- 3}$$

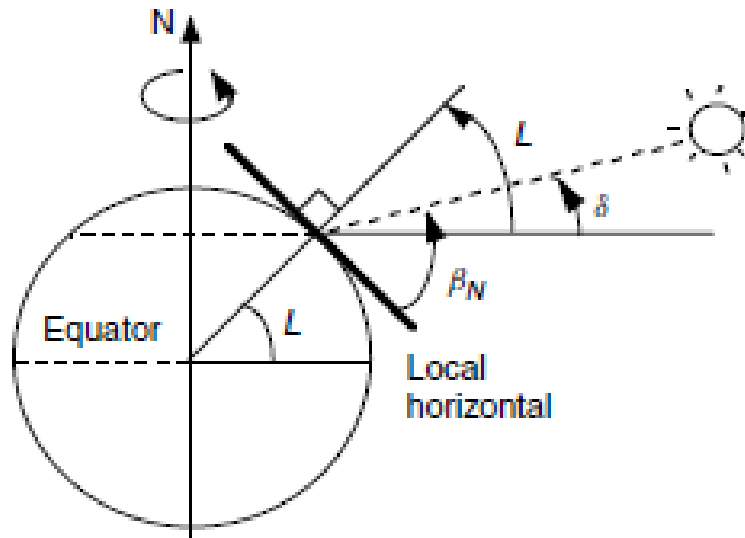


Figure 8: Altitude and Declination Angles [20].

Hour Angle (H)

The hour angle is the number of degrees by which earth moves before the sun is at the line of longitude (local meridian). Hence, the difference between local meridian and the sun's meridian is called Hour angle as shown in Figure 9. Before the sun crosses local meridian (in the morning) Hour angle is taken with positive value while after crossing values occurring with a negative sign [20].

Hour angle can be calculated from Equation 2- 4:

$$H = \frac{15^\circ}{\text{hour}} \times \text{Hours before solar noon} \quad \text{Equation 2- 4}$$

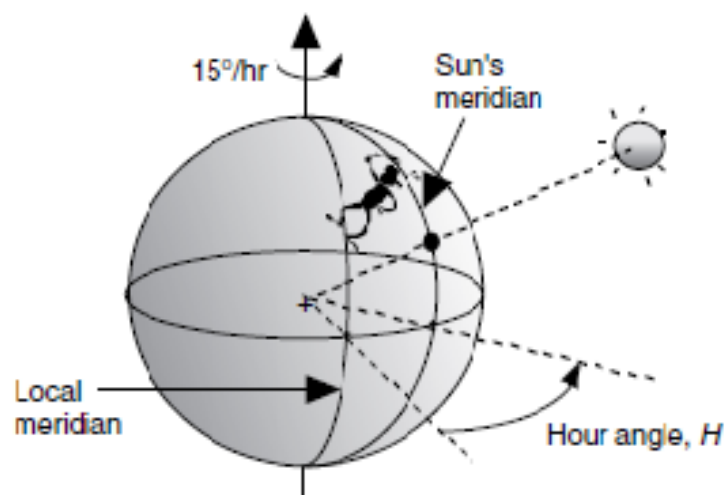


Figure 9: Hour Angle [20].

Declination angle is dependent on a number of the day of the year; however the altitude angle depends on the latitude, day number and most importantly, the time of the day (Hour angle).

The values of 'n' for the first day of the month are given in Table 3.

Table 3: Value of 'n' for the first day of month

January	n = 1	July	n = 182
February	n = 32	August	n = 213
March	n = 60	September	n = 244
April	n = 91	October	n = 274
May	n = 121	November	n = 305
June	n = 152	December	n = 335

In last, to expose the solar array at the maximum irradiation, the optimum tilt angle of the solar array is required. Therefore, an experiment was performed and presented in Chapter 4 using Tindo Karra-250 solar panel to observe the change in power with respect to tilt angles. Later, the optimum tilt angles for the solar array of the Flinders Solar Car are also calculated for all the control stops of the race.

2.5 Temperature Effects

In 2009, Zhangbo et al. [21] presents research that temperature is the most important feature to control the efficiency of solar cell. Due to continuous change in environmental conditions, solar array exhibits a difference of temperature of each solar cell. As the irradiation increase, heat flux that absorbs by solar cell also increases. Since the increase in temperature or heat absorption is the foundation of a significant decrease in output power as shown in Figure 10. It is not just reduction of power but also degrades and reduces the life of the solar cell. Therefore, reliable and controlled cooling system is required [21].

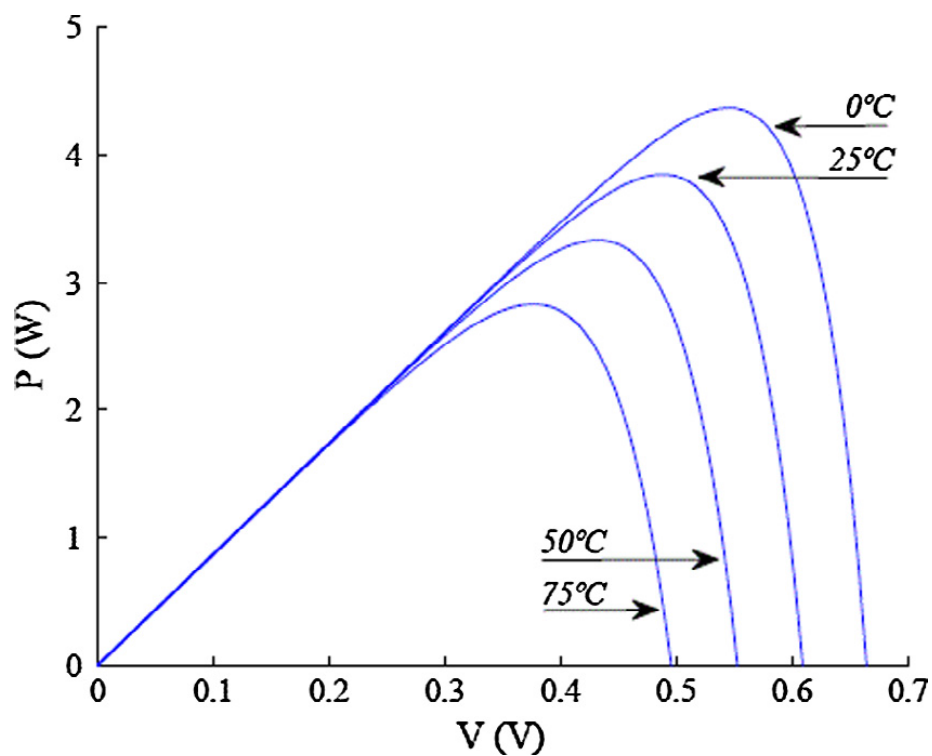


Figure 10 Effect of Temperature on Output Power [22].

In general, there are two types of cooling technologies: active cooling and passive cooling.

a. Active cooling

In this type of cooling, generally a system uses power to cool down the photovoltaic module. However, Zhangbo et al. [21] conducted an experiment and used a heat collector that provides heat energy and worked as heating ventilation for solar module. But, if a heat collector is out of order or non-functional then excessive heat absorbed by solar cells which damage the cells. Therefore, active cooling is a less preferred technique in solar system design [21].

b. Passive cooling

Passive cooling is the mostly preferred technique to be used in solar arrays [21]. In passive cooling, solar cells are cool down by the flow of water or air on the external surface. Air cooling, Water cooling, Heat-pipe cooling, Micro-channel cooling and Fluid jet impingement cooling are the most commonly used passive cooling techniques [21].

2.5.1 Analysis by SABER Modelling

To analyse a solar arrays performance regarding temperature, a modelling program simulation of GPS Block called SABER has been developed by Garcia (1994). This model is implemented by equations described by Rauschenbach (1980). According to this modelling technique; it reveals that:

1.1.1 Hotspot is not effectively minimized by using bypass diodes

2.1.1 Series connections are preferred over parallel because an excess of parallel cells cause high hotspots due to shadowing.

While Garcia (1994) also concludes that SABER modelling technique is for low current ratings while if high current requires parallel connections needed.

2.5.2 Cooling Technique

In 2012, Teo et al. [23] conducted an experiment and presented a cooling technique of solar array, which was based on heat transformation. This technique used external power to operate inlet blower therefore; the technique is an active cooling technique. In this scheme, the efficiency of solar array can be controlled by controlling the temperature via air flow through the air duct [23]. The direct current blower powered by the batteries, extracted air from the surrounding as shown in Figure 11. The extracted air then passed through the control valve, which controls the amount of air and feed the required amount to the air duct. The cool air passed through the air duct underneath the solar array and went out from the outlet as a hot air. This transformation of heat helped to cool down the solar array and significantly increase the efficiency of the PV array.

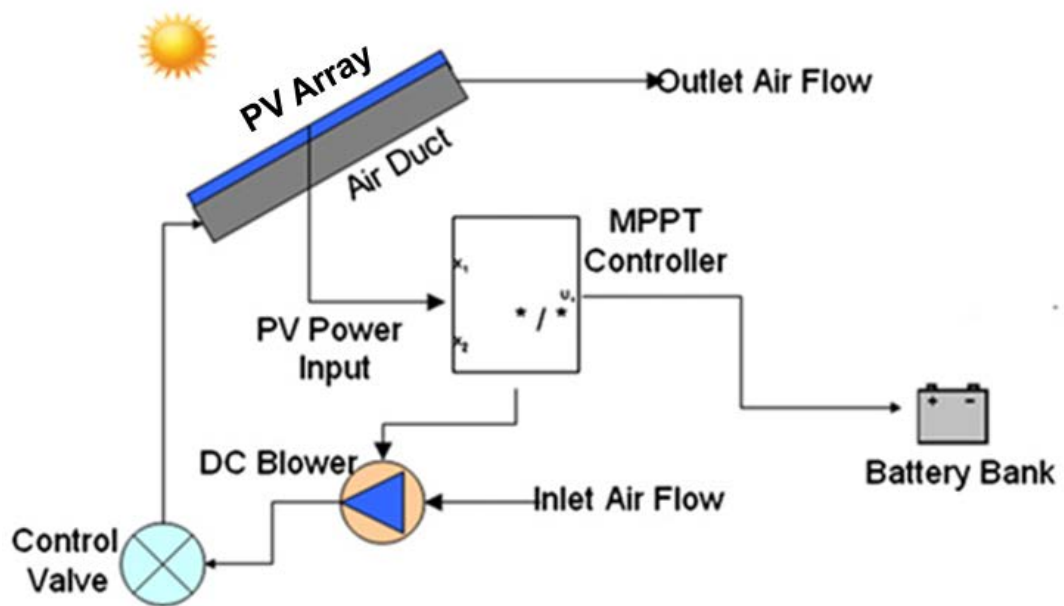


Figure 11 Cooling Technique of a Solar Array [23].

Teo et al. [23] also concluded that solar array temperature is linearly proportional to the irradiation level as shown in Figure 12. With the designed cooling technique, the array temperature increases by 1.4 °C for every 100 W/m² increment in solar irradiation. While, if the array was not cooled down then the temperature increases by 1.8 °C for every 100 W/m².

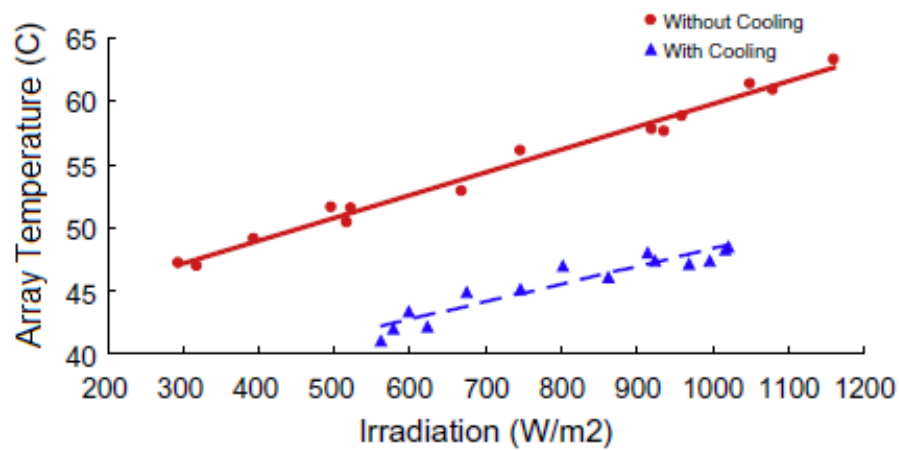


Figure 12: Solar Array Temperature vs. irradiation [23].

2.6 Maximum Power Point Tracker

To increase the overall output power of solar array for a given irradiance, maximum power point tracker (MPPT) is required [24]. However, MPPT reduces the overall efficiency of the system (PV + MPPT). For instance, solar array is 20% efficient and MPPT has 90% efficiency then system efficiency would be 18% ($20\% \times 90\% = 18\%$). During 24 hours of the day, availability of the sunlight is varied and is not constant in most of the cases. It means the output power of the solar array is heavily depends on geographical location (latitude) and weather conditions including sunny weather and cloudy weather. Thus Figure 13 and Figure 14 show the Current-Voltage (I-V) and Power-Voltage (P-V) curves at different irradiance level and operating temperature.

Kharb et al. [24] performed an experiment using an adaptive neuro-fuzzy inference system (ANFIS) based MPPT. A DC-DC boost converter (MPPT) is connected between PV module and load. The Effects of change in irradiation level on maximum power points (MPP) can be seen in Figure 13. As the irradiance level decrease from 900 W/m^2 to 700 W/m^2 , the maximum power point also decreases from MPP1 to MPP2. Furthermore, Figure 13 and Figure 14 shows, at 900 W/m^2 (black curve) the MPP is almost 51W with 17.6V and 2.89Amp. While on MPP2 at 700 W/m^2 (red curve) the overall output power reduces to less than 40W. Hence, the irradiance level proportionally affects short circuit current (I_{SC}) and output power.

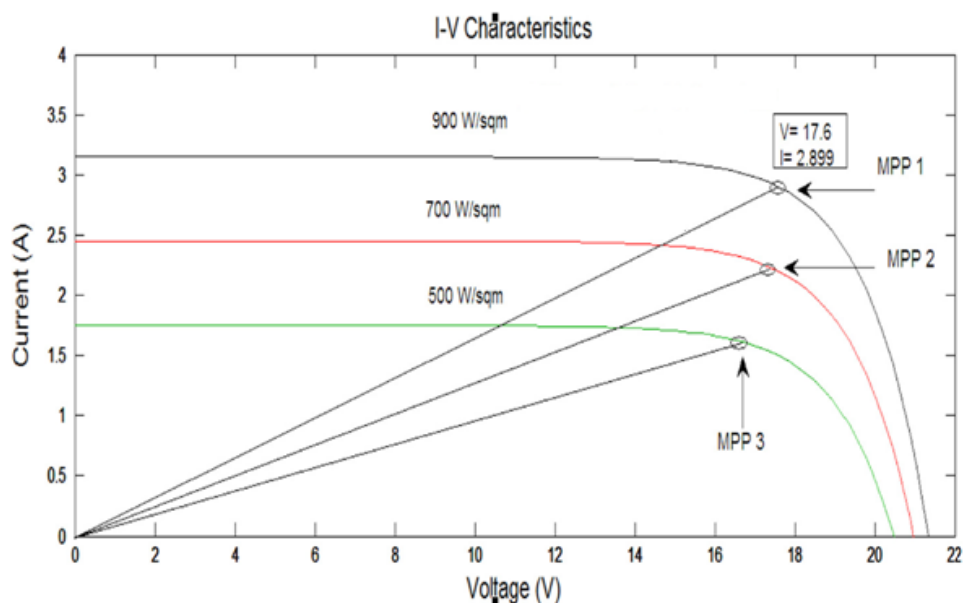


Figure 13: I-V Curve with Different MPP [24].

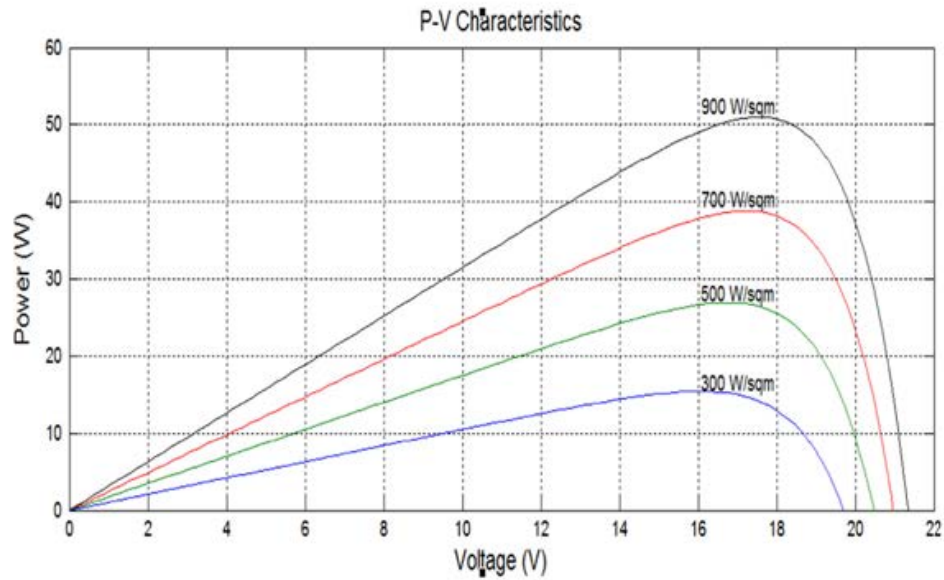


Figure 14: P-V Curve with Different MPP [24].

The principle function of a MPPT is to find the maximum power point of the cell voltage (V_{MPP}) at which PV array should operate to obtain maximum power output (P_{MPP}) with irregular temperature and irradiance level [24]. The improvement with and without using MPPT at an irradiance of $500W/m^2$ on a PV array of $60W$ is shown in Figure 15. It clearly describes the advantage and need of MPPT in PV array system. The power produces without using MPPT shown in red colour i.e. almost $16W$; however, green curve represents the power with MPPT which is $30W$ at an irradiance of $500W/m^2$. As a result, by using MPPT 83% improvement in system output power is observed [24].

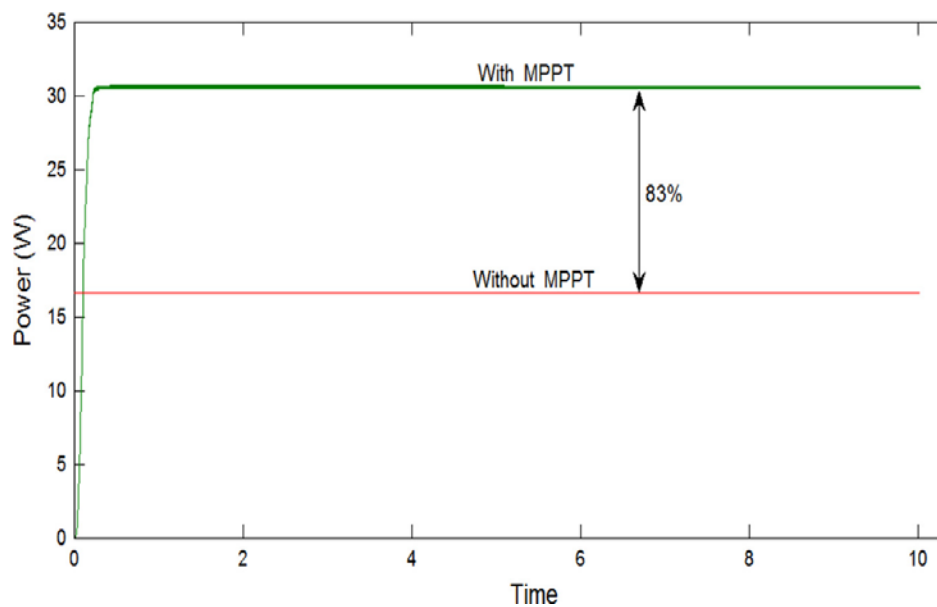


Figure 15: Effect of MPPT [24].

Several algorithm and technique such as Perturb and observe (P&O), Incremental Conductance (IC), Fuzzy Logic Control, Neural network and Ripple Correlation Control (RCC) are developed in recent years for maximum power point tracking [25]. These techniques can respond to change in both irradiance and temperature. They also have the ability to automatically detect the change in the array output power due to shading and aging (getting old) and adjust themselves. According to Esham et al. [25] two MPPT algorithms (P&O and IC) are most commonly follow in designing MPPT and will be further discussed.

2.6.1 Perturb and Observe

Perturb and observe (P&O) algorithm is very simple to design and is the most common MPPT algorithm due to its easiness [26]. In 2002, Hsiao et al. [27] researched that P&O algorithm depends on environmental condition and when circumstances change, current also change from one state to another due to a small threshold. Hence, the overall power output of the solar module changes continuously. Therefore P&O will be less effective when atmospheric conditions changed rapidly.

The operation of the P&O algorithm can be easily understood by the Table 4 and Figure 16. It depicts that, when power increases (change in power is positive) due to perturbation (perturbation is positive) then the perturbation continued (next perturbation is positive). After reaching peak power, the power at the next instant decreases and ultimately perturbation reverses. This method is waving around the peak point unless the steady state is reached. In order to achieve fewer power variations, perturbation size is usually kept very small [28]-[25].

Table 4 : Perturb and Observe (P&O) Procedure [25].

Perturbation	Change in Power	Next Perturbation
Positive	Positive	Positive
Positive	Negative	Negative
Negative	Positive	Negative
Negative	Negative	Positive

The algorithm is developed in such a way that it sets a reference voltage of the solar module with respect to the peak voltage of the module as shown in Figure 16. The operating point of the solar module is moved to the particular voltage level by using PI (Proportional Integral) controller. P&O algorithm unable to track power in a fast varying atmospheric conditions. However, this algorithm is still very popular due to its simplicity [28].

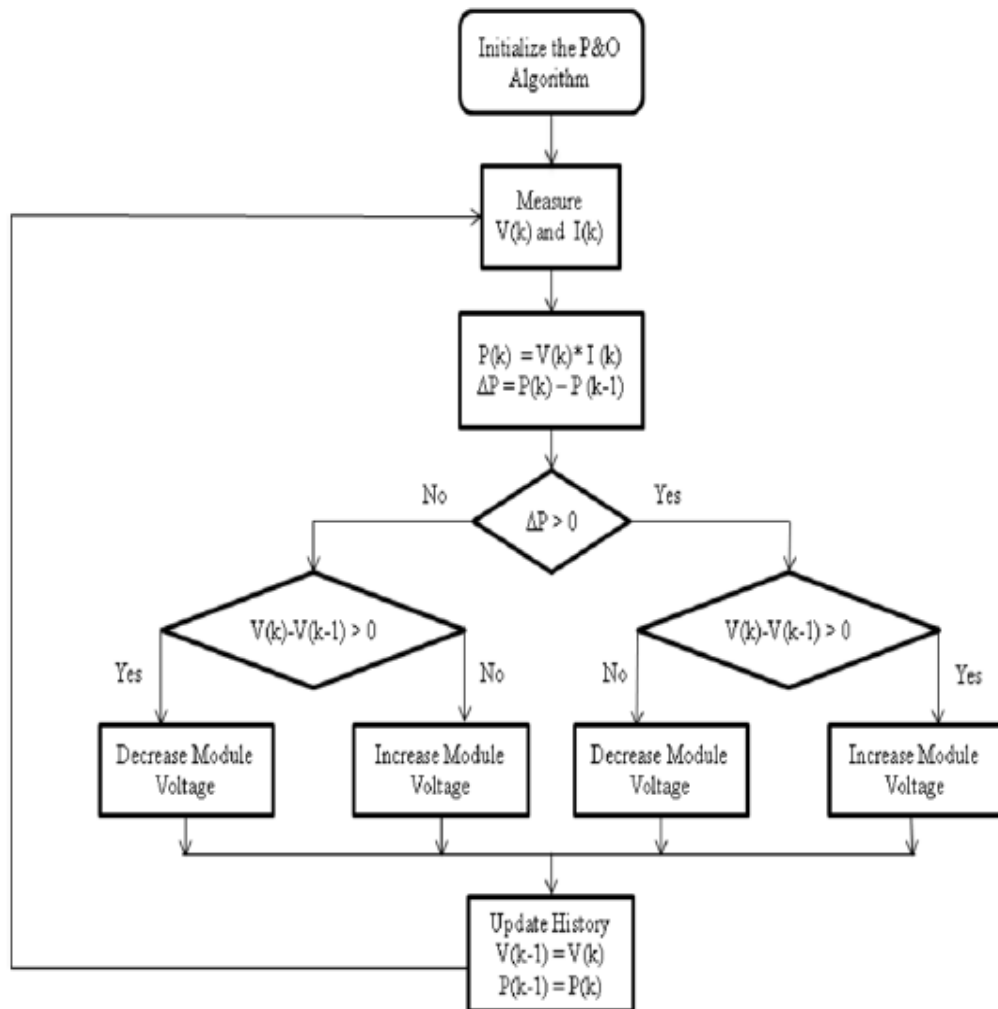


Figure: 16 Perturb and Observe Algorithm [28].

2.6.2 Incremental Conductance

In 1968, Boehringer [29] introduced Incremental Conductance (I&C) method. This method determines whether the maximum power point tracker has reached a maximum point and stops perturbing operating point as well. If P_{MPP} is not met then calculate the relationship between dI/dV and $-I/V$, to find the path in which maximum power point tracker operating point must perturb [25].

Among all other algorithms, incremental conductance is best to implement and gain most of the MPPT. This method will not fail (extremely effective) with the change in atmospheric conditions. As well the, IC method compares the instantaneous immittance of the solar cell with the immittance of the variable quantity. As results, it gains the tracking of the maximum power point and generates output more accurate than Perturb and Observe [25].

2.6.3 Comparison of MPPT Control Algorithm

In 2013, Christopher et al. [28] performed an experiment on 70W PV module to compare the MPPT algorithm. The generalised mathematical model of PV module to test MPPT algorithm developed using MATLAB as shown in Figure 17. However, the specific test models for P&O algorithm and Incremental algorithm are presented in appendix. The study was carried out for Standard Test Conditions (STC) i.e. temperature is 30°C and the irradiation is $1000\text{W}/\text{m}^2$.

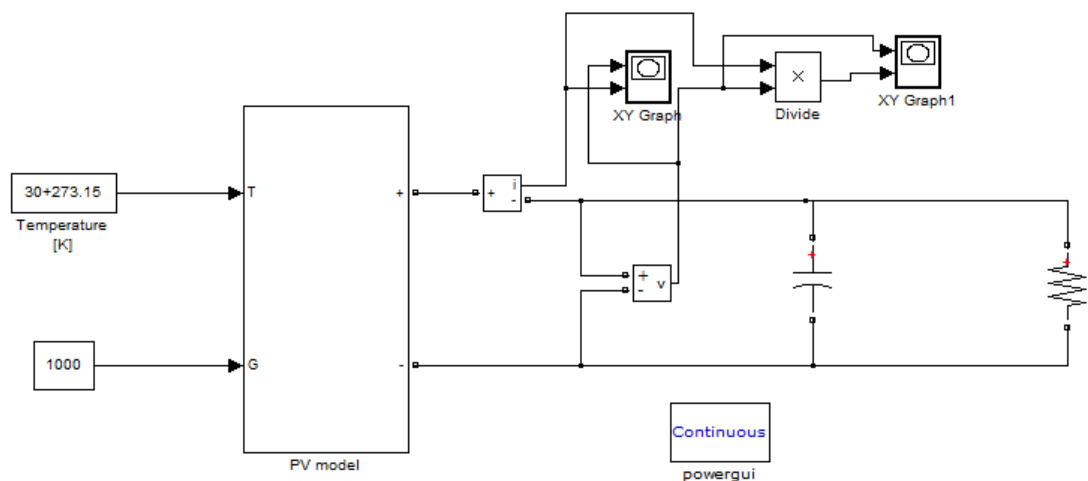


Figure 17: Mathematical Model to Test MPPT Algorithm [28].

The simulation results concluded that Incremental MPPT algorithm is better than P&O algorithm [28] as indicated in Table 5. The response time of P&O is very less as compared to the Incremental algorithm. However, with the change of atmospheric conditions P&O MPPT oscillates close to Maximum Power Point (MPP) while Incremental MPPT finds the MPP perfectly. Therefore, it is proved that Incremental Conductance method gives better performance in changing conditions [28], and best suited algorithm for MPPT of moving objects like solar cars.

Table 5 Comparison of MPPT Algorithms [28]

MPPT Algorithm	Output Current	Output Voltage	Output Power	Time Response	Accuracy
P&O	0.073A	36V	2.6W	0.0175 sec	Less
Incremental	0.087-0.093A	43-47V	3.7-4.7W	0.1 sec	Accurate

2.7 Encapsulation

Photovoltaic modules front surface must protect against all environmental influences whilst allowing light energy to pass through it. Typically, for silicon cells the best transmission of light in the wavelength is 350-1200nm [30]. Also, the reflection from the top surface should be as low as possible to achieve maximum irradiation. The method by which reflection can be reduced and also most commonly use is the anti-reflection coating [30].

This anti-reflection coating is also called encapsulation. An encapsulant acts like an electric insulator between the solar cells and other conductors. Moreover, the encapsulant works as an adhesive component between the top and the rear surface of the photovoltaic (PV) cells. It also remains stable on high ultraviolet (UV) radiation and elevated temperature. Optically transparency and thermal resistivity of the encapsulation will also be discussed in this section as this has a major role on the efficiency of the solar array [31].

High UV radiation and temperature initiates a chemical reaction within encapsulants (mostly oxidation). That is the reason darkens (yellows) the encapsulants over time. This change in colour and degradation due to aging leads to lower the output and efficiency of the photovoltaic cell [32]. Two of the most common encapsulants which are used currently are Ethyl Vinyl Acetate (EVA) and Silicone [33].

The most important consideration for the rear surface of the photovoltaic cell is that the component which will use the rear surface should have very little thermal resistance and must block water or water vapors to enter inside. Tedlar (polymer sheet) are most commonly used in reviewed literature.

In 2009, McIntosh et al. [31] and later in 2015, Lin et al. [33] compares the EVA and Silicone encapsulations. They both found that Silicone encapsulation technique is better than EVA. Silicone can allow shorter wavelength photons to transmit through it comparatively to EVA. Hence EVA blocks some of the shorter wavelengths of the sunlight, so absorption of photons also decreases which in turns decrease in output power or efficiency of a photovoltaic cell as shown in Figure 18.

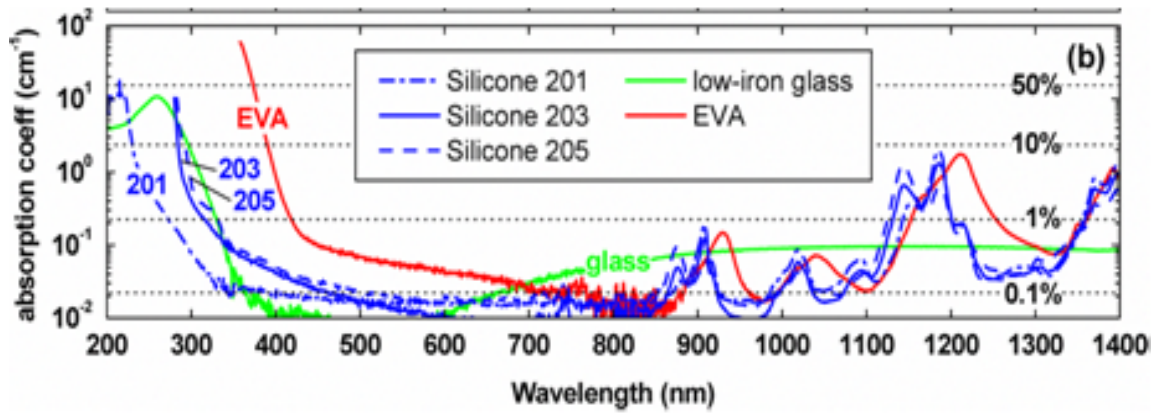


Figure 18: Different Encapsulation Techniques and overall output [31].

Figure 18 compares different types of encapsulation technique and their absorption coefficient. Silicone has multiple varieties such as Silicone 201, 203, 205. Among all components, Silicone 201 has very less absorption of light. However, EVA blocks maximum sunlight and has highest absorption rate.

Current density is also one factor that matters in the efficiency of solar cell. From Figure 19, it can be seen that Silicone in red curve has the higher current density. Therefore, the efficiency of 14.53% whereas EVA encapsulation is 13.26% efficient.

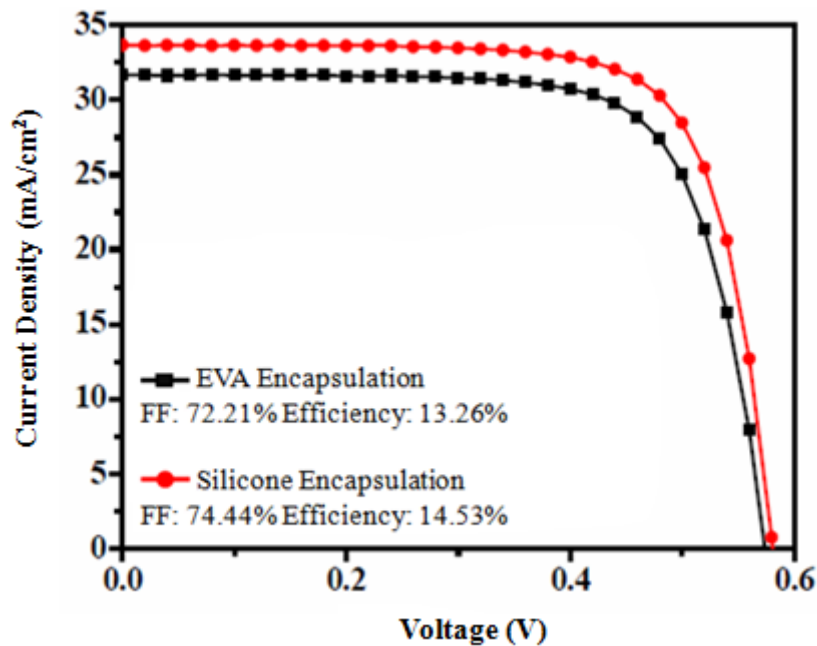


Figure 19: Comparison of EVA and Silicone Encapsulations by I-V Curve [33].

Silicone encapsulation technique is effective, but it requires a rigid material to support [34]. It can also be seen that the amount of silicon required for coating will increase the overall weight of the array. For the vehicle which is going to participate in any challenge must have a low weight to achieve good aerodynamics. Besides the optical clarity of silicone, when it placed under mechanical stress it would break. Furthermore, the cost of silicone encapsulants is another setback [34].

Different tests conducted to investigate the performance of cell with diverse encapsulations. Efficiency, thermal and mechanical testing proved that EVA is the best-suited encapsulant for moving the vehicle [34]. In 2009, Zhao et al. [30] present an approach; in which it is achievable to perform EVA encapsulation and then apply a SiO₂ antireflection coating on top to capture maximum light energy. Total encapsulation losses are about 4%. 1% is optical losses due to anti-reflection coating, 1% calibration differences 0.5% spectral mismatching and 1.5% losses due to the glass surface.

In 1994, Gee et al. [35] investigated the use of multi-layers films for photovoltaic cells encapsulation with EVA. Spectroscopic investigations on PET (polyethylene terephthalate) revealed that due to aging and damp heat test it will lose its efficiency however PVF (polyvinyl fluoride) produce excellent damp heat stability. Thermo analytical investigations and mechanical stress investigations also performed on both types of films as well as on PVDF (poly-vinylidene fluoride). Thermo-analysis results give the edge to PET and PVF film over PVDF. According to requirements in different areas, priorities change to choose the best film that suits conditions on that specific location.

Gee et al. [35] also showed that textured surfaces could also give good results regarding reduction in reflection through the front surface. Reduction in reflection is achieved by confinement of the rays by high refractive index with a material having low refractive index due to internal reflection. This phenomenon of capturing more rays by reducing reflection is also known as optical confinement [35]. An overall result gives maximum absorption of photons and better output. A dicing saw to prepare texture on cells also proposed in research that having high cutting speed than traditional texturing tools [35].

2.8 Design Techniques of Previous Solar Car Teams

The World Solar Challenge (WSC) provides an opportunity to different industries and research groups to design and compete in solar car race. In 2008, students at the University of Kentucky designed a solar car named as Gato Del Sol III. With the designed three wheels solar car, Gato Del Sol III participated in American Solar Challenge 2008 and ranked as eleventh among fourteen teams (americansolarchallenge.org). They used 480 mono-crystalline silicon cells to design the solar array for the solar car which will be judged on its speed [36]. The designed solar array produced power of 1.2kW on 6m² area of the car. The solar cells are encapsulated using XEPS rigid insulation foam and glued on the body of the car as shown in Figure 20 [36]. A brief summary of technical attributes of Gato Del Sol car is given in Table 6.

Table 6 Electrical Specification of Gato Del Sol car

	Gato Del Sol I	Gato Del Sol II	Gato Del Sol III
Solar Array	Polycrystalline cells	Mono-crystalline cells	Mono-crystalline cells
Peak Power	800W	1000W	1200W
Battery	Lead Acid	Nickel Metal Hydride	Lithium Polymer
Weight	449.05 kg	317.51 kg	301.64 kg
Encapsulation	Fibre glass	XEPS rigid foam	XEPS rigid foam
Power Point Tracker	Off the shelf	Off the shelf	Drivetek

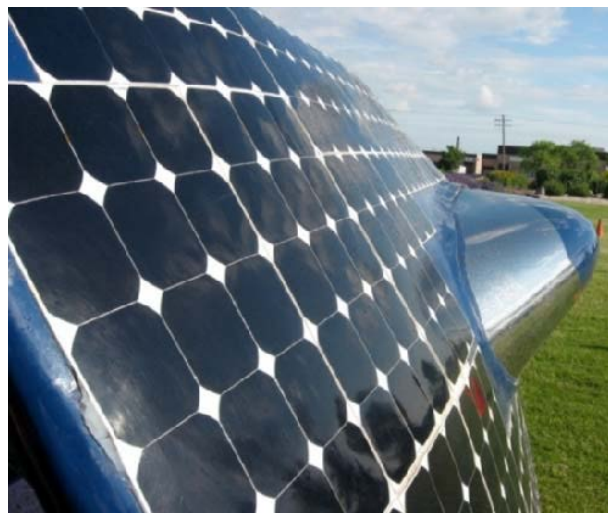


Figure 20 Front Side View of Solar Array of Gato Del Sol Car

Similarly, in 2015, the University of Eindhoven designed a solar car named “Stella Lux” as shown in Figure 21. Eindhoven is the winner of WSC, 2015 in the category of cruiser class. University of Eindhoven completed the distance of 3028.2 km from Darwin to Adelaide within 40hrs 14mins. In a private conversation, the solar array designer of University of Eindhoven said that we used 381 Sunpower mono-crystalline silicon solar cells to build the solar array. In addition, the solar array was encapsulated in flexible plastic material by a German company Gochermann. A brief summary of electrical specification of the solar array is given in Table 7.

Table 7 Electrical Specification of Stella Lux Solar Car

	Stella Lux Solar Car
Solar Array	Mono-crystalline cells by Sunpower, America
Peak Power	1500 W
Encapsulation	Gochermann
Battery	Lithium-Ion
Battery Capacity	15 kWh
Power Point Tracker	Off the shelf



Figure 21: Eindhoven University Solar Car [37].

Likewise, in 2015, students of University of Kogakuin, Japan developed a solar car named “owl” as shown in Figure 22, which was the runner-up in WSC, 2015. Kogakuin solar car team told us in a private chat that they used 391 Sunpower mono-crystalline silicon solar cells. They reached before the Eindhoven solar car and completed the distance of 3028.2 km within 37hrs 52mins (worldsolarchallenge.org). However, they lost marks in the practicality of the car and acquired second position in cruiser class. The specification of the solar array is shown in Table 8.

Table 8 Electrical Specification of Aurora 101 Solar Car

	Kogakuin Solar Car
Solar Array	Mono-crystalline cells by Sunpower, America
Cells efficiency	21%
Peak Power	1100 W
Encapsulation	Gochermann
Battery	Lithium-Ion
Power Point Tracker	Off the shelf



Figure 22: Kogakuin University Solar Car [38].

2.9 Summary

The design fundamentals for a solar array have been reviewed in Chapter 2. The first section discussed the major types of semiconductors that can be used for a solar cell and their advantages and disadvantages. Furthermore, second and third sections have presented few design techniques including configuration of the cells and effect of environmental irregularities. Series connections of the solar cells and parallel connected solar array have been established as the optimized technique to design photovoltaic (PV) system. Moreover, the previous research proposed a bypass diode as a key component that can maintain PV array output under shading conditions.

In the last part of the literature review (Chapter 2), the previous researchers have been examined to increase the efficiency of the solar cells. Maximum Power Point Tracker (MPPT) was found as an essential component that boosts the efficiency of the solar system. MPPT keep tracks on the maximum power point of the solar cell and delivers the maximum power to the load. Furthermore, the Incremental Conductance-based MPPT was suggested for the moving vehicles because it gives the best result with a change in weather conditions.

During the review of past research, the different types of encapsulation or coating of solar cells were also examined for the protection of the solar cells. Among all encapsulation techniques, Silicone encapsulation has been found as the best encapsulant which allows maximum solar irradiation for the solar cell and prevents UV rays of the sunlight from passing through it.

This project is based on the design of the solar array for the Flinders Solar Car. During the race, the car will be running continuously and changes its directions, therefore the optimum angles of the sun for the solar array will also change. While the research reviewed throughout the literature is for the fixed solar array. Therefore a gap in research has been observed regarding the optimum solar array angles for the moving car. Moreover, a gap in research is also observed regarding the isolation of a solar array from other electrical components and prevention for a possible high reverse current flow. However, the mentioned gaps will be under consideration during the design of the solar array for the Flinders Solar Car.

CHAPTER 3

SOLAR ARRAY MODELLING

The prototype of the solar array for the Flinders Solar Car will be modelled in this Chapter, followed by the understanding of a solar cell model and effects of the potential resistances. This Chapter also presents the final solar array configuration for the Flinders Solar Car.

3.1 Solar Cell Model

The simplest and ideal model of the solar cell is given in Figure 23. The circuit contains a photon current source (I_{PH}) and a diode. The photon current (I_{PH}) is produced by the radiations of the sunlight, and this phenomenon is known as the photovoltaic effect. I_{PH} depends on the intensity of the sunlight, quality of the solar cells and weather conditions.

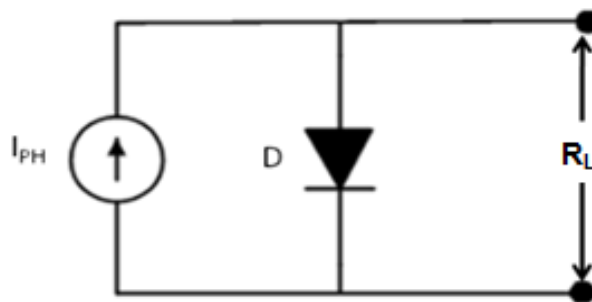


Figure 23: Single Diode Ideal model for a Solar cell [18].

Before the design of the solar array for the Flinders Solar Car, following key characteristics of a photovoltaic cell must be known.

3.1.1 Short Circuit Current (I_{SC})

The short circuit current is the maximum amount of current that a cell can allow to conduct through it. In practical conditions, it completely depends on incident sunlight. Hence, from Figure 23 the I_{SC} is also called photon current (I_{PH}) [20].

3.1.2 Open Circuit Voltage (VOC)

Open circuit voltage is directly proportional to the incident sunlight. But due to increasing the temperature, the saturation current increases. Ultimately, the saturation current decreases the open circuit voltage of a PV cell or increase in temperature decreases V_{oc} [20].

3.1.3 Fill Factor (F.F)

Fill Factor is the ratio of power at the maximum power point to the product of open circuit voltage (V_{oc}) and short-circuit current (I_{sc}) as seen in equation (3.1) [20].

$$F.F = \frac{(V_{MPP} \times I_{MPP})}{(V_{oc} \times I_{sc})} \quad (3.1)$$

Figure 24 outline the parameters which are required to calculate the Fill Factor of a solar cell. The power at maximum power point (P_{MPP}), I_{MPP} , V_{MPP} , V_{oc} and I_{sc} are shown respectively. Hence the Fill Factor is 0.76 ($220/288$) using equation (3.1). As Fill Factor is the ratio of two quantities so, it has no unit.

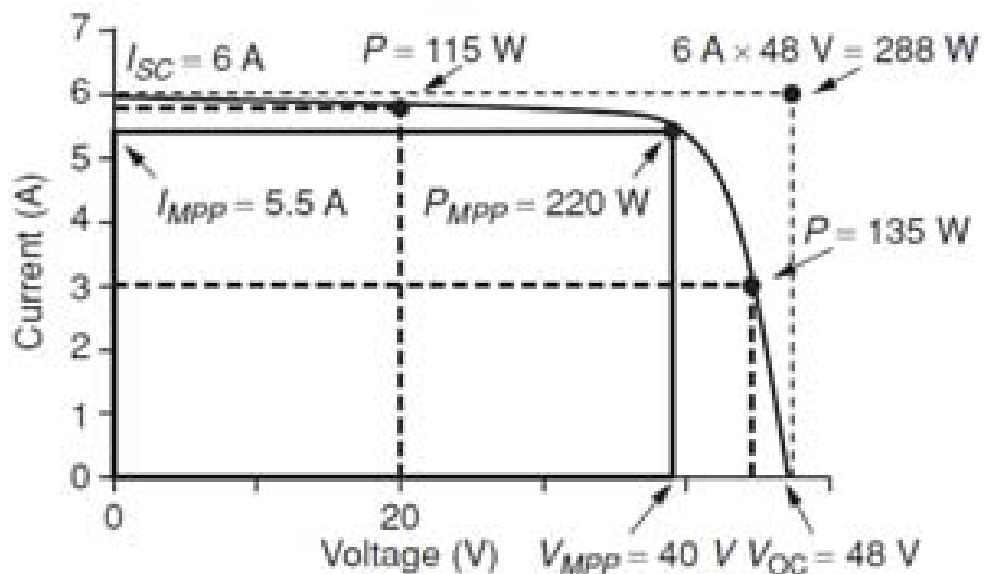


Figure 24: I-V Curve with maximum power points [39]

3.1.4 Maximum Output Power (P_{max})

The maximum amount of power that can be delivered to the load is known as maximum output power. In Solar technology, it is considered as a performance factor of any solar cell/ module. It depends on two parameters open circuited voltage and Fill Factor.

$$P_{max} = F.F \times V_{oc} \quad (3.2)$$

3.1.5 Efficiency (η_{max})

In a PV cell, the ratio of incident sunlight to the output power is known as the efficiency of the PV system. Since the efficiency is the ratio of two quantities, it has unit of % traditionally.

$$\eta = \frac{F.F \times (V_{oc} \times I_{sc})}{P_{in}}$$
$$\eta = \frac{V_{MPP} \times I_{MPP}}{P_{in}} \quad (3.3)$$

Equation (3.3) shows that the efficiency of the solar cells is directly proportional to the maximum power point values of the incident light.

3.2 Software Testing

MATLAB is used as the core software in this project to simulate and analyse the solar array design. Later the results of designed prototype solar array are also analysed mathematically. To start with, Figure 25 shows the Simulink model which is designed to analyse the ideal responses of a 0.8V solar cell. Figure 26 shows the ideal power vs. voltage (P-V) curve of the modelled solar cell. The power increases linearly and at a certain point power starts decreasing, this point is called maximum power point (P_{MPP}) indicated in Figure 26.

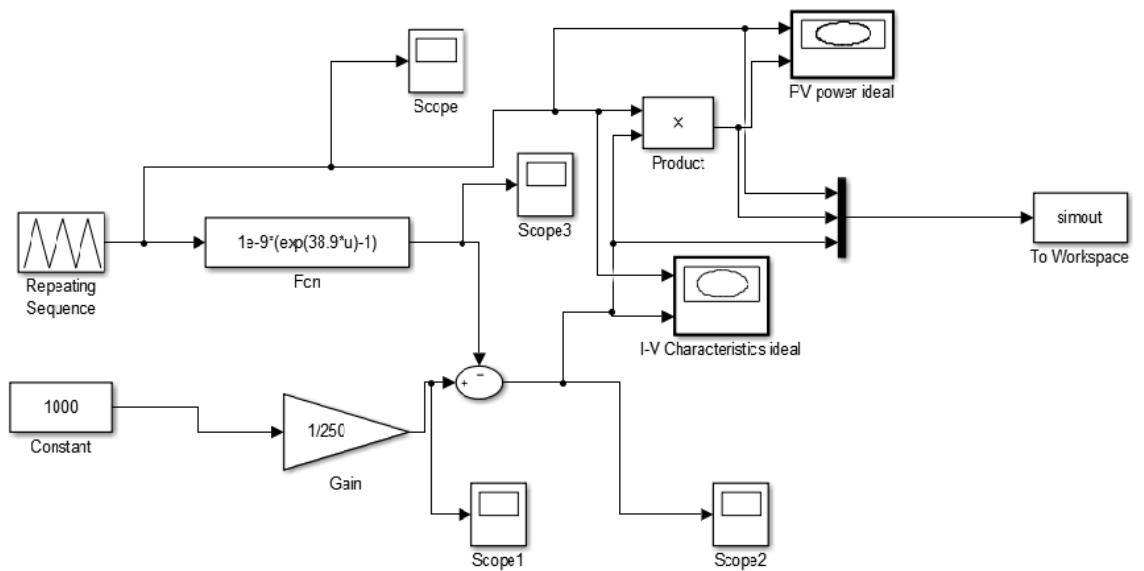


Figure 25: MATLAB Simulation for P-V and I-V Curve

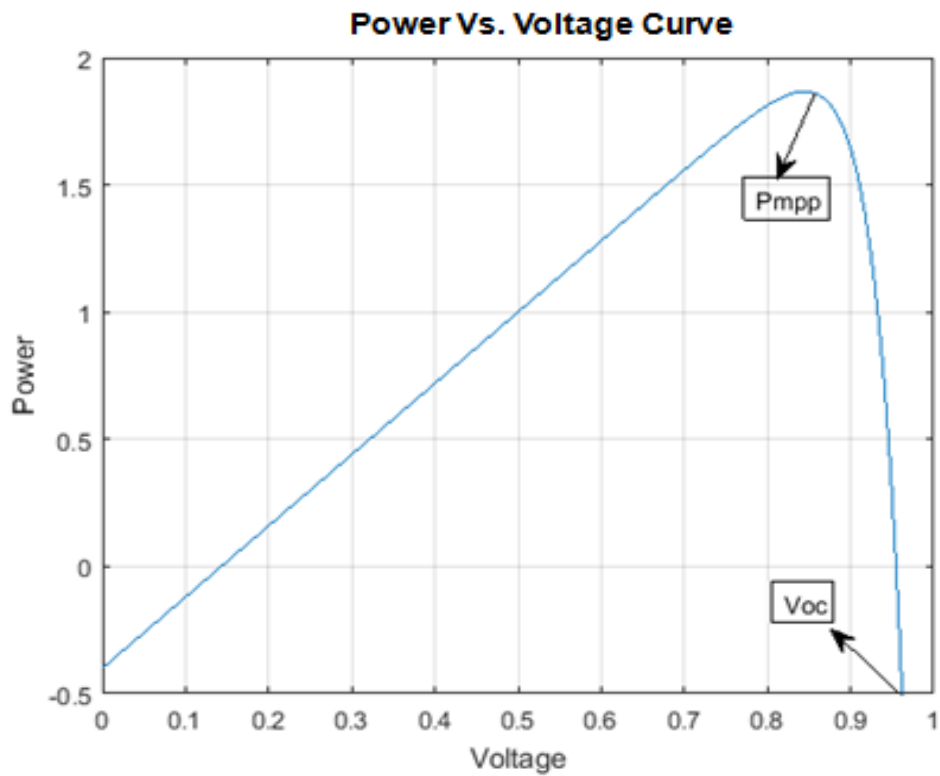


Figure 26: Power-Voltage (P-V) Curve.

Similarly, Figure 27 represents the ideal current-voltage (IV) curve of a modelled solar cell. The best performance of the solar array is achieved when all the solar cells are works at the maximum power point.

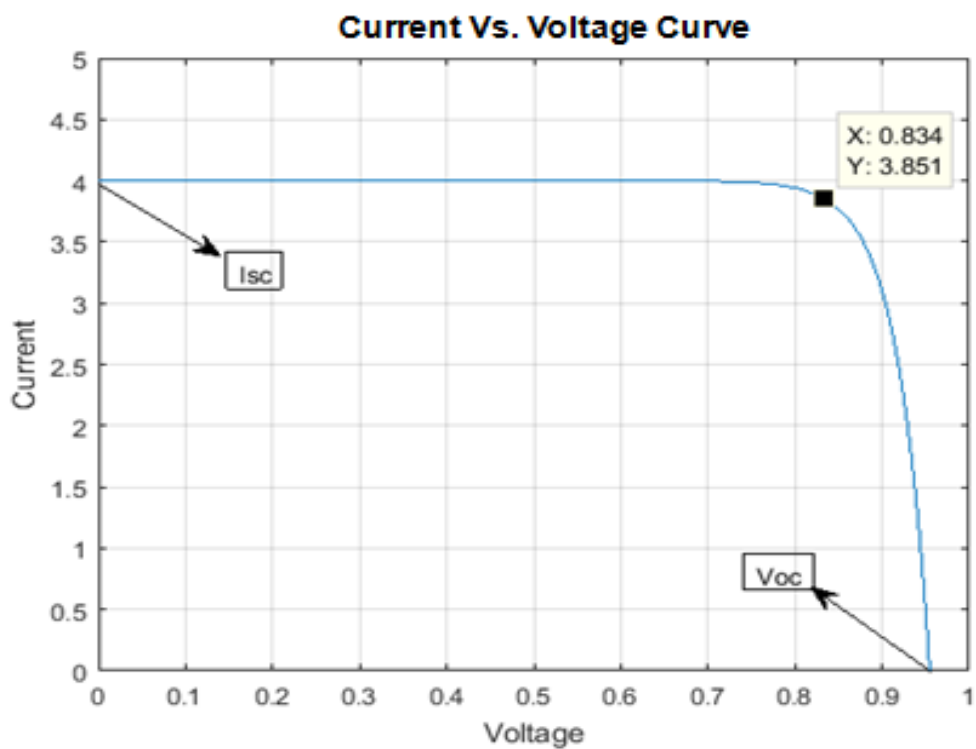


Figure 27: Current-Voltage (I-V) Curve.

3.3 Resistance Effect

In shading condition, a shaded solar cell acts as a virtual resistance to other cells in the solar array. The value of resistance can minimize or maximize the amount of power delivered. The solar cells which are connected in series are acts like series resistance. Conversely, the parallel connected solar cells act as parallel resistance. Figure 28 shows the one-diode model connected in series and parallel (shunt) resistance. Both types of resistances reduce the amount of power delivered to the load as shown in Figure 29.

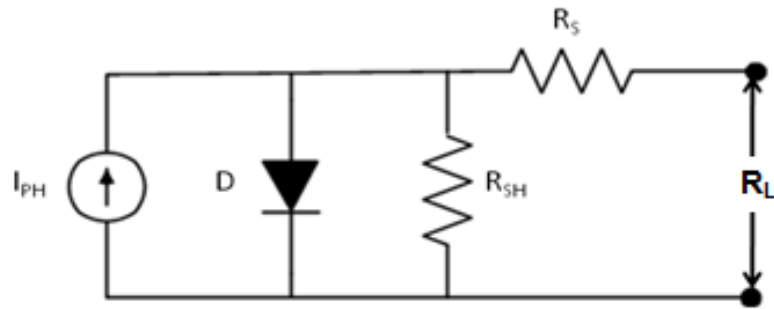


Figure 28: Single Diode Solar Cell Model with Parasitic Elements [39].

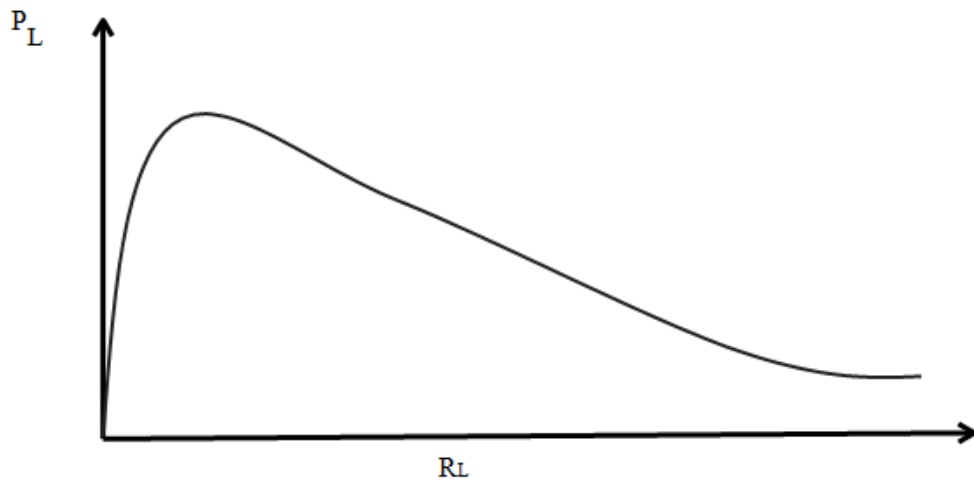


Figure 29: Power vs Load Resistance Curve [39].

3.3.1 Series Resistance (R_s)

Series resistance appears in the solar cell due to following reasons.

- a) Metal contact and silicon contact also acts as R_s .
- b) Internal diode resistance due to improper manufacturing.

3.3.2 Series Resistance R_s on I-V Characteristics Curve

Using the Simulink model shown in Figure 25, the parametric analysis is carried out by varying the series resistance R_s from 0.05Ω to 0.5Ω and the load resistance R_L is varied between 0.01Ω to 3Ω . In results, Figure 30 shows the effect on I-V curve with the increase in series resistance. The red curve is the original curve with 0.05Ω resistance while blue curve is the deviated curve because of increase in resistance. Hence, the maximum power point is reduced significantly.

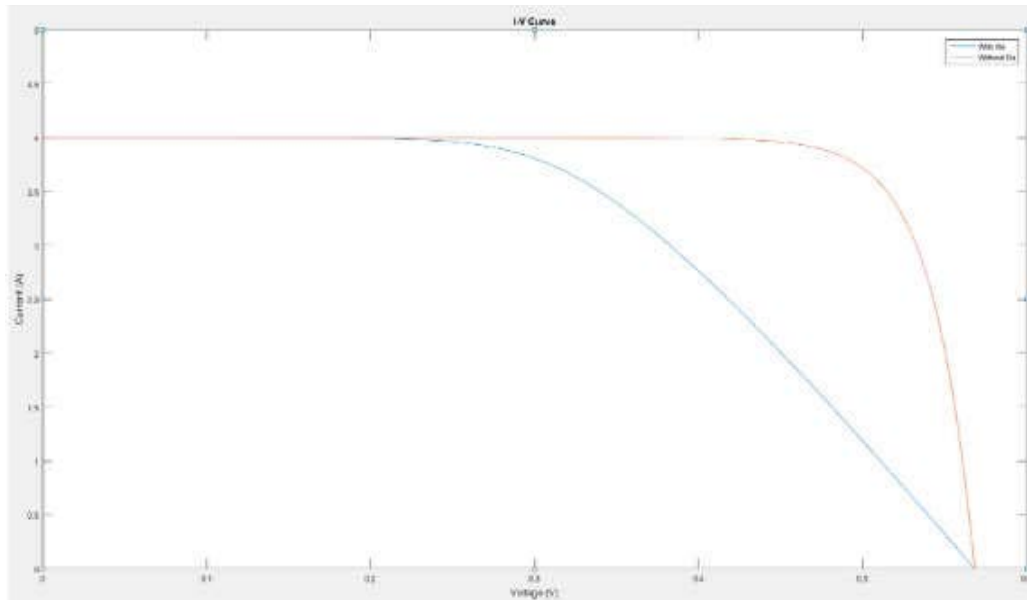


Figure 30: I-V Characteristics with Varying Series Resistance at Fixed Illumination.

3.3.3 Shunt Resistance

Following are the reasons of generating shunt resistance effect in the solar cell.

- a) Inadequate cell design or poor manufacturing
- b) The flow of leakage current between different polarity contacts.

3.3.4 Shunt Resistance R_{SH} on I-V Characteristics Curve

Similarly, a parametric analysis is carried out by varying the shunt resistance R_{SH} from 0.1Ω to 10Ω , and the load resistance R_L is varied between 0.01Ω to 3Ω . Figure 31 illustrates that there is not a big change in the response of a solar cell due to increasing in parallel (shunt) resistance. However, the original output curve deviates and the maximum power point (P_{MPP}) is reduced.

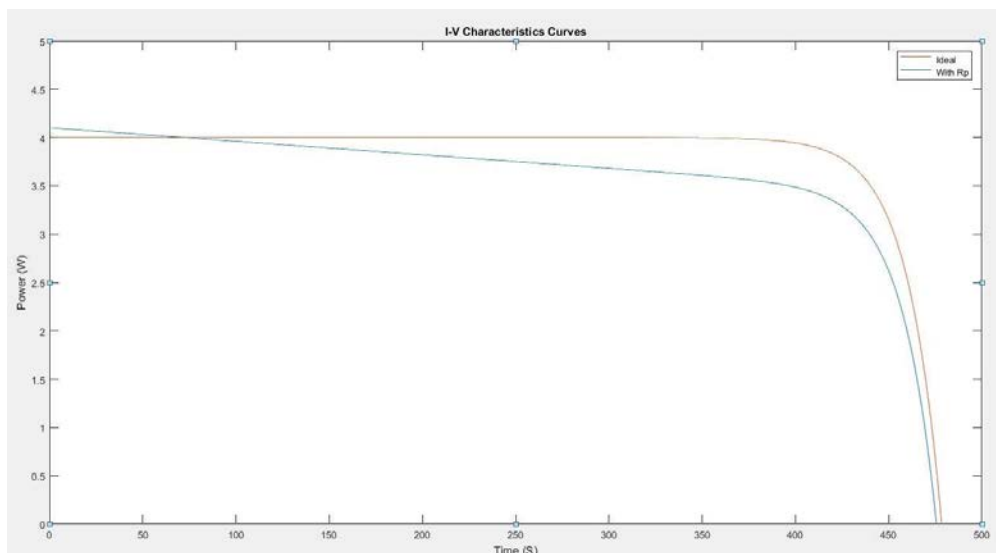


Figure 31: I-V Characteristics with Varying Shunt Resistance at Fixed Illumination.

3.3.5 Results and Discussion

The above simulations result helps to determine the parameters for the optimal design of the solar array for the Flinders Solar Car. The best performance solar array should have R_S equals to zero or minimum as much as possible, while the shunt resistance (R_{SH}) must be equal between parallel connected solar arrays, to allow equal current flow in all solar arrays

3.4 Proposed Solar Array Design

The mono-crystalline silicon solar cells are selected to design the solar array for the Flinders Solar Car, as these cells provides best efficiency at cheap prices. On the other hand, thin film technology (Gallium arsenide cells) has higher efficiency than silicon, but they are very expensive. Hence, there is a trade-off between quality and cost due to this silicon technology is preferred for electric vehicles.

3.4.1 General Design

The fundamental architecture of a photovoltaic (PV) system on the solar car is presented in Figure 32. The PV system is usually divided into number of groups/sections of the solar arrays that are mounted on the roof, hood, and doors of the car depending upon the total area available for the solar cells on the car. According to World Solar Challenge regulation [2.4.2], cruiser class vehicles are allowed to use 5m² area for the silicon solar cells. The general deigned solar array shown in Figure 32 gives an overview and covers the complete roof, hood and doors of the car. All the three solar arrays are connected in series with the one MPPT. Hence, the complete PV system in series and connected to the battery pack as shown in Figure 32.

The general design is considered as less efficient design because of series solar array connection. At the moment, when one solar array is shaded then overall power output is reduced as discussed earlier in Section 2.3.

Therefore, the design configuration of the solar array for the Flinders Solar Car is different to the design shown in Figure 32. Although, the solar array is divided into three sections while separate MPPT is connected to each solar array in series. The MPPT connected with each solar array maintains the similar output from the solar arrays that connected in parallel and terminated to the battery packages will be discuss under Section 3.5.

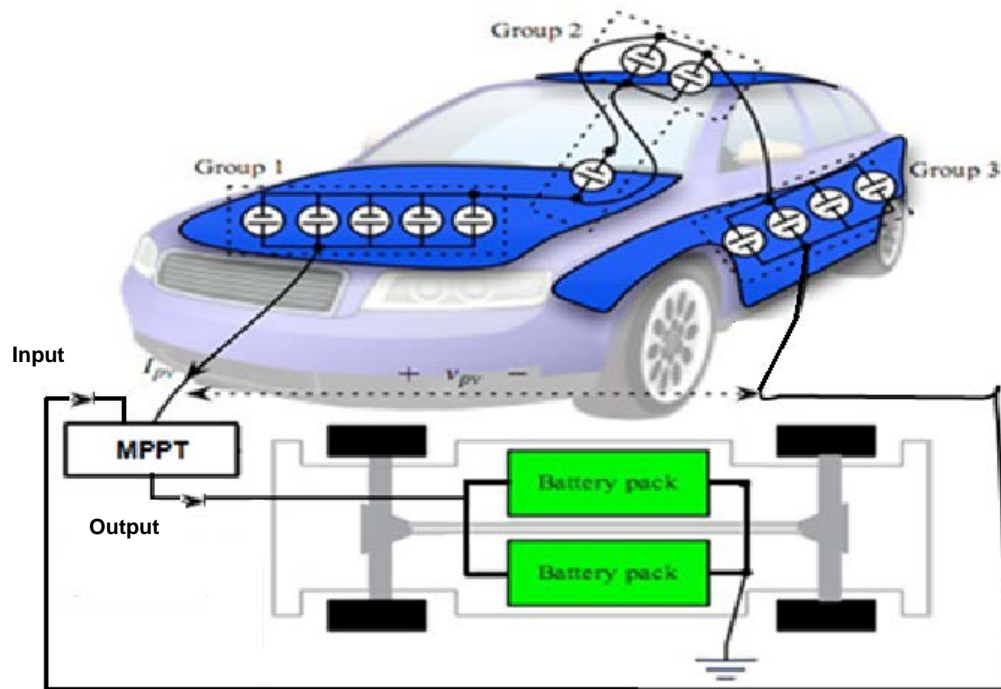


Figure 32: System diagram of a PV system on solar car [40].

3.4.2 Partial Shading

Sometimes the PV cells connected in the solar array are unable to receive uniform sunlight. Mostly for the moving object (cars) irradiance level change continuously and few cells in the array are partially shaded due to moving vehicles, clouds, buildings, change in directions of the vehicle, etc. Change in direction results in a change in incident angle of sunlight. The partially shaded cells act as a resistance for all the other solar cells connected in the solar array as discussed in Section 3.3. As a result, the partially shaded solar cells deviate the maximum power point of the complete solar array. Thus the overall produced power of the PV array decreases.

For the mentioned reason the bypass diodes are connected in parallel with each module of the solar array as shown in Figure 33. The diodes are connected in reverse direction as compared to the flow of solar module current. Therefore, it will conduct when a particular module is shaded, and the resistance of the module is greater than the barrier potential of the bypass diode. This connection provides an alternative path for the current to flow and reduced the effect of shading.

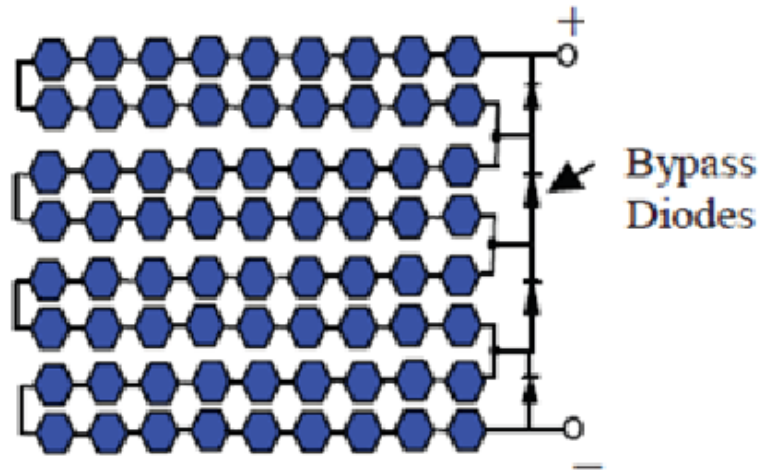


Figure 33: Influence of Bypass diode [40].

The impact of bypass diodes on the I-V curve of the particular solar array is shown in Figure 34. The blue curve shows the maximum power output of 173.25W when the complete solar array in full sun conditions. However, the yellow curve shows the effect of shading when no bypass diode and one solar module is shaded, the output power is reduced to 96.75W. Whereas, a significant amount of power loss is avoided using bypass diode under shading conditions as shown in red curve in Figure 34 which produced the power output of 139.05W.

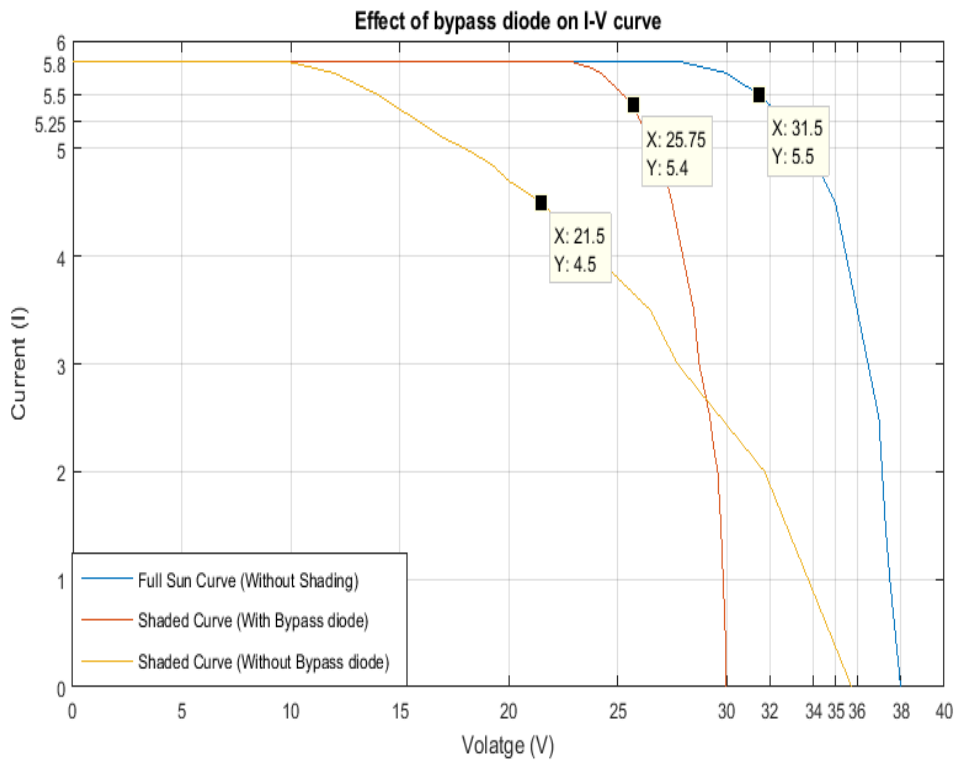


Figure 34: Influence of Bypass diode [41].

3.5 Final Solar Array Design

Among all the solar cell manufacturers, the Sunpower C60 maxeon cells technology is chosen to design our solar array. The main reason for choosing SunPower is that they are providing most efficient mono-crystalline silicon solar cells at a reasonable price in all over the solar cell market. SunPower claimed their C60 maxeon solar cells to be 21% efficient that is more than our 2nd option which is Tindo at 19% efficiency [42] - [43]. Table 9 and Table 10 shows the electrical and physical specification of C60 solar cells. However, at the same time, the Tindo solar company is also in our consideration to get some sponsorships or cells for our car.

Table 9 : Electrical characteristics of Sunpower C60 cell [42]

Electrical Characteristics of Typical Cell at Standard Test Conditions (STC)					
STC: 1000W/m ² , AM 1.5g and cell temp 25°C					
P_{MPP} (W)	Eff. (%)	V_{MPP} (V)	I_{MPP} (A)	V_{oc} (V)	I_{sc} (A)
3.34	21.8	0.574	5.83	0.682	6.24

Table 10 : Physical characteristics of Sunpower C60 cell [42]

Physical Characteristics	
Construction:	All back contact
Dimensions:	125mm × 125mm (nominal)
Thickness:	165μm ± 40μm
Diameter:	160mm (nominal)

According to the World Solar Challenge (WSC), 2017 regulation [2.4.2] the cruiser class is allowed to use only 5 m² area of the car for the solar cells. Therefore, with our chosen solar cells we can use 320 cells to design the complete solar array. However, it is mentioned in the regulation [3.18.2] of the WSC 2017 that the cruiser class teams can recharge the energy storage system at any time except control stops (stop point after every 300km) but this recharge time will deduct the energy efficiency score. For this reason, we have to design our array in an optimum way that the solar array will not

exceed the allowed area and in the meantime it can deliver enough power to run the car on a complete day. By the specifications and physical dimensions shown in Table 9 and Table 10, the preliminary design for the Flinders Solar Car is proposed in Figure 35.

3.5.1 Design Scheme of Solar Array

By studying several design schemes and their responses in the literature review section of Chapter 2, an optimum design approach is chosen to build the complete solar array for the Flinders Solar Car. Figure 35 shows the arrangements of the photovoltaic (PV) system for the Flinders Solar Car. The three solar arrays are used on the overall body of the car as shown below. All the three solar arrays have an equal number of solar cells connected in series. While the solar arrays are connected in parallel with each other, to built a complete PV system for the Flinders Solar Car. In addition, Maximum Power Point Tracker (MPPT) attached with each solar array in series which matches the output power of each solar array connected in parallel as shown in Figure 35.

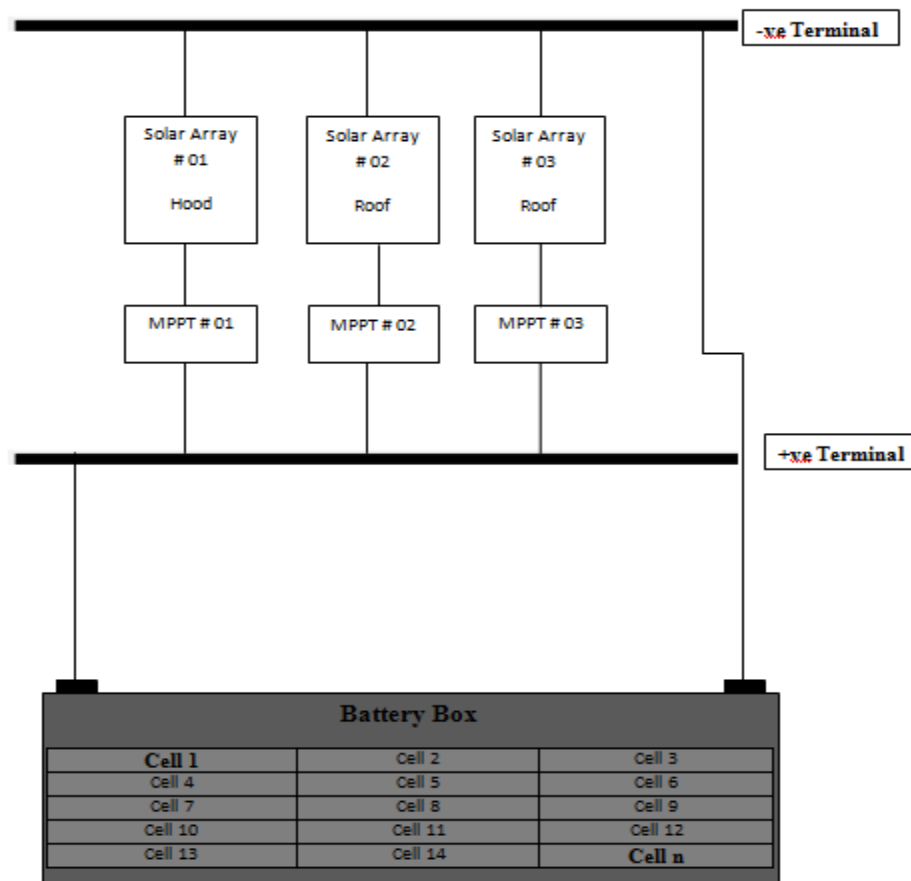


Figure 35: Preliminary Solar Array Design

3.5.2 Prototype Design

Since the purchase order of the solar cells for the Flinders Solar Car is under process. Therefore, a few low-grade SunPower maxeon C60 solar cells are purchased from the vendor (not original manufacturer) for testing and experimental works.

Before making a solar array, the solar cells are tested individually. Individual testing reveals that the output power of the solar cells is non-identical. Among ten, only two solar cells have the same power output ratings. Hence, it proves the mismatching effect which was discussed in Chapter 2 and Chapter 3. To avoid mismatching, we designed a prototype of two solar arrays using the same design approach as discussed above under the heading of Design Scheme of the solar array 55. All the solar cells are connected in series to form a solar array while the solar arrays are connected in parallel to form a complete PV system. The solar arrays are connected in parallel, to increase the current output of the overall system and reduce battery charging time. The prototype of the solar array is designed by connecting the four closely matched solar cells in series using tabbing wire as shown in Figure 36.



Figure 36: Prototype of Solar Array.

After that, the design prototype of the solar array shown in Figure 36 was tested under the full sun on 13th October, 2016 at an irradiance of 6.9kWh/m² [44]. The produced power from one sample of the solar array was observed as 5.14W (2.42V × 2.12A). As these solar cells are low-grade cells and bought from vendor just for testing purpose, therefore, it is observed that the output current is significantly lower than the stated output current by SunPower Company (i.e. 5.83A) outlined in Table 9.

As the Flinders Solar Car model includes a rear wing spoiler on the trunk of the car for efficient aerodynamics as shown in Figure 37, therefore, the solar array will not be attached to the rear of the car. The reason for not using an array at the back is because of the flip, which causes the solar cells to be shaded. Even if a few cells of any array are under shade, the whole string output is reduced as observed in Section 3.4.2.

Since the solar cells are attached only on the roof and hood of the solar car. Therefore, we distributed the cells architecture into three (3) solar arrays. The considerations which were taken in mind before designing the complete solar array are as follows.

- All arrays must have equal numbers of cells, to make sufficient potential difference to charge the battery.
- Battery voltage is approximately 110 Volt, for that reason solar power is boosted by MPPT to charge the battery packs.
- By considering space on the body of the car, each array built by connecting 67 cells in series
- Single array will generate 38-volt output by 67 cells (1 cell = 0.574 Volt outlined in Table 9)
- The galvanic isolated maximum power point tracker (MPPT) used to maintain the solar output. MPPT boosts the solar arrays output more than the battery voltage to charge the battery sufficiently.
- All arrays are connected in parallel to add current, bus wires should be used to connect arrays together.
- Finally, the complete PV system will produce the power of 645 Watt whereas, each array will generate almost 215 Watt.

Design/body works of the car are still in process, and some minor changes regarding aerodynamics might be done in the future. However, this will not significantly affect the solar array design as we have left space for any minor adjustments in the body design of the car. Our estimated area for one array is 1.05m^2 which is less than the available space on hood and roof. The space on the roof is left empty because of the two reasons. Each array should have equal number of the solar cells to get similar output voltage (because arrays are connected in parallel if the voltage is dissimilar then mismatching occurs). Secondly, the solar array design will remain unaffected if the available area for the solar cells decreases by any reason such as aerodynamics.

The rear side of the car is the optimum place to attach the solar array. However, the rear spoiler at the back side of the car seen in Figure 37 will shade the solar cells in result, the overall output of the PV system will be reduced. Therefore, the solar array is not attached to the back of the car.



Figure 37: Final Model of the Solar Car.

3.5.3 Strength and Weaknesses of the Design

- Trunk (rear) space is wasted regarding the solar array because rear side will be shaded by the rear spoiler as it easily seen in Figure 38.
- As roof has a total area of 2.52m^2 and hood has only 1.68m^2 area shown in Figure 38, and we have to distribute solar arrays evenly because at the end all arrays will be connected in parallel. Therefore 67 cells are the optimal number of cells that can be used which covers an area of 1.05m^2 ($67 \text{ cells} * 0.015625\text{m}^2$ area of one cell = 1.046m^2). Due to that some of the parts of the hood will be useless.

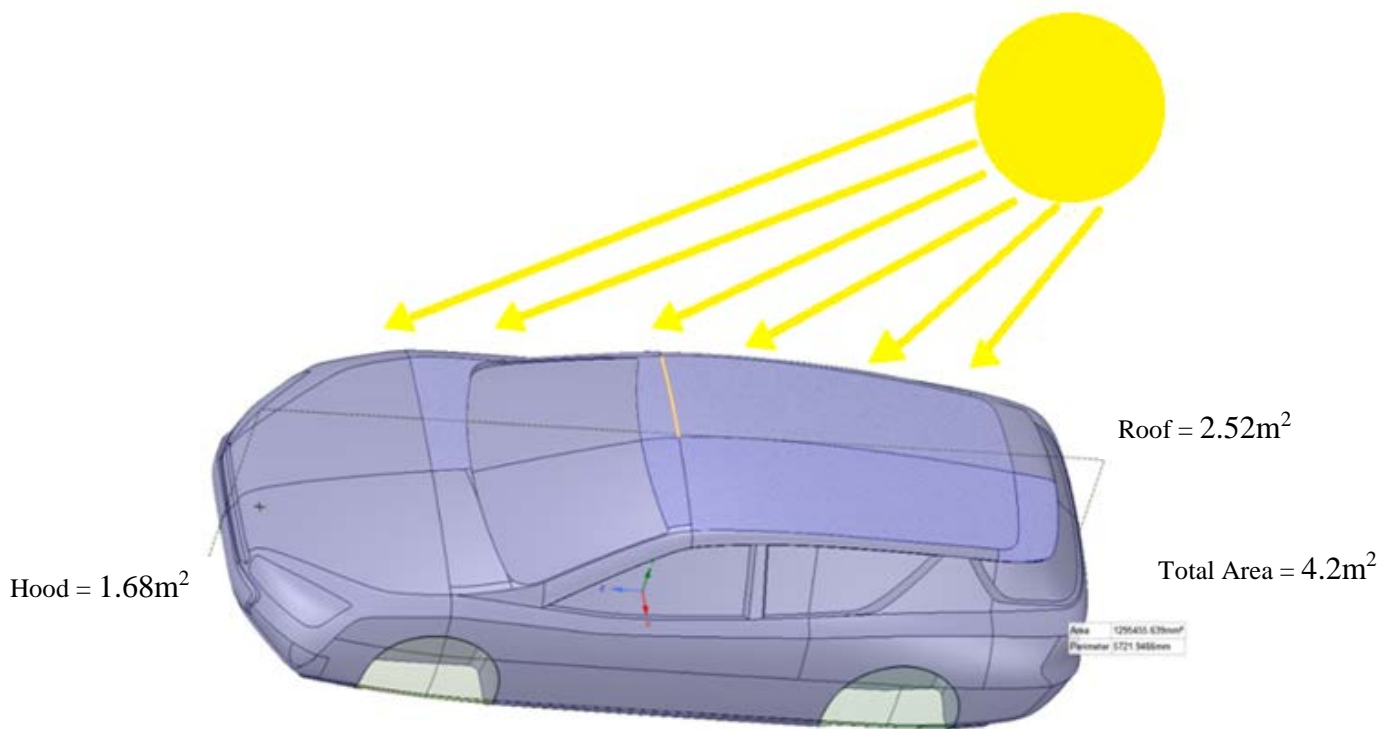


Figure 38: Total Area for Solar Cells.

- The WSC, 2017 regulations allowed the cruiser class teams to use 5m² for the silicon solar cells on the body of the car. While, we are just using 3.15m² area for the solar array on the body of the car, which will significantly decrease the output of the solar array. However, if the allowed area (5m²) of the body of the car is used then the designed solar array will produce the power of 860W instead of 645W. But there is a trade-off between the aerodynamics and the solar array output. Given the fact that, during the race, teams are allowed to recharge the energy storage systems, therefore Flinders Automotive Solar Team is more focussed and concerned about the aerodynamics of the car.

3.6 Maximum Power Point Tracker

The output power from the solar cells mainly depends on irradiation from the sun, output current and voltage draw from the cells. Maximum power can be achieved when the solar cells are operating at maximum power point (knee point on of I-V curve).

Flinders Automotive Solar team has planned to purchase maximum power point tracker (MPPT) rather design in house. The reason for purchasing MPPT is the output efficiency. It has a high probability that we will not achieve high efficiency if we design by ourselves. While, there are various MPPT available in market at low cost.

Several MPPT's are analysed considering the designed solar array for Flinders Solar Car. Few names of the companies are mentioned below:

1. AERL RACEMAX
2. Symtech Technology
3. DriveTek
4. Dilithium Power Systems

All the above Maximum power point trackers meets our solar array and battery specifications. Though, we are going to use it as a step-up function that boosts the low voltages of the solar array to the high battery voltages. Due to that reason isolation between two voltages must need to be made. If there is no isolation between the solar array and battery, then the solar array will damage due to reverse high current flow from battery packs to the solar array.

The two most common types of isolations are: by using any semiconductor component (generally blocking diode), or by a transformer (galvanic isolation). According to the safety aspects, the galvanic isolation is the most powerful isolation and has fewer chances to fail as compared to the semiconductor device.

The performance comparison of three different MPPT's is presented in Table 11.

Table 11 Comparison of Different MPPT [45],[46],[47]

Specifications	Aurora Symtech MPPT	DriveTek MPPT	AERL RACEMAX MPPT
Input Voltage Range	20V – 60V	26V – 60V	40V – 135V
Output Voltage Range	110V – 170V	28V – 140V	72V, 96V, 120V, 144V, 168V
Efficiency	98.5%	97.5%	98%
Isolation	3kV Galvanic	Transistor/diode	Transistor/diode
Weight	790 gm	650 gm	720 gm
Interface	CAN bus	CAN bus	N/A
Operating Temperature	-20°C to +85°C	+70°C	+50°C

The above mentioned companies provide the isolation between input (low voltage) and output (high voltage) using semiconductor. While only the Symtech Technology provides transformer isolation between the input and output. Symtech also provided MPPT's to previous teams that participated in the World Solar Challenge. A transformer and associated circuitry achieve the galvanic isolation from input to the output as shown in Figure 39. The galvanic isolation alleviates the requirement for circuit breakers to be installed on the PV side of the Tracker as mentioned in WSC, 2017 regulation [1.29.1]. To achieve the high efficiency resonant soft switching technology is used over a broad range of power and voltages.



Figure 39: MPPT Hardware Module of Aurora/Symtech [45].

The efficiency of the Symtech MPPT is 97.5% as shown in Figure 40. Moreover, the Symtech MPPT is also advantageous because the Flinders Automotive Solar Team uses Controller Area Network (CAN) bus communication and the mentioned MPPT supports the CAN communication as outlined in Table 11. The Symtech provides 1Mbps CAN bus interface to report the voltage, current and temperature of the particular solar array to which it is attached. The overload protection will be turned on after 5 minutes and the Symtech MPPT is passively cooled by the natural convection.

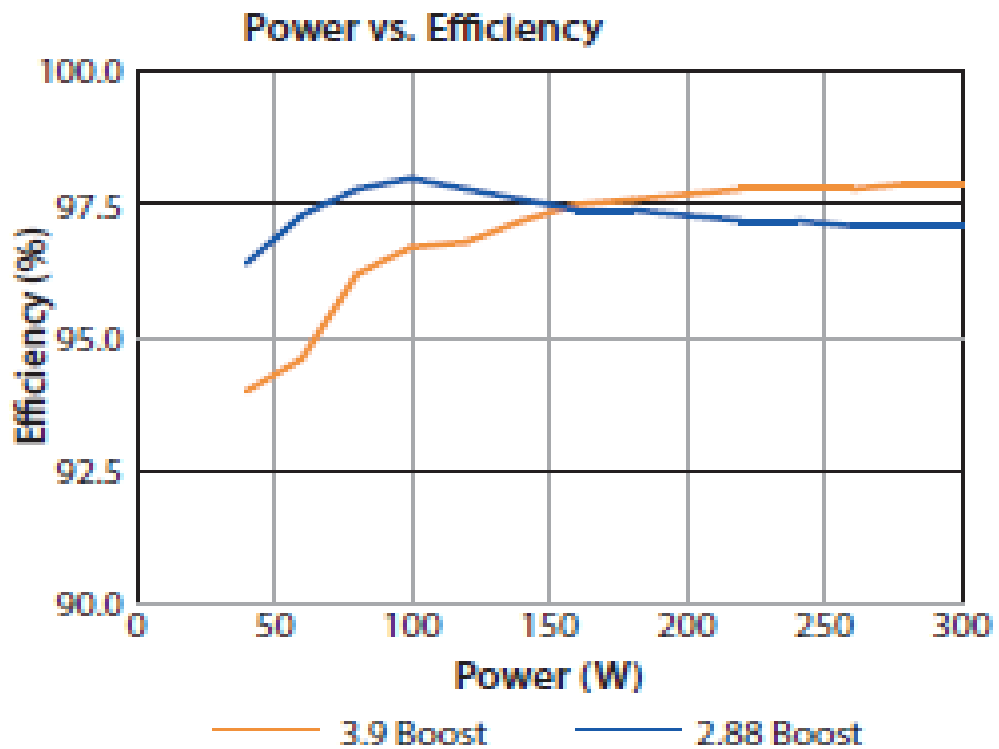


Figure 40: Power vs Efficiency Graph of Aurora/Symtech MPPT [45].

CHAPTER 4

PERFORMANCE ANALYSIS OF DESIGNED SOLAR ARRAY

This Chapter presents the performance analysis of the solar array for the race from Darwin to Adelaide. The parameters which significantly reduce the power output includes temperature of the solar array, shading and optimum tilt angle are discussed in this Chapter. Moreover, this Chapter also outlines the strategy to achieve the optimum power output from the proposed design of the solar array.

4.1 Temperature Effects

To calculate the power produced by the solar array, the temperature of the solar cells must be considered. The temperature of the solar cells is non-uniform due to several reasons, including non-uniform manufacturing of the solar cells, non-uniform illumination of a sunlight and position of the solar cells in the solar array as discussed in Section 2.3. Therefore, a solar array must possess some cooling system to reduce the high-temperature effects. A water cooling system is the most efficient way to maintain the temperature of the solar cells. However, the World Solar Challenge (WSC), 2017 regulation [3.28.1] do not allow to use water on the solar array.

Therefore, it is required to propose an optimum cooling technique for the Flinders Solar Car. Since the moving car cuts the massive amounts of air, the solar arrays are attached to the body of the car in such a way that air will cool down the solar array. As mentioned in the design Section 3.4, the solar arrays are attached to the hood and roof of the car which will have enormous contact with the surrounding air.

Initially, the temperature analysis was performed for Standard Test Conditions (STC). STC assumes that the ambient temperature ($T_{\text{ambient}} = 25^{\circ}\text{C}$) and the solar irradiations (irradiation) = 1000 W/m^2 or 1-sun (S). Later, the temperature analysis will also be conducted for the local temperature of Darwin on the first day of the race (October 08, 2017).

The comparison of difference in power output with the change in temperature is shown in Table 12. As, the solar cell temperature is always more than the temperature at surrounding due to a continuous flow of electrons from one band to another. Therefore, the Sunpower C60 solar cell is heated up to 56.25°C under STC (at 25°C). The increase in temperature causes the output power of Photovoltaic (PV) cell to reduce by 3.23W as shown in Table 12. In addition, the overall output of the solar array at STC was also reduced with the increase in a cell temperature as depicted in Table 12.

Similarly, the mathematical analysis was performed for the local temperature of the Darwin at the start of the race 08th October, 2017. The predicted ambient temperature at Darwin on 08th October, 2017 will be 35°C [accuweather.com]. As the solar cell temperature will rise to 66.25°C at an ambient temperature of 35°C. Therefore, the SunPower solar cell will produces 3.2W at 35°C and the overall solar array output will decrease from 645W to 618.39W as shown in Table 12. The percentage loss in power output of the solar array with the increase of temperature at irradiation of 1kW/m² is calculated below.

$$\text{Percentage Loss} = \frac{\text{Total power at STC} - \text{Total power at } 66.25^{\circ}\text{C}}{\text{Total power at } 66.25^{\circ}\text{C}} \times 100$$

$$\text{Percentage Loss} = 4.3\%$$

Since, the first two analyses are based on 1-sun (1kW/m²) irradiation as shown in first two columns of Table 12. While, this is the ideal case and practically 100% irradiation is not captured by the solar array. The Bureau of Meteorology [44] provides that the average solar irradiation at Darwin is around 0.7kW/m². Thus, the final calculation according to expected temperature and radiations at Darwin on October 08, 2017 are shown in column three in Table 12.

The power calculated to analyse the effect of temperature did not include the maximum power point tracker (MPPT). However, in reality, MPPT is attached to each array which will boost the solar array output and force to work at maximum power points as discussed in Section 3.6.

With ground realities and under practical conditions, a significant amount of power lost as compared to the previous cases. Due to increase in ambient temperature and decrease in irradiation, the overall photovoltaic array observes 47.5% reduction in the power output. Hence the results showed that, the designed solar array for the Flinders Solar Car will produce 437.11W at Darwin on 08th October, 2017, if used without Maximum Power Point Tracker (MPPT).

Table 12 Effect of Temperature on Output Power for Ideal Radiations (1kW/m²)

Output Power Analysis under Standard Test Conditions (STC). (Irradiation = 1kW, Temp. = 25°C)	Output Power Analysis under Full Sun at Darwin Temperature. (Irradiation = 1 kW, Temp. = 35°C)	Output Power Analysis under Darwin Conditions. (Irradiation = 0.7 kW, Temp. = 35°C)
$T_{Cell} = 56.25^{\circ}C$	$T_{Cell} = 66.25^{\circ}C$	$T_{Cell} = 56.87^{\circ}C$
$P_{Cell} = 3.23W$	$P_{Cell} = 3.20W$	$P_{Cell} = 2.26W$
$P_{Array} = 624.84W$	$P_{Array} = 618.39W$	$P_{Array} = 437.11W$

Because, the purchase order of the proposed solar cells (SunPower C60 maxeon cells) for the Flinders Solar Car was under process. Another experiment was conducted using the Tindo Karra-250 solar panel to analyse the temperature effects of the solar cells. The Tindo solar panel was placed under the sunlight at Tonsley, Adelaide at an angle of 27° on 14th October, 2016. The observed latitude and irradianations at solar noon (01:02pm) of the test day are 63° and 7.0kWh/m² respectively [44].

Figure 41 (a) shows the difference of temperature within a single panel at the start of the experiment. The ambient temperature observed during the test was 21°C whereas the temperatures of the solar cells are observed higher than the ambient temperature. The zero point (P0) indicated in Figure 41(a) has the highest temperature of 26.7°C while the average solar cells temperature is 22.2°C as indicated by A0.

Similarly, Figure 41(b) shows the rise in temperature with the rise in ambient temperature to 23.5°C within two hour of the test. The cell on the top right corner exhibits the significant rise in temperature from 26.7°C to 37.5°C as shown in Figure 41(b). In result, the overall output current of the solar panel was also decreased from 7.4A to 6.2A due to non-uniform change in temperature across the panel. Hence, the above analysis proved that the rise in temperature of one cell can decrease the overall array output.

At the end of the test, the water was sprayed on the test panel. The spray of water as a coolant significantly decreases the temperature and cooled down the solar cells as depicted in Figure 41(c). Moreover, the decrease in temperature results in an increase in output current of the solar panel again from 6.2A to 7A. Therefore, the solar array design for the Flinders Solar Car was considered the effect of temperature increment and designed the solar array prototype in Section 3.5, accordingly with closely matched cells. Furthermore, for cooling purpose during the race, the passing air will be used to maintain the solar array temperature as spraying of water is not allowed according to regulation [3.28.1] of World Solar Challenge.

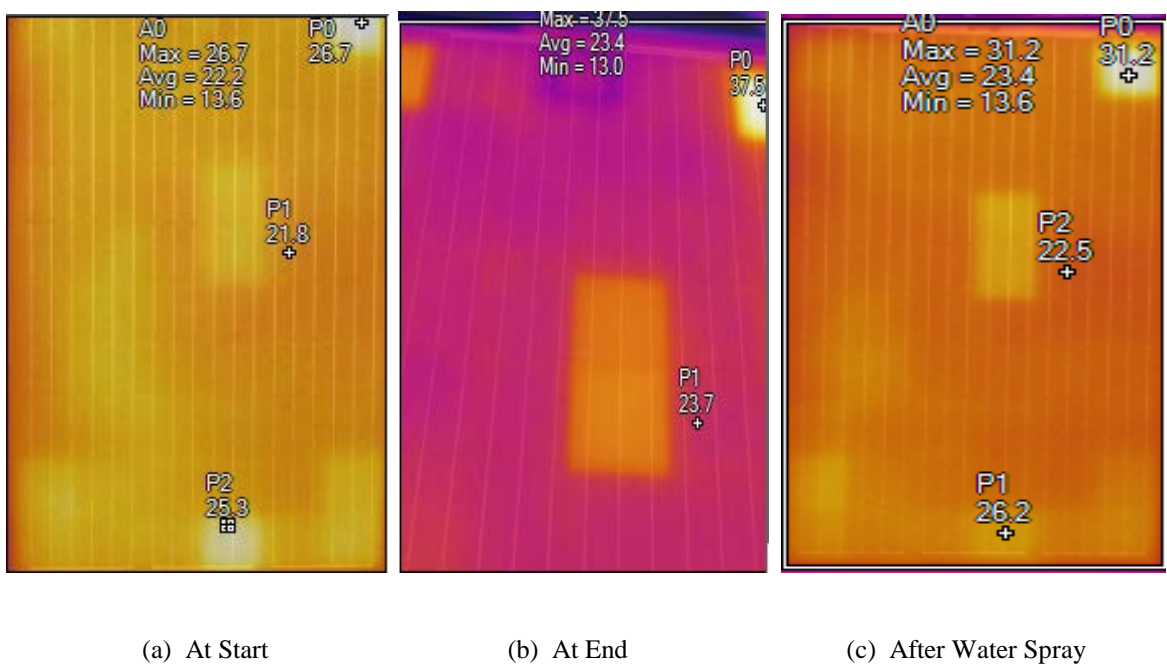


Figure 41: Temperature Variations of Solar Panel.

4.2 Shading Analysis

The photovoltaic (PV) system for the Flinders Solar Car is designed in such a way that it consists of 3 solar arrays. Each solar array is made up of 67 series connected solar cells as described in detail in Chapter 3. Shading of the solar cells leads to the mismatch condition. Whenever a solar cell or an array is shaded and unable to produce the power equal to the other arrays, then the cells are mismatched.

An experiment has been performed using designed solar array prototype in order to analyse the effect of partial shading. At start, all the three solar arrays placed in full sun at the irradiation level of 6.9 kWh/m^2 at solar noon on 14th October, 2016 [44]. The total power produced by the designed prototype system was 3.23W as shown in Figure 42 in blue curve. After that, out of the three arrays, one solar array was shaded by an obstacle during experiment considering an array attached to the hood of the car comes under shade during sunset. However, the other two solar arrays were under full sun. Hence, the shading of one array caused mismatched condition and reduced the overall output power to 2.054W as shown in Figure 42 in yellow colour.

The bypass diode (schottky diode) is then connected in parallel with each array in order to analyse the advantage of bypass diode. The similar experiment was conducted again by shading one solar array out of the three arrays. In result, the maximum power point increased from the previous case where no bypass diode attached. Hence, the considerable amount of power loss was avoided. The red curve shows the response of solar array using bypass diode, the power output is now 2.812W which is 36.95% more than the output of the previous case when no bypass diode (yellow colour).

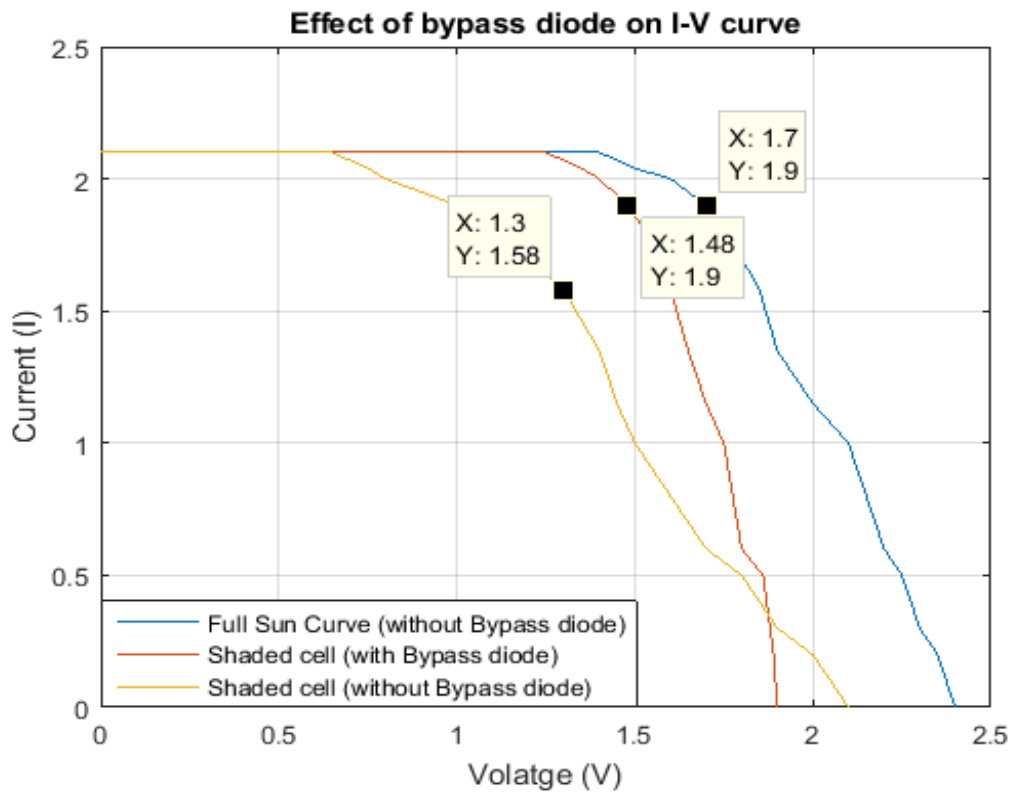


Figure 42: Effects of shading with and without bypass diode.

Using I-V curve of Figure 42, mathematical calculations are performed to examine the effect of a shaded solar cell and advantage of a bypass diode in the solar array. In addition, for the proposed solar array of the Flinders Solar Car schottky diode is considered as it has minimum voltage drop. Therefore, the calculation performed in this section is according to the electrical ratings of schottky diode.

The value of parallel resistance (R_P) is not given in the datasheet of Sunpower C60 solar cells. Therefore an R_P is assumed to be 1Ω during calculations. The results of the calculations are presented in Table 13. However, the complete calculation can be seen in appendix.

Table 13 Effect of Bypass Diode on Output Power

Output Power Variations	
Power under Full Sun	3.230W
Power under Shading (With bypass diode)	2.812W
Power under Shading (With bypass diode)	2.054W

Hence, the maximum power (P_{max}) produced by the designed solar array with one shaded solar cell and no bypass diode is 2.054 W. This power is 26.95% less than the power produced by the solar array having bypass diode.

The above calculation explained the effect of shading and revealed the importance of the bypass diode (schottky diode). As compare to the power output of the solar array under full sun condition in Eq. (13), the shaded cell without bypass diode reduced the solar array output by 36.41% from 3.23W to 2.054W in Eq. (15). Whereas using the bypass diode a significant amount of power loss is voided, and only 12.94% power losses are observed from 3.23W to 2.812W.

However, at this moment the analysis was performed for the designed solar array prototype to observe the shading effect. While in similar manner, the shading effect will reduce the power output of the final solar array for the Flinders Solar Car. Therefore, the proposed solar array design in Chapter 3 for the Flinders Solar Car was having bypass diode (schottky diode), which will help to optimise the efficiency of the solar array by providing another path for current flow under the shading condition.

4.3 Analysis of Optimum Tilt Angle

On the sunny day of 13th October 2016, the experiment was performed to analyse the change in power with the change of the tilt angle. Initially, the Tindo Karra-250 Solar panel was used to perform the experiment. While after the design of the solar array, the same experiment was performed with the prototype of the solar array to observe the effect of tilt angles over the power output. The electrical specifications of the solar panel are given in Table 14.

Table 14 Electrical Specifications of Tindo karra-250 (tindosolar.com.au)

Tindo Solar Panel Electrical Specifications	
Maximum Load Power (P_{max})	250 W
Open Circuit Power (P_{max})	358 W
Current (I_{mpp})	8.3 A
Volatge (V_{mp})	30.0 V
Short Circuit Current (I_{sc})	9.5 A
Open Circuit Voltage (V_{oc})	37.7 V
Efficiency (η)	19%

4.3.1 Power and Efficiency Losses vs. Tilt Angles

At solar noon, the sun crosses the meridian at the highest elevation in the sky. At this time the maximum sunlight reaches to the earth, and solar panel can work at its maximum efficiency. Therefore, the test was conducted at 01.02 pm to 01:45 pm as solar noon occurred at 01.02 pm (bom.gov.au). The panel was placed at an angle of 27.2° from ground as the altitude of the sun was 62.7 ° on 13th October, 2016 [44].

The results of the experiment shows that change in power with the change in tilt angles of the designed solar array and the Tindo solar panel was in similar proportion. Hence, the effect of the change in tilt angle of the Tindo solar panel over the power output is illustrated in Figure 43. The maximum power of 335.4W was achieved by the solar panel at the tilt angle of 27.2° which was the optimum tilt angle for the experiment day (13th October, 2016). While at an angle of 5° from the ground, the minimum solar power is produced.

Figure 43 also shows that, the output current of the solar panel changes significantly from the tilt angle of 5° to 27.2° and 35° to 45° and so on. However, from an angle of 27.2° to 35° very little amount of current changed. Similarly, the slight change in power is observed at the particular range of tilt angle from 27.2° to 35° . In addition, Figure 43 depicts that, output voltage of the solar panel is almost constant and tilt angles doesn't change the output voltage in a significant amount.

In result, the experiment concludes that the output power is reduced in very little amount with the slight deviations in the tilt angle from the optimum angle. However, the deviation of the tilt angle more than 10° from an optimum angle will have a significant impact on the output power.

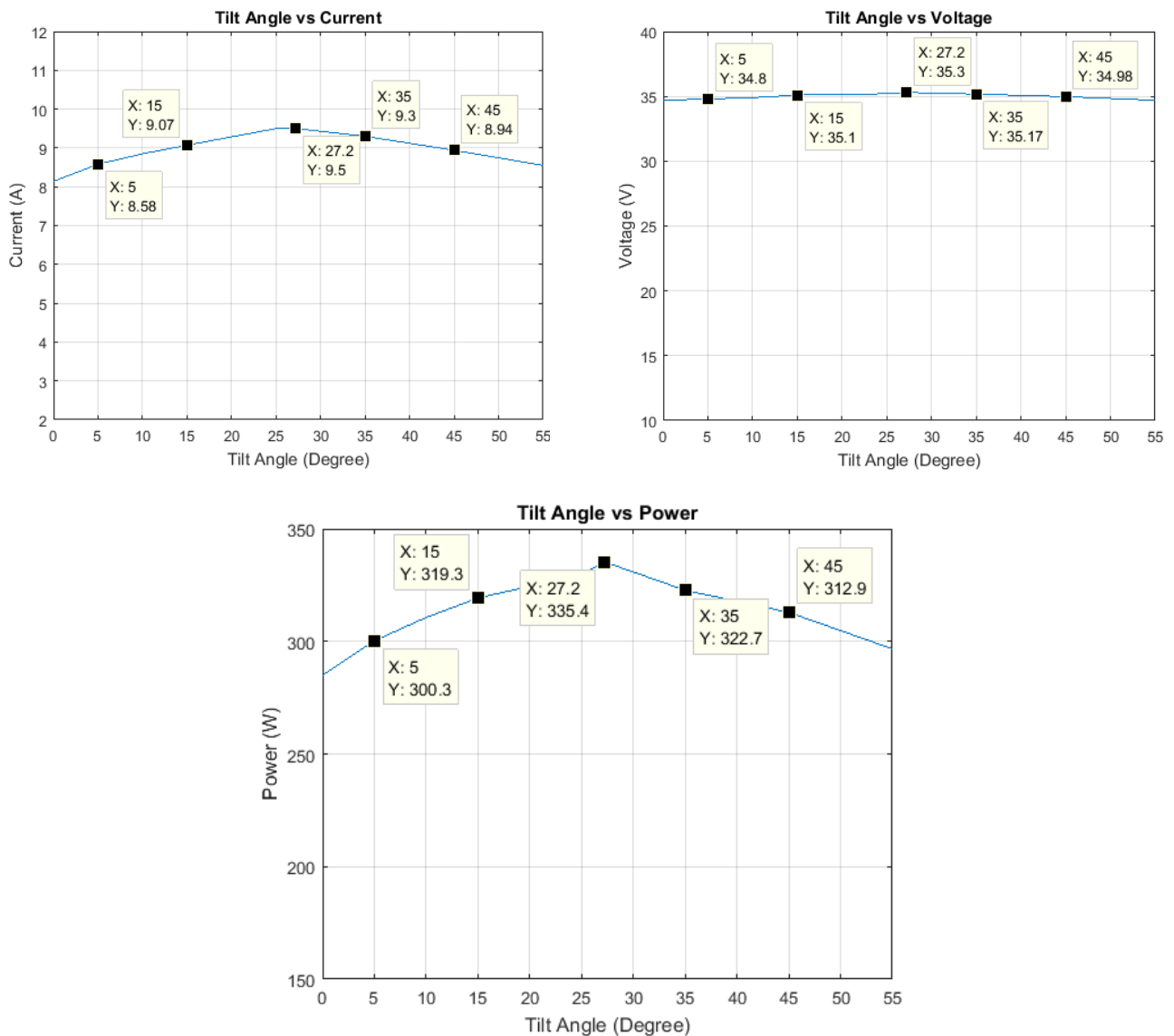


Figure 43: Change in Current, Voltage and Power vs. Tilt Angle.

Similarly, the efficiency loss with the change of tilt angle of the solar panel and the designed solar array was similar. Hence, the efficiency response of the Tindo solar panel versus tilt angle can be seen in Figure 44. The Tindo Company declares the maximum efficiency of the solar panel is 19% in ideal conditions as mentioned in Table 14. However, the maximum efficiency of 18.74% was achieved in practical when the solar panel is tilted at an angle of 27.2° on the experiment day (13th October, 2016). While at 0° and 180° the efficiency of the solar panel is minimum which is 15.92% and 17.49% respectively. On the other hand, Figure 44 also shows that loss in efficiency with the 5° deviation from the optimum tilt angle is very less as compare to more than 10° deviations from the optimum tilt angle.

Consequently, the experiment concludes that the optimal tilt angle for the designed solar array and the Tindo solar panel at Tonsley, Adelaide is 27.2° on the day of experiment conducted. Moreover, the experiment concludes that the solar panel including the designed prototype solar array have the tolerance of 5° in the deviation of the tilt angle. However, the deviation more than 5° will cause a significant loss in the power and the efficiency as shown in Figure 43 and Figure 44.

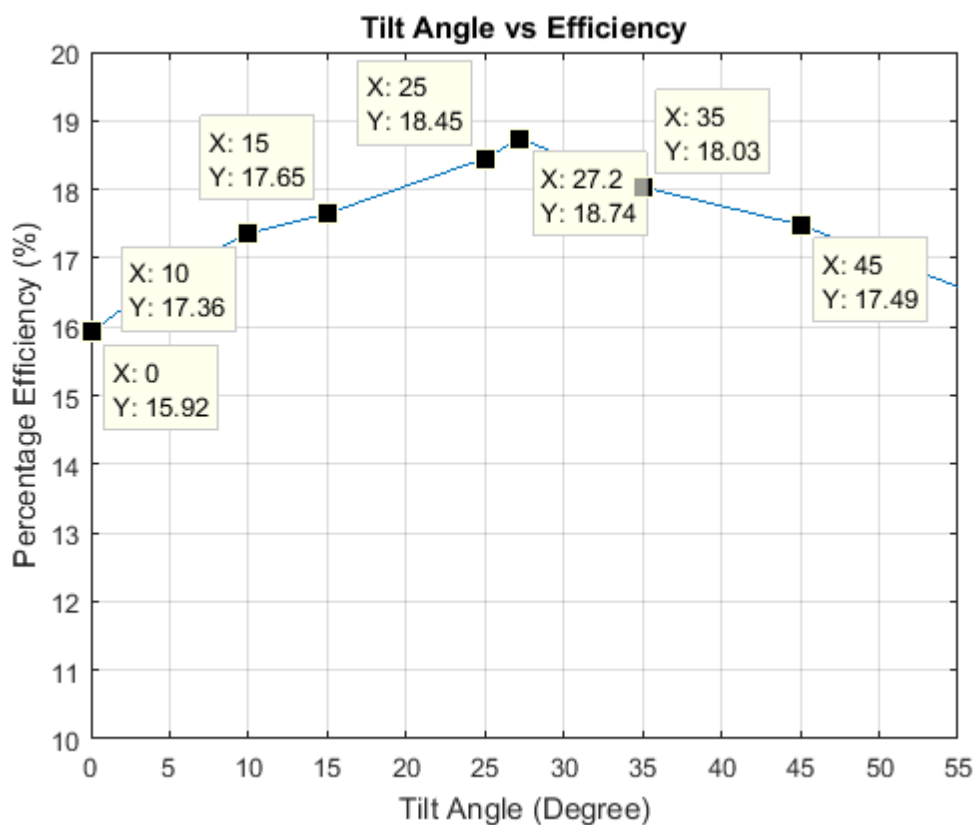


Figure 44: Change in Efficiency vs. Tilt Angle.

The race will start on October 08, 2017 at 8 am from Darwin which has latitude (L) of 12.4634°S (australia.places-in-the-world.com). Flinders Automotive Solar Team (FAST) strategy makers calculated that, at the finish time of the day one of the race, the car will travel about 380km from start point. Therefore, at 5 pm (finish time of day one) we consider the same latitude of the Darwin. Hence, the optimum tilt angle for the Darwin at the start time of the race to the finish time of the same day is shown in Table 15.

Table 15 Optimum Tilt Angle for Complete Day at Darwin

Optimum Tilt Angle for Darwin	
Time of the Day	Tilt Angle
8 th October, 2017 at Start Time (8:00 am)	68°
8 th October, 2017 at Solar noon (12:34 pm)	07°
8 th October, 2017 at Finish Time (5:00 pm)	66°

For a complete day at Darwin, a plot is generated by using MATLAB simulink as shown in Figure 45. It shows that at the start time around 8 am, the tilt angle is the maximum. However, as the sun moves towards west, tilt angle reduces. At solar noon (12:34pm), the tilt angle of the solar array at Darwin on 8th October, 2017 is minimum i.e. 7°. After the midday, the tilt angle again increases and later, the optimum tilt angle for maximum power output reaches to the highest value of 66° at 5pm.

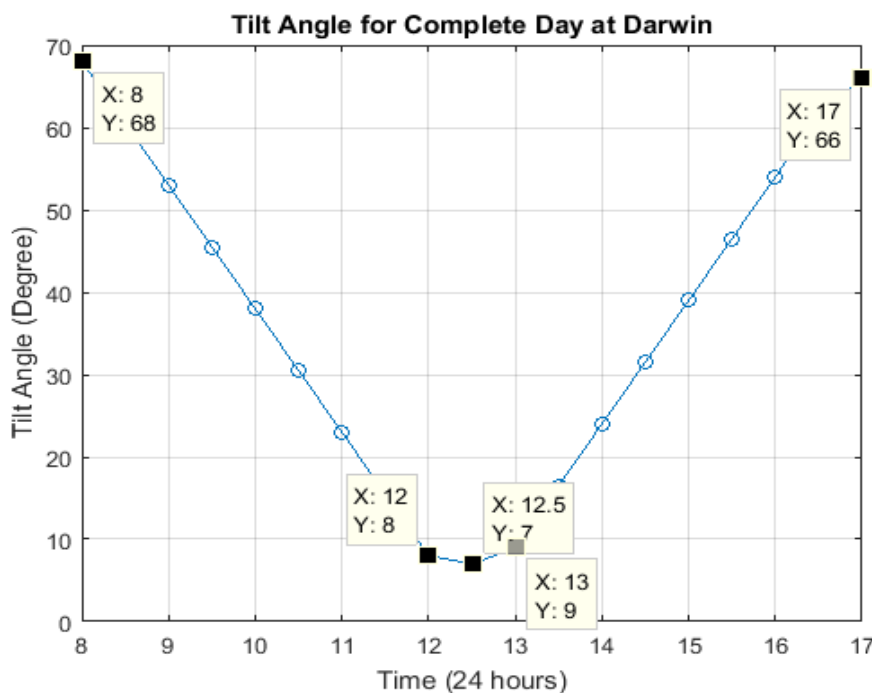


Figure 45: Optimum Tilt Angle for Darwin from 8 am to 5 pm.

The FAST strategy planners provide the plans of arrival or departure from the control stops (the stop point after every 300km) during the race. Thus, the optimum tilt angles for the solar array from Darwin to Adelaide including all the control stops at solar noon are calculated in Table 16.

Table 16 Optimum Tilt Angles for Complete Race at Solar Noon

Location	Date	Optimum Tilt Angle	Distance from Start Point
Darwin	October 08, 2017	7°	0 km
Katherine	October 08, 2017	9°	317.1 km
Dunmarra	October 09, 2017	11°	633.6 km
Tennant Creek	October 10, 2017	13°	989 km
Barrow Creek	October 11, 2017	14.5°	1,216 km
Alice Springs	October 12, 2017	16°	1,496.4 km
Kulgera	October 13, 2017	18.5°	1,812.8 km
Cooper Pedy	October 13, 2017	21°	2,183 km
Glendambo	October 14, 2017	22.5°	2,436.3 km
Port Augusta	October 15, 2017	24.2°	2,723.2 km
Adelaide	October 15, 2017	26°	3,028.2 km

From Darwin to Adelaide the tilt angle for the solar array is shown in Table 16 and Figure 46. Figure 46 shows that the tilt angle can be seen continuously increasing as moves towards Adelaide. However, the Flinders Solar Car will have stationary solar array system. Therefore, the optimum tilt angle for the Flinders Solar Car is obtained by an average of the tilt angles at all control stops. Hence, the optimum angle for the Flinders Solar Car is 16.61°.

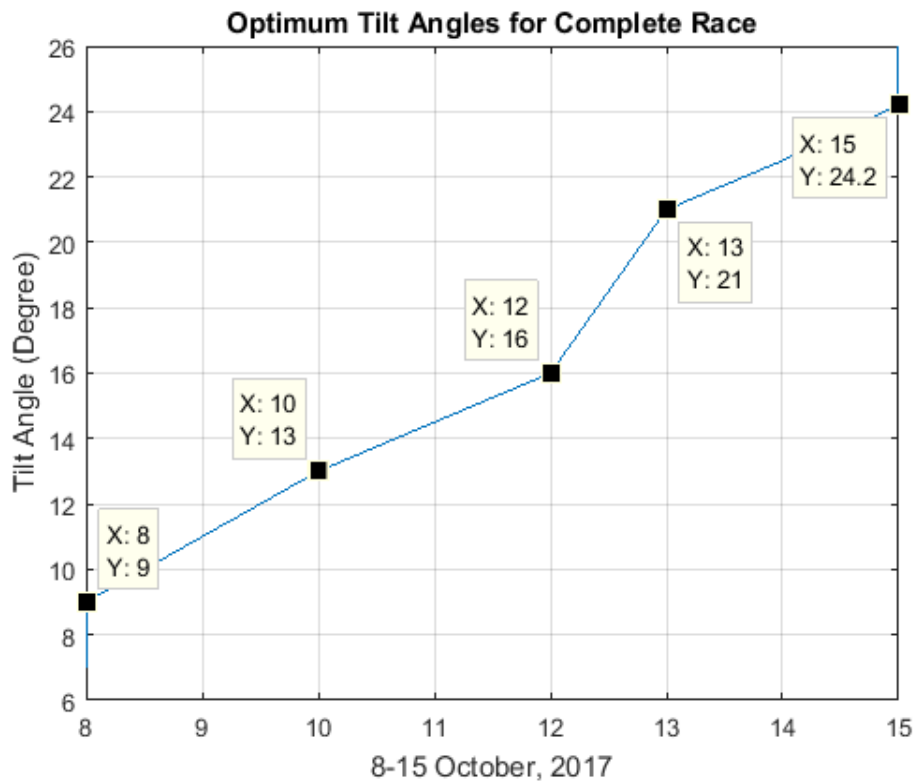


Figure 46: Optimum Tilt Angle from Darwin to Adelaide.

However, the current body design of the Flinders Solar Car has not achieved the mentioned optimum angle (16.61°) as the car has maximum angle of 8.79° on the roof of the car shown in Figure 47. Hence, the total difference in the optimal angle and current angle is calculated below:

$$\text{Difference in Angles} = \frac{\text{Current angle}}{\text{optimum angle}} \times 100$$

$$\text{Difference in Angles} = \frac{8.79}{16.61} \times 100$$

$$\text{Difference in Angles} = 52.92\%$$

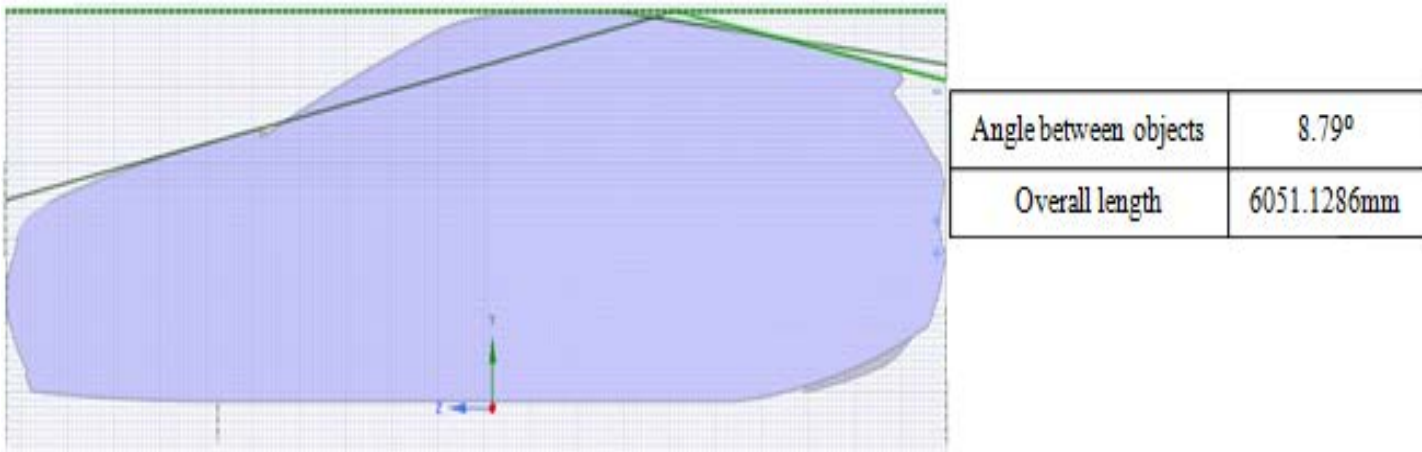


Figure 47: Angle at Current FAST Car Model.

Thus, on average 52.92% loss in power will be observed at all locations due to the current body design of the car. That means, on average the solar array of the Flinders Solar Car will produce 304W instead of 645W. Therefore, FAST has been planned to recharge the batteries as recharging of battery is allowed by the WSC, 2017 regulations. However, the PV system of the solar car is considered as a supplement for the energy storage system.

CHAPTER 5

DESIGN CHALLENGES AND CONSTRAINTS

5.1 Area Limitations

Until mid of the year 2016, WSC, 2017 regulations was not released and the Flinders Automotive Solar Team (FAST) was working according to the previous (2015) regulations. As in the year 2015, the allowable area for the photovoltaic (PV) cells was 6m^2 . According to 6m^2 , the proposed output power was about 1000 Watt under full sun condition by using the SunPower C60 solar cells.

After the release of WSC, 2017 regulations, we changed the design scheme of the solar array for the Solar Car. By the 2017 regulations of the World Solar Challenge (WSC), it is obligatory that area for the solar collectors will not exceed more than 5m^2 . This limitation imposed a significant effect on the design of the Flinders Solar Car. Due to a reduction in the area of the solar collector by 1m^2 , fewer solar cells can be attached on the body of the car. Using 5m^2 area of the solar car, the proposed solar array design produces 833.33W. It is significant cutback of PV output power. Therefore, and the challenge was to propose such an optimum configuration of the solar array that has the least power losses and maximum solar power output using a limited area on the body of the car.

5.2 Aerodynamics vs. Solar Array

The race begins from Darwin to Adelaide, which is the southern hemisphere. Therefore, the backside portion of the car is vital in designing of the solar array for the Flinders Solar Car. Solar cells facing towards north will be exposed to more sunlight relatively than cells facing other directions. As well as, the angle of rear windshield is optimum to absorb maximum solar irradiation.

Additionally for the racing event, the aerodynamics test of the vehicle is most important. Hence, to improve aerodynamics under the WSC, 2017 regulations, FAST proposed a design that has rear spoiler at the rear window as seen in Figure 37. That rear spoiler will provide a late cut off the air

and improve the aerodynamics of the solar car. On the other hand, that rear spoiler at the back of the car will reduce the number of solar cells on the body of the car. It is because, by connecting cells under rear spoiler of the car, PV cells would be under shade. As discussed in Section 4.2, shading has the worst impact on the solar output. Side by side, one shaded cell connected in series with others will reduce overall solar array output.

Due to downsizing in the available area for solar cells, the total power output produced by PV cells is also expected to decrease. The current design of solar array proposed in Figure 35 will cover the 4m² area on car's body. Under the full sun conditions and using specified (Sunpower C60) cells that design will produce 645Watt output power. Thus, due to area limitations and aerodynamics of the car, the reduction in overall output power can be seen in Table 17.

Table 17 Reduction in Total Power

Change in Power due to Regulations		Change in Power due to Aerodynamics	
2015 (6m ²)	2017 (5m ²)	Before Aerodynamics	After Aerodynamics
1000 Watt	833.33 Watt	645 Watt	304 Watt

5.3 Soldering and Reconfiguration

Another major challenge was the connection of all the solar cells perfectly to make a complete solar array. As all cells are connected in series in an array, if one of them is connected (soldered) improperly, it will act as series resistance (R_s). The effect of R_s was seen in Figure 30, where a significant power reduction occurred. For that reason, during the final solar array design, each solar module should be carefully examined before moving to another module or encapsulating the solar array.

Since, the WSC regulations changes after every two years. Therefore, the proposal of the reconfigurable solar array design for the Flinders Solar Car was required. Thus, the design proposed in Section 3.4 can be easily reconfigured by using the same design approach having series connections for the solar cells and parallel connection of the solar arrays.

CHAPTER 6

CONCLUSION

Optimal design of a solar array is a key principle to compete and win the World Solar Challenge (WSC). According to the WSC regulation [2.4.2], only a 5 square metre area can be used for the solar cells on the body of the solar car. Therefore, it is necessary to utilize that space with the most efficient design of the photovoltaic (PV) string.

This project proposes the efficient design of the solar array for the Flinders Solar Car as well as discussed the design techniques used by previous solar car teams in Section 2.8. Competent designing includes pre-design calculations for the available area on the body of the car and optimum angles for the solar cells. Which is followed by the designing Section 3.4 that discusses the optimized configuration scheme of the solar array and then post-design Section 3.6 includes the techniques to boost the designed solar array efficiency using Maximum Power Point Tracker (MPPT). Photovoltaic arrays give their best performance when they are built by considering factors that directly affect the output of a solar array. These factors include the proficient wiring of solar cells, efficient maximum power point tracking system, optimum tilt angle and encapsulation of the solar array.

At the outset, the solar output power is significantly affected if the PV cells are not wired proficiently. Different configurations of the solar cells can yield to different output powers. The solar array output can be reduced up to 50% due to unbalanced connections of the solar cells as seen in Figure 7 in configuration Section 2.3.

Another aim of this project was to set all PV cells to work at their maximum operating point. However, in cloudy weather or when an obstacle comes between the solar car and the sun, then a few of the cells of the solar array could become shaded. In this situation, the particular solar array is unable to produce the desired output. Thus, an efficient configuration technique using bypass diode was employed and discussed in Chapter 3, which fills this design gap and improves the solar output.

The facing of the solar cells towards the sun is an important factor that is considered during the design of the solar array. In order to gain high irradiation, the maximum number of cells should be

placed on the body of the car in such a way that they directly face the sun. Therefore, the tilt angle of the solar cells is the principle consideration during the design of a solar array for a solar car.

To achieve the above-discussed aims and to fill the design gaps, the optimum solar array design is presented to Flinders Automotive Solar Team (FAST) in Section 3.4. However, the current body of Flinders Solar Car is designed for optimum aerodynamics response rather optimum tilt angles of the solar cells because PV system is considered as supplement for energy storage system. As cruiser class teams are allowed by the regulations to charge battery throughout the race. Therefore, the present design and angles of the car, propose solar array will produce 304W due to difference from optimum angle which is 52.92% as discussed in Section 4.3.1.

The key finding of this project is the optimum design of the solar array that produces maximum power with the limited solar cells on the limited area of the car. Solar cells are configured in series to make a complete array. Series connection provides the addition of cell voltage to produce enough voltage to charge the battery of the car. Similarly, all the other arrays are designed with the same principle and then all arrays are connected in parallel. Since parallel connection adds array current, therefore, it provides high charging current to the battery. The result is to help battery charger to reduced charging time of the battery.

For Flinders Solar Car, the designed solar array will produce 36V at full irradiation while the battery voltage is 110V. Therefore, the Maximum Power Point Tracker (MPPT) attached with each array. MPPT boosts the solar power output and forces the solar cells to operate at their maximum ratings, in order to match the battery power points. Since the solar array operates at low voltages whereas the battery has high voltage, therefore, electrical isolation is necessary between the solar array and the battery. Thus, a galvanic isolated MPPT is employed to design a safe system. In this way, there is no potential harm that could damage the solar array due to high reverse current from the battery.

As this the first time Flinders University is going to participate in the World Solar Challenge, we needed to start work from the ground up. Hence, in the limited time of the one-year project, the crucial findings of the optimum design of the solar array have been established. However, some areas require more work and considered as future work to make the most efficient design of the solar arrays.

6.1 Future Work

6.1.1 Increment of Solar Cells

One of the most important aims of the project is to produce the maximum amount of power. Therefore, the number of solar cells will be increased by modification of the body design of the solar car. The optimal design for the World Solar Challenge (WSC) event is the north facing solar array, and the rear side of the car will face north during the race from Darwin (North) to Adelaide (South) as discussed in Section 3.4. If the body design is modified in such a way that allows more space at the rear side of the car, then more energy can be captured from sunlight.

For future work, during the modification of car's body design, shading effect of solar cells need to be considered. The design should be modified in a way that body parts will not shade the solar cells. As happened in the current design, due to rear spoiler at the rear windshield shown in Section 3.5.2 Figure 37. If upcoming students need to enhance the photovoltaic (PV) array, they can easily wire more cells by using current design technique discussed in designing Chapter 3. The proposed technique includes extremely optimized procedure to design the solar array, especially for the solar car. Extension of the solar array should be connected in parallel with the existing solar arrays. However, cells in PV cells should be in series to form an array.

6.1.2 Data Logging

The continuously changing variables need to be stored to keep track on the system efficiency. The present system design uses a Maximum Power Point Tracker (MPPT) to acquire information about output voltage, output current, and temperature of the solar array. However, this design will display the values in current time and does not have memory to store the acquired information. Therefore, for future work, some special data logging technique should be included. By doing so, the chance of damaging solar array due to over-heat (high temperature) can be avoided. Moreover, the output current and voltage log helps to analyse the solar array performance throughout the race.

6.1.3 Additional Sensors

Further work may require adding sensors on particular solar modules. Sensors will help to know about the performance of the individual PV module. In the current solar array design, the MPPT gives the output of performance variables but only for the complete solar arrays rather individual solar modules. Therefore, more emphasized performance reporting can be done in future by using separate sensors on each solar module. Individual sensors on the solar modules will help in the reconfiguration of the solar array, error handling and makes complete PV string more proficient. However, there is a matter of cost that need to be consider for a better trade-off.

Sensors can be used for voltage, current and temperature reporting. Using these parameters array output can be easily optimized to produce maximum power.

6.1.4 Efficient Enclosure and Encapsulation

Optimum enclosure design is necessary in order to fix the solar arrays on the body of the car. The enclosure design requires mechanical design using software such as Solid Works or Inventor. Solar array enclosure considers following things:

- Easy access to passengers of car
- Trouble-free reconfiguration technique
- Proper alignment of solar cells to face the sun
- Secure mounting on body

Therefore, to achieve these things, the current design can be enhanced by future students. It will present a clearer picture of solar arrays mounting on solar car. As well as, solar arrays position can be easily adjusted in later if required.

REFERENCES

- [1] P. Sarikprueck, S. K. Korkua, W.-J. Lee, and P. Lumyong, "Developing important renewable energies in Thailand," in *Power and Energy Society General Meeting, 2011 IEEE*, 2011, pp. 1-8: IEEE.
- [2] T. Key, "Future of renewable energy development & deployment," in *Power & Energy Society General Meeting, 2009. PES'09. IEEE*, 2009, pp. 1-1: IEEE.
- [3] L. Berzi, M. Delogu, and M. Pierini, "A comparison of electric vehicles use-case scenarios: Application of a simulation framework to vehicle design optimization and energy consumption assessment," in *Environment and Electrical Engineering (EEEIC), 2016 IEEE 16th International Conference on*, 2016, pp. 1-6: IEEE.
- [4] S. Car. (2010). Available: <https://www.sciencelearn.org.nz/resources/1753-exploring-solar-power>
- [5] V. Tyagi, N. A. Rahim, N. Rahim, A. Jeyraj, and L. Selvaraj, "Progress in solar PV technology: research and achievement," *Renewable and sustainable energy reviews*, vol. 20, pp. 443-461, 2013.
- [6] M. Agrawal, A. Nainani, and M. Frei, "Design and optimization of next generation high aspect ratio periodic thin film photovoltaic cells," in *Photovoltaic Specialists Conference (PVSC), 2011 37th IEEE*, 2011, pp. 000848-000851: IEEE.
- [7] W. Xiao, N. Ozog, and W. G. Dunford, "Topology study of photovoltaic interface for maximum power point tracking," *IEEE Transactions on Industrial Electronics*, vol. 54, no. 3, pp. 1696-1704, 2007.
- [8] U. Stutenbaeumer and B. Mesfin, "Equivalent model of monocrystalline, polycrystalline and amorphous silicon solar cells," *Renewable Energy*, vol. 18, no. 4, pp. 501-512, 1999.
- [9] S. Fang *et al.*, "Gallium arsenide and other compound semiconductors on silicon," *Journal of Applied Physics*, vol. 68, no. 7, pp. R31-R58, 1990.
- [10] Available: <http://www.sun-life.com.ua/doc/sunpower%20C60.pdf>.
- [11] S. c. chart. Available: <http://energyinformative.org/solar-cell-comparison-chart-mono-polycrystalline-thin-film/>
- [12] Gohermann. Available: http://www.gohermann.com/solar_cells/

- [13] N. Núñez, J. González, M. Vázquez, C. Algora, and P. Espinet, "Evaluation of the reliability of high concentrator GaAs solar cells by means of temperature accelerated aging tests," *Progress in Photovoltaics: Research and Applications*, vol. 21, no. 5, pp. 1104-1113, 2013.
- [14] A. Silicon. (26 April). *Thin Film*. Available: <https://www.enfsolar.com/>
- [15] H.-Y. Chen *et al.*, "Polymer solar cells with enhanced open-circuit voltage and efficiency," *Nature photonics*, vol. 3, no. 11, pp. 649-653, 2009.
- [16] J. Yuan *et al.*, "Structure, band gap and energy level modulations for obtaining efficient materials in inverted polymer solar cells," *Organic Electronics*, vol. 14, no. 2, pp. 635-643, 2013.
- [17] C. B. Honsberg, S. Bremner, J. Lee, A. Bailey, and S. Dahal, "Hybrid advanced concept solar cells," in *2011 37th IEEE Photovoltaic Specialists Conference*, 2011, pp. 001903-001906.
- [18] V. Di Dio, D. La Cascia, R. Miceli, and C. Rando, "A mathematical model to determine the electrical energy production in photovoltaic fields under mismatch effect," in *Clean Electrical Power, 2009 International Conference on*, 2009, pp. 46-51: IEEE.
- [19] C. Vimalarani and N. Kamaraj, "Modeling and performance analysis of the solar photovoltaic cell model using Embedded MATLAB," *Simulation*, vol. 91, no. 3, pp. 217-232, 2015.
- [20] G. M. Masters, *Renewable and efficient electric power systems*. John Wiley & Sons, 2013.
- [21] Y. Zhangbo, L. Qifen, Z. Qunzhi, and P. Weiguo, "The cooling technology of solar cells under concentrated system," in *Power Electronics and Motion Control Conference, 2009. IPEMC'09. IEEE 6th International*, 2009, pp. 2193-2197: IEEE.
- [22] K. Moharram, M. Abd-Elhady, H. Kandil, and H. El-Sherif, "Enhancing the performance of photovoltaic panels by water cooling," *Ain Shams Engineering Journal*, vol. 4, no. 4, pp. 869-877, 2013.
- [23] H. Teo, P. Lee, and M. N. A. Hawlader, "An active cooling system for photovoltaic modules," *Applied Energy*, vol. 90, no. 1, pp. 309-315, 2012.
- [24] R. K. Kharb, S. Shimi, S. Chatterji, and M. F. Ansari, "Modeling of solar PV module and maximum power point tracking using ANFIS," *Renewable and Sustainable Energy Reviews*, vol. 33, pp. 602-612, 2014.

- [25] T. Esram and P. L. Chapman, "Comparison of photovoltaic array maximum power point tracking techniques," *IEEE Transactions on energy conversion*, vol. 22, no. 2, pp. 439-449, 2007.
- [26] Y. Kim, H. Jo, and D. Kim, "A new peak power tracker for cost-effective photovoltaic power system," in *Energy Conversion Engineering Conference, 1996. IECEC 96., Proceedings of the 31st Intersociety*, 1996, vol. 3, pp. 1673-1678: IEEE.
- [27] Y.-T. Hsiao and C.-H. Chen, "Maximum power tracking for photovoltaic power system," in *Industry Applications Conference, 2002. 37th IAS Annual Meeting. Conference Record of the*, 2002, vol. 2, pp. 1035-1040: IEEE.
- [28] I. W. Christopher and R. Ramesh, "Comparative study of P&O and InC MPPT algorithms," *American Journal of Engineering Research*, vol. 2, 2013.
- [29] A. F. Boehringer, "Self-Adapting dc Converter for Solar Spacecraft Power Supply Selbstanpassender Gleichstromwandler für die Energieversorgung eines Sonnensatelliten," *IEEE Transactions on Aerospace and electronic Systems*, no. 1, pp. 102-111, 1968.
- [30] J.-H. Zhao, A. Wang, E. Abbaspour-Sani, F. Yun, M. A. Green, and D. L. King, "22.3% efficient silicon solar cell module," in *Photovoltaic Specialists Conference, 1996., Conference Record of the Twenty Fifth IEEE*, 1996, pp. 1203-1206: IEEE.
- [31] K. R. McIntosh, J. N. Cotsell, J. S. Cumpston, A. W. Norris, N. E. Powell, and B. M. Ketola, "An optical comparison of silicone and EVA encapsulants for conventional silicon PV modules: A ray-tracing study," in *Photovoltaic Specialists Conference (PVSC), 2009 34th IEEE*, 2009, pp. 000544-000549: IEEE.
- [32] G. Oreski and G. Wallner, "Aging mechanisms of polymeric films for PV encapsulation," *Solar Energy*, vol. 79, no. 6, pp. 612-617, 2005.
- [33] S.-Y. Lin, S.-J. Chang, Y.-E. Wu, H.-C. Wu, and T.-J. Hsueh, "An excellent encapsulation of silicone on an optimized-ZnO-nanowires anti-reflection layer for crystalline-Si photovoltaic devices," in *Photovoltaic Specialist Conference (PVSC), 2015 IEEE 42nd*, 2015, pp. 1-4: IEEE.
- [34] W. S. Hurter, H. du Plessis, and N. J. van Rensburg, "Simplified encapsulation of solar cells using glass fibre reinforced polymers," in *AFRICON, 2013*, 2013, pp. 1-5: IEEE.

- [35] J. M. Gee, W. K. Schubert, H. L. Tardy, T. Hund, and G. Robison, "The effect of encapsulation on the reflectance of photovoltaic modules using textured multicrystalline-silicon solar cells," in *Photovoltaic Energy Conversion, 1994., Conference Record of the Twenty Fourth. IEEE Photovoltaic Specialists Conference-1994, 1994 IEEE First World Conference on*, 1994, vol. 2, pp. 1555-1558: IEEE.
- [36] R. Mangu, K. Prayaga, B. Nadimpally, and S. Nicaise, "Design, development and optimization of highly efficient solar cars: Gato del Sol I-IV," in *Green Technologies Conference, 2010 IEEE*, 2010, pp. 1-6: IEEE.
- [37] Eindhoven. (26th October). Available: <https://solarteameindhoven.nl/>
- [38] Kogakuin. (26th October). Available: <http://www.ns.kogakuin.ac.jp/~wws1034/>
- [39] J. Galtieri and P. T. Krein, "Designing solar arrays to account for reduced performance from self-shading," in *Power and Energy Conference at Illinois (PECI), 2015 IEEE*, 2015, pp. 1-8: IEEE.
- [40] J. Kim, Y. Wang, M. Pedram, and N. Chang, "Fast photovoltaic array reconfiguration for partial solar powered vehicles," in *Proceedings of the 2014 international symposium on Low power electronics and design*, 2014, pp. 357-362: ACM.
- [41] Y.-H. Liu, J.-H. Chen, and J.-W. Huang, "A review of maximum power point tracking techniques for use in partially shaded conditions," *Renewable and Sustainable Energy Reviews*, vol. 41, pp. 436-453, 2015.
- [42] SunPower. (07, May). Available: <https://us.sunpower.com/why-sunpower/high-efficiency-solar-technology/>
- [43] Tindo. (05 May). Available: <http://www.tindosolar.com.au/>
- [44] B. o. Meteorology. Available: <http://www.bom.gov.au/>
- [45] Aurora. (25 june). *MPPT*. Available: <http://www.aurorasolarcar.com>
- [46] DriveTek. (02 july). *MPPT*. Available: <http://www.drivetek.ch/index.php?id=28>
- [47] AERL, "MPPT," (in English).

A. APPENDICES

A.1 Appendix A- Sunpower Solar Cell Datasheet

SUNPOWER
C60 SOLAR CELL
MONO CRYSTALLINE SILICON

BENEFITS

Maximum Light Capture
SunPower's all-back contact cell design moves gridlines to the back of the cell, leaving the entire front surface exposed to sunlight, enabling up to 10% more sunlight capture than conventional cells.


Superior Temperature Performance
Due to lower temperature coefficients and lower normal cell operating temperatures, our cells generate more energy at higher temperatures compared to standard c-Si solar cells.

No Light-Induced Degradation
SunPower n-type solar cells don't lose 3% of their initial power once exposed to sunlight as they are not subject to light-induced degradation like conventional p-type c-Si cells.

Broad Spectral Response
SunPower cells capture more light from the blue and infrared parts of the spectrum, enabling higher performance in overcast and low-light conditions.

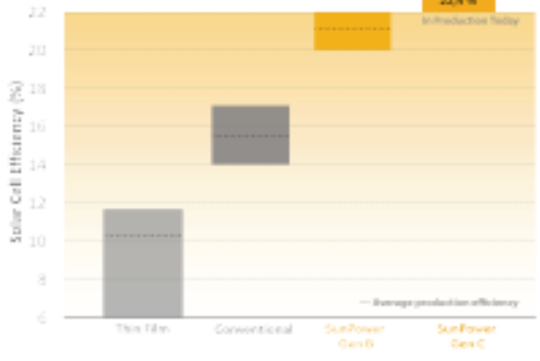
Broad Range Of Application
SunPower cells provide reliable performance in a broad range of applications for years to come.

The SunPower™ C60 solar cell with proprietary Maxeon™ cell technology delivers today's highest efficiency and performance.





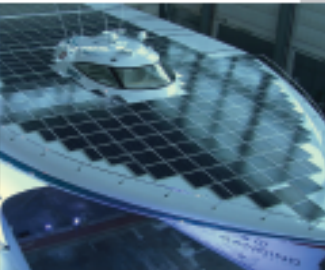
The anti-reflective coating and the reduced voltage-temperature coefficients provide outstanding energy delivery per peak power watt. Our innovative all-back contact design moves gridlines to the back of the cell, which not only generates more power, but also presents a more attractive cell design compared to conventional cells.

SunPower's High Efficiency Advantage



Technology	Solar Cell Efficiency (%)
Thin Film	~11.5
Conventional	~16.5
SunPower Gen B	~19.5
SunPower Gen C	22.4

--- Average production efficiency

C60 SOLAR CELL

Electrical Characteristics of Typical Cell at Standard Test Conditions (STC)

STC: 1000W/m², AM 1.5g and cell temp 25°C

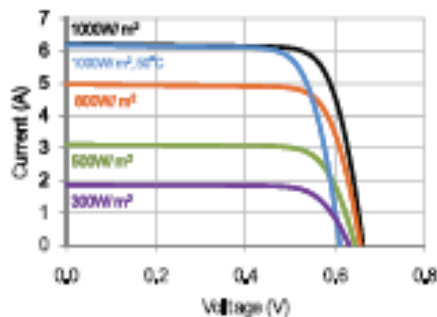
Bin	P _{mp} (Wp)	εF (%)	V _{mp} (V)	I _{mp} (A)	V _{oc} (V)	I _{sc} (A)
G	3.34	21.8	0.574	5.83	0.682	6.24
H	3.38	22.1	0.577	5.87	0.684	6.26
I	3.40	22.3	0.581	5.90	0.686	6.27
J	3.42	22.5	0.582	5.93	0.687	6.28

All Electrical Characteristics parameters are nominal
Unlimited Cell Temperature Coefficients
Voltage: -1.8 mV / °C Power: -0.32% / °C

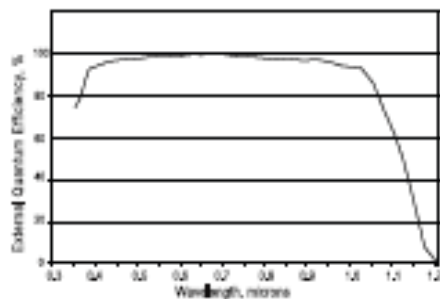
Positive Electrical Ground

Modules and systems produced using these cells must be configured as "positive ground systems".

TYPICAL I-V CURVE



SPECTRAL RESPONSE



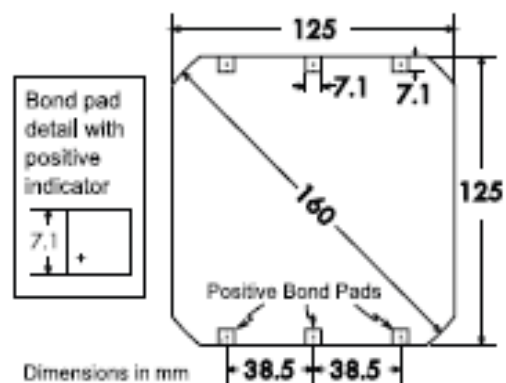
About SunPower

SunPower designs, manufactures, and delivers high-performance solar electric technology worldwide. Our high-efficiency solar cells generate up to 50 percent more power than conventional solar cells. Our high-performance solar panels, roof tiles, and trackers deliver significantly more energy than competing systems.

Physical Characteristics

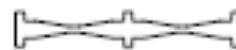
Construction:	All back contact
Dimensions:	125mm x 125mm (nominal)
Thickness:	165µm ± 40µm
Diameter:	160mm (nominal)

Cell and Bond Pad Dimensions



Bond pad area dimensions are 7.1mm x 7.1mm
Positive pole bond pad side has "+" indicator on leftmost and rightmost bond pads.

Interconnect Tab and Process Recommendations



Tin plated copper interconnect. Compatible with lead free process.

Packaging

Cells are packed in boxes of 1,200 each; grouped in shrink-wrapped stacks of 150 with interleaving. Twelve boxes are packed in a water-resistant "Master Carton" containing 14,400 cells suitable for air transport.

Interconnect tabs are packaged in boxes of 1,200 each.

A.2 Appendix B- MPPT Datasheets



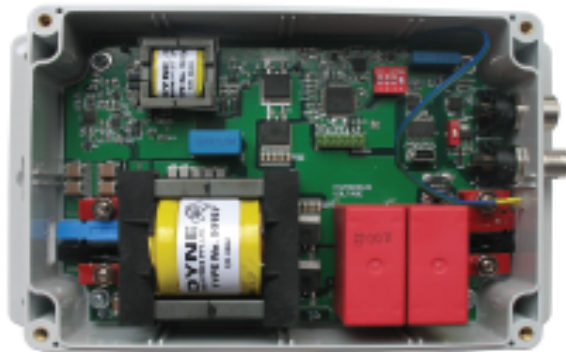
Symtech Maximum Power Point Tracker



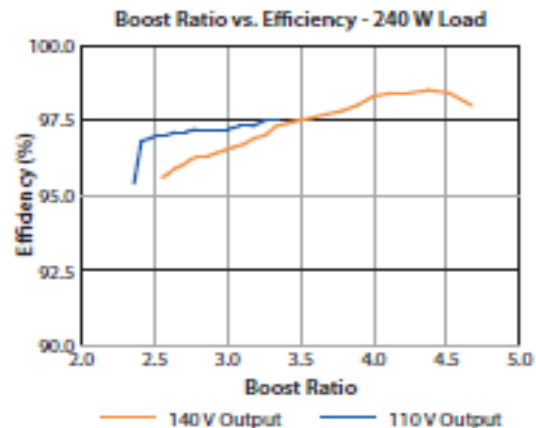
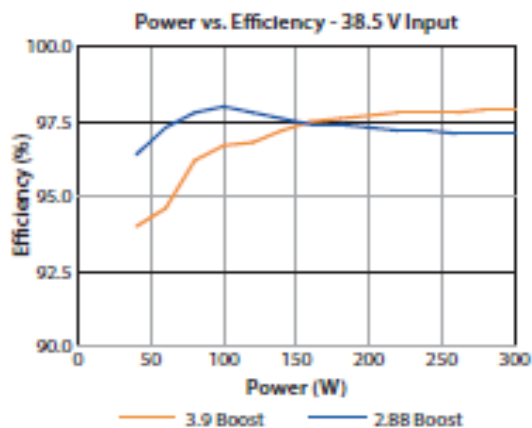
The Aurora/Symtech Maximum Power Point Tracker represents the next generation of high efficiency converters for solar powered vehicles.

Designed to boost the PV voltage to the battery voltage the Tracker utilises the latest resonant soft switching technology to achieve the highest efficiency over a broad range of power and voltages.

A transformer and associated circuitry achieves galvanic isolation from input to output which alleviates the need for circuit breakers to be installed on the PV side of the Tracker – a new World Solar Challenge regulation.



A powerful DSP running a fast tracking algorithm ensures the PV panels stay locked onto their maximum power point and to recover quickly in the event of variable shading.



Ratings

- Rated to 240 W
- Overload rated to 300 W for 5 minutes
- Nominal Input Voltage Range: 20 - 55 V
- Maximum Input Voltage: 60 V
- Nominal Battery Voltage Range: 110 - 165 V ⁽¹⁾
- Maximum Battery Voltage Range: 170 V
- 3 kV Galvanic Isolation from input to output
- Peak Efficiency: 98.5%

Environmental & Packaging

- Operating Temperature Range: -20 to +85 °C
- Passively Cooled through natural convection
- Dimensions: 122 x 200 x 58 mm
- Weight: 790 g

1 Mbps CAN Bus Interface

- Voltage Reporting
- Current Reporting
- Internal Temperature Reporting
- Shut down via the CAN Bus

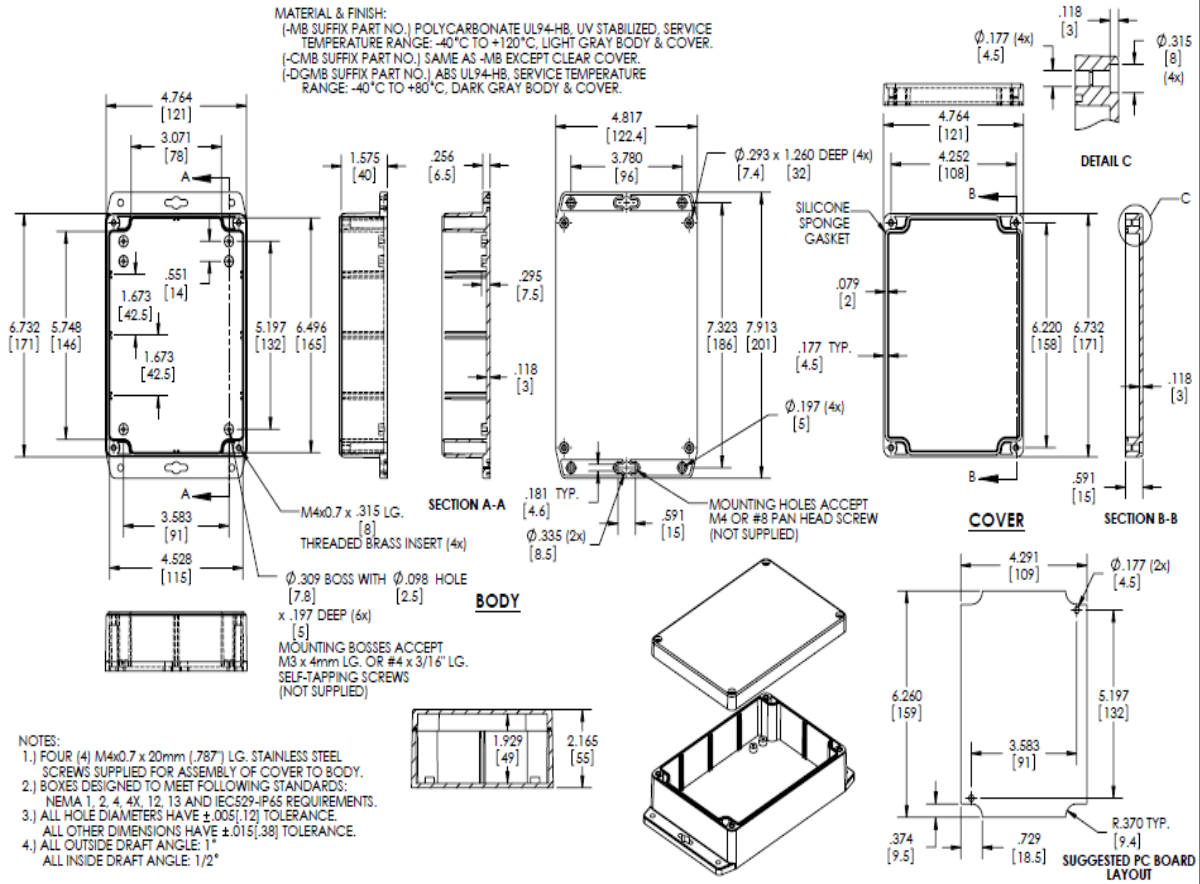
Note (1): At low battery voltage of 110V and rated power of 240W, the lowest Vmp voltage is 33V. However this voltage range extends lower at reduced powers and/or higher battery volts. Other voltage ranges are available on request.

Contact

Email: ross@sym-tech.com.au
Symetric Technologies Pty Ltd, Blackburn Australia

PART NAME	NEMA 4X PLASTIC BOX w/EXTERNAL MTG. BRKT.	PART No.	PN-1324-MB PN-1324-CMB PN-1324-DGMB	REVISION DATE	5-26-11
-----------	---	----------	-------------------------------------	---------------	---------

MATERIAL & FINISH:
 (-MB SUFFIX PART NO.) POLYCARBONATE UL94-HB, UV STABILIZED, SERVICE TEMPERATURE RANGE: -40°C TO +120°C, LIGHT GRAY BODY & COVER.
 (-CMB SUFFIX PART NO.) SAME AS -MB EXCEPT CLEAR COVER.
 (-DGMB SUFFIX PART NO.) ABS UL94-HB, SERVICE TEMPERATURE RANGE: -40°C TO +80°C, DARK GRAY BODY & COVER.



MPPT-Race V 4.0

Low Voltage Setup

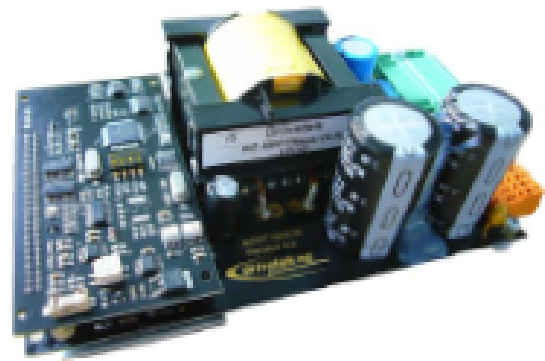


Technical Specification

25 - 540 W DC/DC-Boost Maximum Power Point Tracker

Features:

- High Conversion Efficiency up to 97.5%
- Seeks and Tracks MPP with closed loop algorithm
- Wide I/O Range
- High Reliability and Durability due to Low Thermal Stress
- Separate Control and Power Part
- Data Transmission via CAN Bus
- Input and Output Protection
- End of charge current control
- Fully customized design according to customer specifications

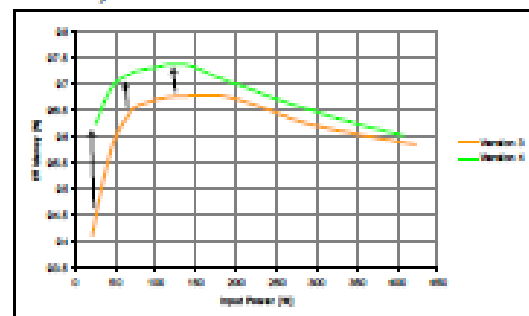


The 4th generation of drivetek's well-proven MPPT-Race. Optimized for solar boat applications with a low input voltage range (< 80V). The absence of almost any switching losses makes this converter ideal for solar cars and any solar power application which needs extremely high efficiency over a wide power range. Current and voltage limits are customized to increase accuracy of MPPT algorithm. High efficiency allows an operation temperature range up to +70°C.

Characteristics¹

Parameter	Unit	Minimum	Typical	Maximum
Input Power Continuous	W	5		540
Input Power Peak ²	W			600
Input Current	A _{oc}			9
Peak Efficiency ³	%		97.5	
Input Voltage Range	V _{oc}	26		60
Output Voltage Range ⁴	V _{oc}	28		140
Output Shutdown Voltage ⁷	V _{oc}			236
Output to Input Voltage Ratio ⁵	-	1.05		3
Length	mm		170	
Width	mm		100	
Height	mm		80	
Weight	g		650	
Operating Temperature	°C	0		70
CAN interface Specification				
Supply Voltage	V _{oc}	6		18
Supply Current Recesive ⁶	mA	15		50
Supply Current Dominant ⁶	mA	60		100
Transmission Rate	kB/s		125	
Bus Length	m			500
Standards	-		ISO 11898	
¹ At 25°C ambient temperature				
² At 140W input power, 40V input and 50V output voltage				
³ During maximum 5min. per hour				
⁴ Output voltage must be higher than input (boost topology)				
⁵ V _{in} =V _{out} , I _{load} =5.5V, R _L =60Ω				
⁶ Use a transmission ratio close to 1.05 for best efficiency				
⁷ Maximum output voltage in case of a sudden load drop				

Efficiency¹ (at 100-140 W)



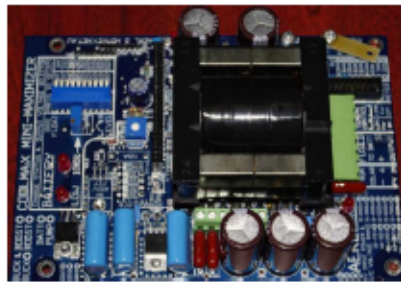
Big winner of the Fribourg Solar Challenge 2010 is the Private Energy Solarboat team using drivetek's MPPT-Race V4.0.

drivetek ag, industriestrasse 37, ch-2555 bruegg
 phone +41 32 332 78 32, fax +41 32 332 78 31
 www.drivetek.ch

1 **PRODUCT OVERVIEW**

AERL RACEMAX 600B

A high current, high efficiency, boost-only race-trim maximum power point tracker.



FEATURES:

- High 98 – 99% operating efficiency.
- Compatible with all types of solar cells and battery arrays.
- Passive cooling & no moving parts results in highly reliable operation to 50°C .
- Output voltage options of 72, 96, 120, 144, 168V.
- Compact and lightweight design, weighing only 750g.
- Charges higher voltage battery packs from lower voltage solar arrays.



Australian Energy
Research Laboratories Pty Ltd

PRODUCT DATASHEET

RACEMAX 600B
Australian Energy Research Labs
AER02.001 – ver 2
30 March 2010

2 MODEL SPECIFICATIONS

Performance Data

Symbol	Parameter	Max
T_{amb}	Maximum ambient air temperature	50°C
$I_{sc-const}$	PV panel short circuit current - constant	6A
$I_{sc-trans}$	PV panel short circuit current – transient	8A

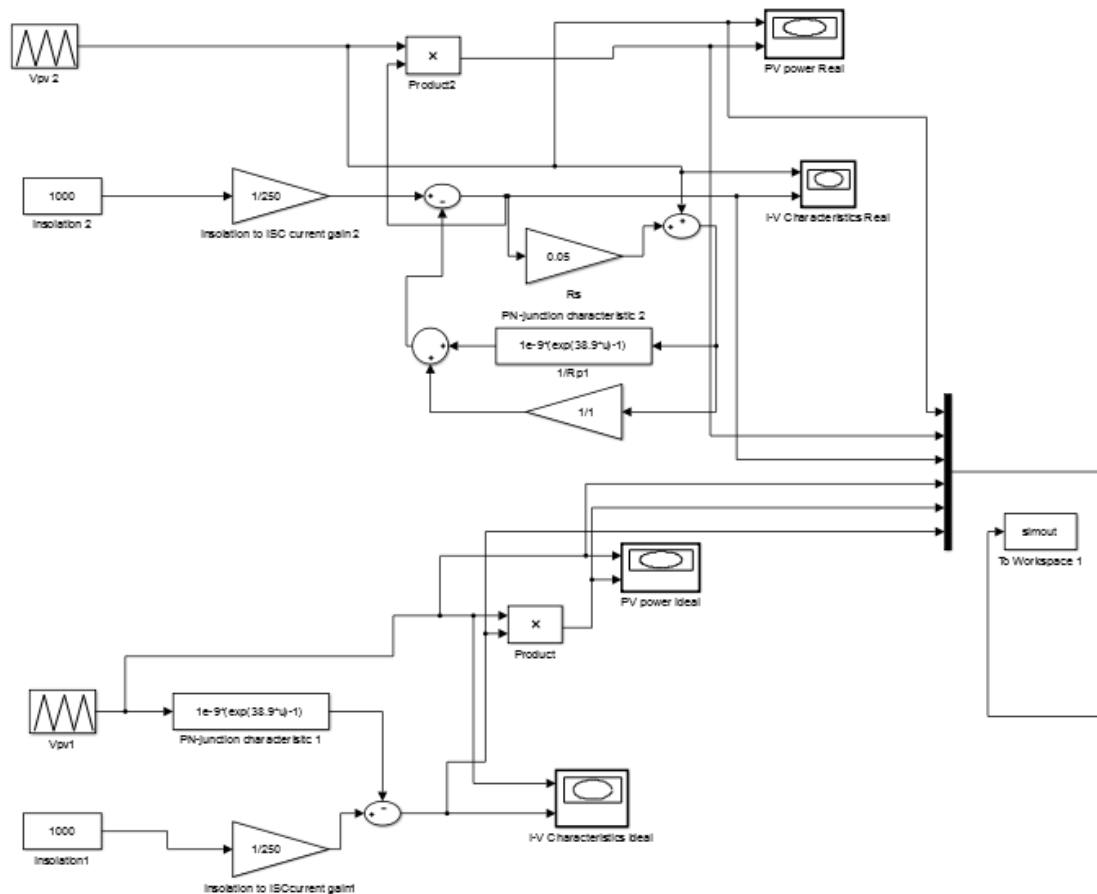
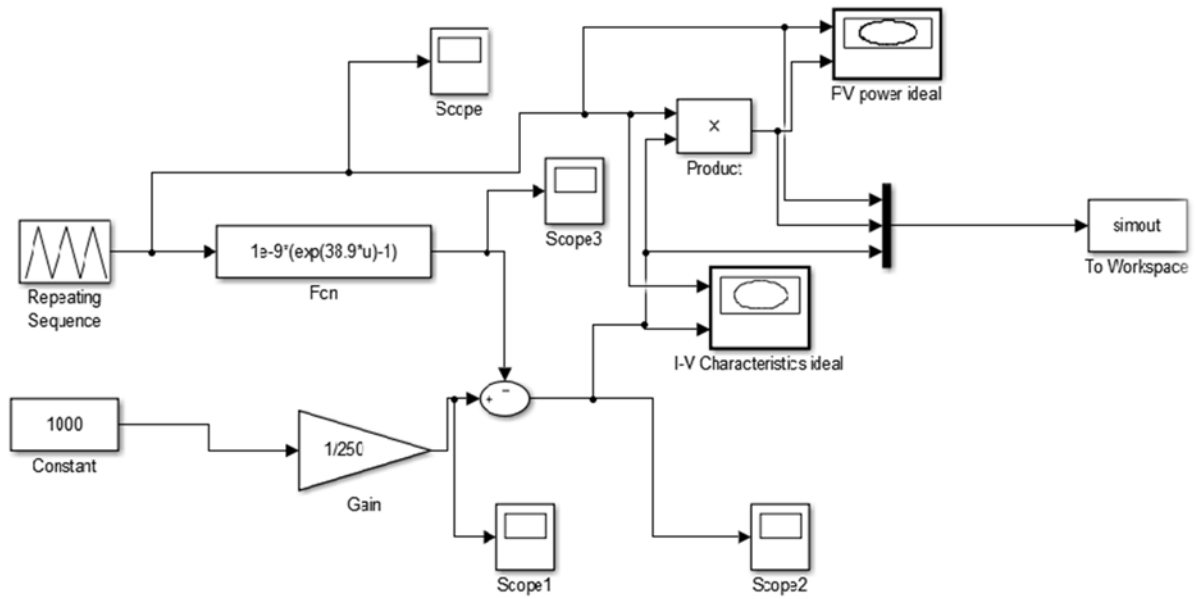
Electrical Characteristics

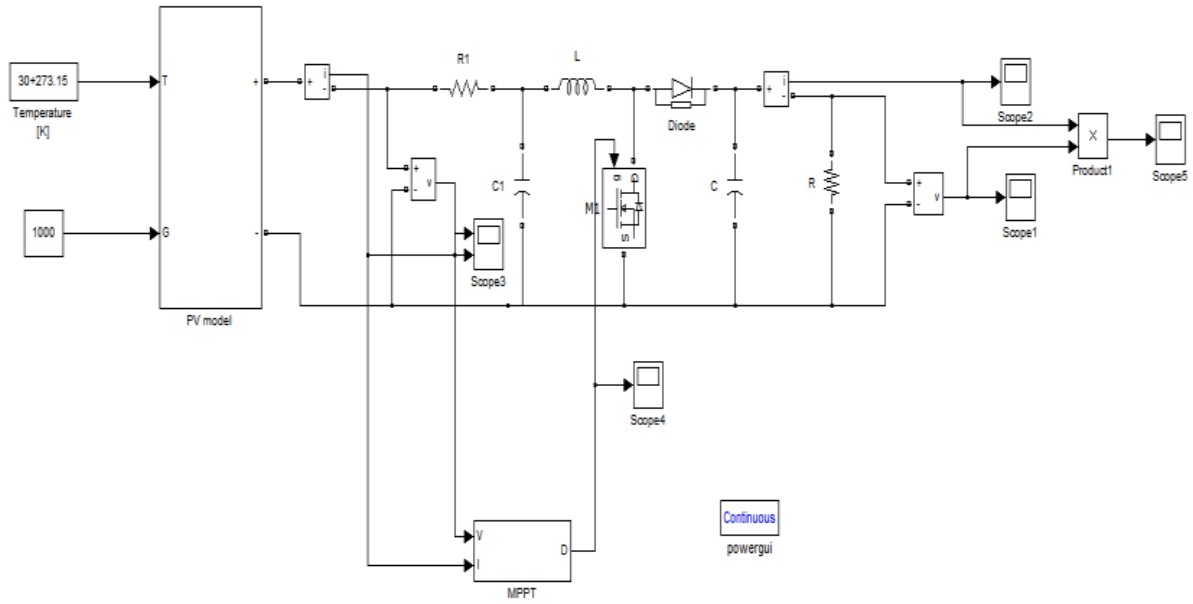
Symbol	Parameter	Min	Max
P_{mp}	Solar panel peak power	0W	600W
V_{oc}	PV panel open circuit voltage	40V	135V
η	Efficiency @ 6A, 100Vmp, & 25°Camb	98.00%	-
V_{bat}	Battery Voltage (Selectable)	72, 96, 120, 144, 168V	

Physical Characteristics

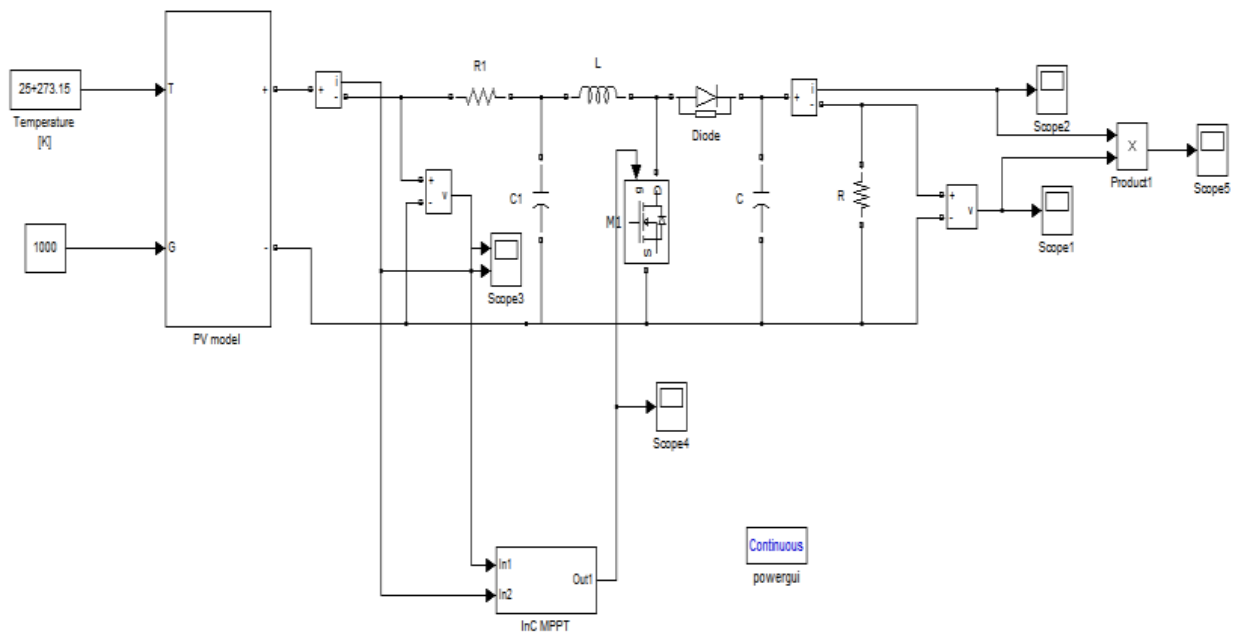
Parameter	Typical
Weight	720g
Dimensions (L x W x H)	170 x 120 x 65 mm

A.3 Appendix C- MATLAB Simulink Models and Coding





P&O Algorithm test model



Incremental Algorithm test model

```

function S2 = DATA(day,localTime,latitude, longitude,area,eff)

if rem(day,1) ~= 0 | day < 0 | day > 365
error('Error: "day" needs to be expressed as a whole number between 1
(Jan 1st) to 365 (Dec 31st)')
end

if localTime < 0 | localTime > 24
error('Error: "time" needs to be expressed in hours as a number between
0 to 24')
end

if latitude < -90 | latitude > 90
error('Error: "latitude" needs to be expressed in degrees between -90
to 90')
end

if area < 0 | eff < 0
error('Error: "area" and/or "eff" need to be greater than zero')
end

%Declination Angle: Dependent on day of year
dec = 23.45*sind((360/365)*(281+day)); %declanation angle from 8 Oct
GMT = 9; %Greenwich Mean Time (Same for both darwin and Adelaide)

%Local standard time meridian
LSTM = 15*GMT; %in degrees

%Correction to local solar time(LST) due to time zone effect
TC1 = 4*(longitude - LSTM); %minutes

B = (360/365)*(day - 81); %deg

%Equation of time
EOT = 9.87*sind(2*B) - 7.53*cosd(B) - 1.5*sind(B); %min

%Total time correction
TC = TC1 + EOT; %min

%Local solar time
LST = localTime + (TC/60);

%Hour Angle
H = 15*(LST-12); %deg

%Elevation angle
EA = asind(sind(dec)*sind(latitude) +
cosd(dec)*cosd(latitude)*cosd(H));

%Zenith angle
zen = 90 - EA; %deg

%Azimuth Angle

```



```

az = acosd((sind(dec)-
sind(latitude)*cosd(zen))/(cosd(latitude)*sind(zen)));

%sunrise time in hours
sunrise = 12 - (1/15)*acosd(-tand(latitude)*tand(dec)) - (TC/60);

%sunset time in hours
sunset = 12 + (1/15)*acosd(-tand(latitude)*tand(dec)) - (TC/60);

%Solar constant:(mean value) (incidence angle 0)
Gsc = 1367; %W/m^2

%Solar constant:(exact value) (incidence = 0)
Gon = Gsc*(1+0.033*cosd((360*day)/365)); %W/m^2

%Radiation incident on the surface tangent
%to the outer surface of the atmosphere
Go = Gon*cosd(zen); %W/m^2

%Power output of a PV array
power = Go * area * eff;

S2 = [power, sunrise, sunset];

clc
close all
clear all

for i = 1:900
    time(i) = 8+(i-1)*0.01;
    Power(:,i) = DATA(1,time(i),12.46,130.84,4,0.19);
end

figure
plot(time,Power(1,:))

```

A.4 Appendix D- Temperature and Shading Calculations

Temperature Effect on Output Power:

At Darwin: (08th October, 2017)

Temperature = 35°C [accuweather.com].

Therefore,

$$T_{\text{cell}} = T_{\text{ambient}} + \left(\frac{\text{NOCT} - 20^{\circ}\text{C}}{0.8} \right) * S$$

$$T_{\text{cell}} = 35^{\circ}\text{C} + \left(\frac{45^{\circ}\text{C} - 20^{\circ}\text{C}}{0.8} \right) * 1$$

$$T_{\text{cell}} = 66.25^{\circ}\text{C}$$

For One cell:

$$P_{\text{max}} = 3.34 \text{ W} [1 - 0.1\% \text{ per } ^{\circ}\text{C} \times (66.25^{\circ} - 25^{\circ})]$$

$$P_{\text{max}} = 3.20 \text{ Watt}$$

For Complete Solar Array:

$$P_{\text{max}} = 645 \text{ W} [1 - 0.1\% \text{ per } ^{\circ}\text{C} \times (66.25^{\circ} - 25^{\circ})]$$

$$P_{\text{max}} = 618.39 \text{ Watt}$$

Under Radiations = S = 0.7kW/m². (bom.gov.au)

$$T_{\text{cell}} = T_{\text{ambient}} + \left(\frac{\text{NOCT} - 20^{\circ}\text{C}}{0.8} \right) * S$$

$$T_{\text{cell}} = 35^{\circ}\text{C} + \left(\frac{45^{\circ}\text{C} - 20^{\circ}\text{C}}{0.8} \right) * 0.7$$

$$T_{\text{cell}} = 56.87^{\circ}\text{C}$$

For One cell:

$$P_{\text{max}} = 3.34 \text{ W} \times 0.7 \times [1 - 0.1\% \text{ per } ^{\circ}\text{C} \times (56.87^{\circ} - 25^{\circ})]$$

$$P_{\text{max}} = 2.26 \text{ Watt}$$

For Complete Solar Array:

$$P_{\text{max}} = 645 \text{ W} \times 0.7 \times [1 - 0.1\% \text{ per } ^{\circ}\text{C} \times (56.87^{\circ} - 25^{\circ})]$$

$$P_{\text{max}} = 437.11 \text{ Watt}$$

Shading Effect on Output Power:

At Darwin: (08th October, 2017)

Power under Full sun (without Shading)

$$\therefore P_{\max} = V \times I$$

$$P_{\max} = 1.7 \times 1.9$$

$$\mathbf{P_{\max} = 3.23 W}$$

Power under shading (with bypass diode)

Maximum Current = $I_{MPP} = 1.9A$ and Maximum Voltage = $V_{MPP} = 1.48V$

$$\therefore P_{\max} = V \times I$$

$$P_{\max} = 1.48 \times 1.9$$

$$\mathbf{P_{\max} = 2.812 W}$$

Power under shading (without bypass diode)

From Figure 42: Maximum Current = $I_{MPP} = 1.58A$ and Maximum Voltage = $V_{MPP} = 1.3V$

$$\therefore P_{\max} = V \times I$$

$$P_{\max} = 1.3 \times 1.58$$

$$\mathbf{P_{\max} = 2.054 W}$$